TEXTILE RESEARCH JOURNAL

Publication of

TEXTILE RESEARCH INSTITUTE

VOLUME 30 AUGUST 1960 NUMBER 8

TEXTILE RESEARCH JOURNAL

Volume 30 *August 1960* Number 8

Editor: **Richard K. Toner**

Production Editor: **Candida Frenking**

Advisory Board

Herbert J. Ball
Earl E. Berkley
John Boulton
C. H. Fisher
Walter J. Hamburger
Milton Harris
R. M. Hoffman
Harold P. Lundgren
Herman Mark
Edward R. Schwarz
George Switlyk
Helmut Zahn

TEXTILE RESEARCH JOURNAL, published monthly at Prince and Lemon Streets, Lancaster, Pa., is devoted to the interest of research in textile and allied industries. It is published by Textile Research Institute.

Manuscripts and communications should be sent to the Publications Department, P.O. Box 625, Princeton, N. J.

Second-class postage paid at Lancaster, Pa.

Subscription rates: $25.00 per year; additional for postage, 50 cents to Canada, $1.00 to all other countries. Single copies, $2.50 each.

Contents copyright © 1960 by Textile Research Institute. Advertising rates applied on request.

IN THIS ISSUE

A Quantitative X-Ray Diffraction Study of the Alpha–Beta Transformation in Wool Keratin. *E. G. Bendit* 547

The Log-Normal Distribution of the Diameter of Wool Fibers in Top Slivers as Studied by R. Henon and J. Ott. *Franz Monfort* 556

Load Deflection Analysis of Fibers with Plane Crimp. *R. Chicurel and E. Suppiger* 568

Durability of Oleophobicity of Cotton Fabrics Imparted by Fluorochemicals. *Ralph J. Berni, Ruth R. Benerito, and Frederick J. Philips* 576

The Determination of Moisture in Wool with Karl Fischer Reagent. *John R. Wilson and M. M. Sandomire* 587

Some Observations on Kinetic Friction of Jute. *A. C. Chakravarty* 592

Studies of the Movement of Wool Fibers in Fabrics During Felting, with Particular Reference to the Permanency of Pleasts. Part III: Felting in a Woolen Fabric. *K. Rachel Makinson* 598

The Bilateral Structure of Crimped and Steely Wools and the Origin of Fiber Crimp. *D. F. Louw* 606

Studies on Wool. Part V: Partial Hydrolysis in Acid Reducing Medium. *Pierre Pigache and Gerard Biserte* 612

LETTERS TO THE EDITOR

A Ballooning Yarn Apparatus with Linear Yarn Movement. *D. Brunnschweiler, P. J. Cotterill, and N. Hodgkinson* .. 616

Cotton Fiber Weight Distribution. *Jamnadas Shah* 618

Linear Densities of Fibers in Selected Length Groups of 42 Domestic and Foreign Cottons. *Jack E. Sands, Gain L. Louis, and John D. Tallant* 619

A Note on the Effects of Humidity and Actinic Exposure on Fabric Strength. *Joseph J. Moder* 620

The X-Ray Diffraction Pattern of Iodinated Wools. *A. R. Haly and M. Feughelman* 622

The Differential Thermal Analysis of Textile and Other High Polymeric Materials. *Robert F. Schwenker, Jr. and Louis R. Beck, Jr.* 624

Ultraviolet Light and Conduction in Keratin. *J. E. Algie and A. R. Haly* 627

Continuous Simultaneous Measurements of Rigidity and Regain in a Filament During a Sorption Process. *B. H. MacKay and J. G. Downes* 628

BOOK REVIEWS 630

REPRINT REQUESTS SHOULD BE DIRECTED TO THE AUTHORS

SEE ARTICLES FOR ADDRESSES

TEST FOR **STATIC** *WITH*

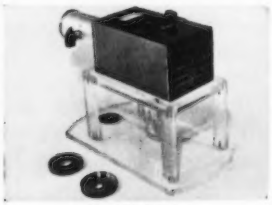

Model CS-66

The ELECTROSTATIC VOLTMETER (CS-66) was developed by the Institute of Textile Technology to detect and measure electrostatic charges on moving or stationary equipment or materials.

The ELECTRICAL RESISTANCE TESTER (CS-51) has been developed for measurement of electrical resistance of fabrics, fibers, film and other materials to determine the static propensities of the materials.

Model CS-51

FOLDERS AND PRICE UPON REQUEST

CUSTOM SCIENTIFIC INSTRUMENTS, Inc.

541 Devon St. Kearny, N.J.

AUGUST 1960
VOL. 30 NO. 8

TEXTILE RESEARCH JOURNAL

A Quantitative X-Ray Diffraction Study of the Alpha–Beta Transformation in Wool Keratin

E. G. Bendit

C.S.I.R.O. Wool Research Laboratories, Division of Textile Physics, Ryde, N.S.W., Australia

Abstract

The α–β transformation has been investigated with a Geiger counter x-ray diffractometer by observing the variations of peak intensity of the three prominent reflections (5.1 Å, 4.65 Å, 9.8 Å) of the wide-angle x-ray diagram of wool during extension under different conditions of temperature and humidity. It is found that the α–β transformation always starts at extensions of 5% or less, and that the extent of transformation is frequently proportional to fiber extension, or approximately so. (These results are at variance with the generally accepted view, based on photographic evidence, that the onset of the α–β transformation always occurs at 20–30% extension, and that most of the transformation takes place in the range 30–50% extension.) In general, the transformation proceeds more rapidly at low than at high relative humidities; i.e., at a given strain, it has proceeded further in the case of dry than that of wet fibers; the rate of the transformation is the same at 50° C. as it is at 20° C. It is frequently found that during the α–β transformation a decrease in the α-reflection at 5.1 Å is not accompanied by a related increase in the β-reflection at 4.65 Å, and a similar lack of correspondence is noted if extended fibers are allowed to relax in water. In this connection, the difficulty of relating the intensity of x-ray reflections to the actual amount of diffracting material is briefly discussed.

Some incidental observations, such as the effect of x-radiation on the α–β transformation, are also reported. A brief outline of a correction procedure which takes account of counting loss, air scattering, and variation of absorption and diffracting material during extension is included.

Introduction

The pioneer research by Astbury and his colleagues [1, 2, 3] some 25 years ago on the "Structure of Hair, Wool and Related Fibres" established that the x-ray diagram of stretched keratin is quite different from that of unstretched keratin. Astbury found that the x-ray photograph remains essentially unchanged up to 20% or 30% extension (α-pattern), undergoes a marked transformation between 30% and 50% extension, and changes little at higher extensions (β-pattern); he interpreted this finding in terms of a configurational change in the keratin molecule from a folded α- to an extended β-form. The nature of the fold involved in the α-form has been the subject of many proposals, but it now

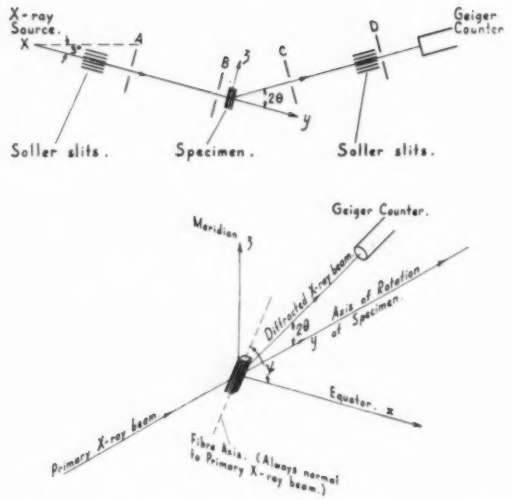

Fig. 1. Diffraction geometry of transmission technique; (top) x-ray optical arrangement, (bottom) specimen geometry. The divergence slit A is a rectangular aperture 2 mm. high × 3 mm. wide, and the circular apertures B, C, and D have diameters 2 mm., 2 mm., and 4 mm. respectively.

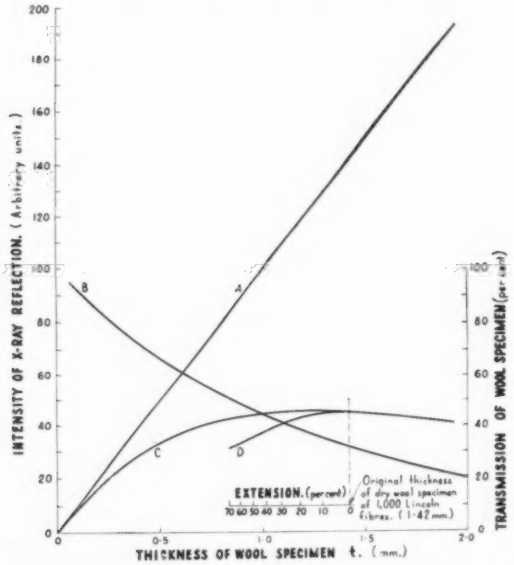
INTENSITY OF X-RAY REFLECTION. (Arbitrary units.)
TRANSMISSION OF WOOL SPECIMEN (per cent)
THICKNESS OF WOOL SPECIMEN t. (mm.)
EXTENSION. (per cent)
Original thickness of dry wool specimen of 1,000 Lincoln fibres. (1·42 mm.)
A
B
C
D

Fig. 2. Curve A: Variation of diffracted intensity as a function of specimen thickness in the absence of absorption. Curve B: Variation of percentage transmission as a function of specimen thickness for the 5.1 Å reflection. Curve C: Intensity variation due to changes in specimen thickness for the 5.1 Å reflection (obtained by multiplying corresponding ordinates of Curves A and B). Curve D: Experimental intensity variation of the 5.1 Å reflection during the α–β transformation normalized to agree with Curve C at 0% extension.

seems universally accepted that basically the structure is closely related to the α-helix of Pauling, Corey, and Branson [16], although some modification of this is necessary to account for details of the diffraction photograph of keratin [7, 18] and also to achieve the closer packing required by density considerations [12, 18]. In contrast, the origin of the β-pattern has never been controversial, and Astbury's original β-structure is still regarded as essentially correct, although it is now replaced by Pauling and Corey's [17] more precisely determined pleated sheets.

While it is true to say that the majority opinion has always accepted Astbury's original hypothesis that the change from the α- to the β-pattern is directly related to a configurational change in the keratin molecule, alternative explanations have been advanced from time to time. Moreover, several recent studies have emphasized the chemical and physical heterogeneity of the wool fiber and suggest that the cortex of the fiber is largely made up of two types of protein which are very different both chemically and physically. This suggestion, linked with the stereochemical difficulty [4, 12] of converting α-helices into the pleated sheet configuration, raises the possibility that the α- and β-photographs may have their origin in different parts of the cortex. It was thought that some light might be shed on this and other aspects of the α–β transformation by a quantitative study. Preliminary results have been published earlier [5], and this paper reports the results in greater detail.

Experimental

All tests were carried out with a Norelco high-angle x-ray diffractometer. The normal reflectance x-ray optical arrangement of the instrument was modified to permit use of a transmission technique (Figure 1-top). After emerging from the x-ray tube, the radiation passes through the divergence slit A and is incident normally on a fiber specimen which is mounted behind the aperture B. The diffracted radiation passes through apertures C and D before entering the Geiger counter. The bracket holding aperture C is attached to the rotating arm of the wide-angle goniometer on which the Geiger counter and aperture D are mounted. The angular resolution of this optical system was found to be better than $2\theta = 1°$ "half-width" both radially and azimuthally.

Copper radiation was used throughout, generally at 35 kVP. The radiation was not filtered, as tests showed that for this type of investigation the advantage of a "cleaner" x-ray diagram is outweighed by the disadvantage of reduced diffracted intensity. The specimen consisted of about 1000 Lincoln wool fibers of dry diameter 45 ± 5 μ, and was held between stretching jaws in a chamber at controlled temperature and humidity. The x-ray diagrams obtained with this technique were in the form of strip chart recorder traces of diffracted intensity as a function of Bragg angle through a section of the x-ray diagram. Different sections were obtained by rotating the specimen about an axis coincident with the primary x-ray beam (Figure 1-bottom).

In view of the small intensity differences which had to be measured, reproducibility of Geiger counter traces was of great importance. As neither direct beam monitor nor electronic stabilizer was available, the intensity was periodically checked with a standard specimen. The specimen chosen consisted of a number of thicknesses of beaten "Dutch metal" which, being free from preferred orientation, gave Debye-Scherrer rings and was therefore unaffected by slight positional errors. It was also shown to be unaffected by x-radiation and humidity. Tests over a long period showed that, at any given time after switching on the equipment, the standard trace was reproducible to within $\pm 1\%$, but that during a day's run the peak reading increased by 2–3%, presumably due to heating up of electronic components.

This investigation deals mainly with a determination of the intensity variation of the three prominent reflections of the wide-angle x-ray diagram of wool: the meridional α-arc (a group of reflections at about 5.1 Å), the equatorial β-spot at 4.65 Å, and the equatorial spot common to both α- and β-patterns (a group of reflections at about 9.8 Å). The fine structure of these reflections is not resolved by the present x-ray optical arrangement, which is designed for maximum diffracted intensity rather than optimum resolution.

Correction Procedure

The most satisfactory way of presenting the α–β transformation quantitatively (see below) is by plotting the peak intensity of a reflection against extension, but before this can be done, the following corrections must be applied to the observed peak heights.

1. Counting loss in the Geiger counter due to finite dead-time; this was allowed for by using the expression [15]

$$N = N_o/(1 - N_o \tau)$$

where N_o and N are the observed and corrected counting rates and τ is the resolving time of the Geiger counter.

2. Background due to air scatter and scattering at the apertures; this was determined by taking Geiger counter traces without wool specimens, while at the same time attenuating the direct beam suitably to get conditions equivalent to those obtaining during diffraction tests.

3. Variation of specimen geometry during stretching. Extension of the wool specimen reduces both the amount of irradiated diffracting material and the absorption within the sample. The first effect causes the intensities of the x-ray reflections to decrease linearly with decreasing specimen thickness, because the width of the wool bundle is held fixed between guides. The second effect causes the intensities of the reflections to increase with decreasing specimen thickness in an approximately exponential manner, the precise manner of variation depending on the particular reflection under investigation. Figure 2 shows the relative magnitude of these effects (Curves A and B).

The intensity variation of an x-ray reflection during stretching, as represented by Curve C, arises entirely from changes in specimen geometry, and the effect of a true, intrinsic change of the x-ray diagram, such as occurs during the α–β transformation, causes the experimental curve to be different from Curve C. For example, the disappearance of the 5.1 Å meridional reflection during the transformation, as observed from peak height measurements of the recorder trace at different extensions, may be represented by an intensity–thickness graph (Curve D). The true intensity variation of this reflection is given by the difference between the ordinates of Curves C and D. Included in Figure 2 is a scale which showes the percentage extension of a wool bundle of original thickness 1.42 mm. and which allows determination of the intensity of x-ray reflections at various extensions. A plot of the difference between Curves C and D as a function of extension represents the graph of true peak intensity against extension (Figure 3).

As a check on the procedure of correcting the

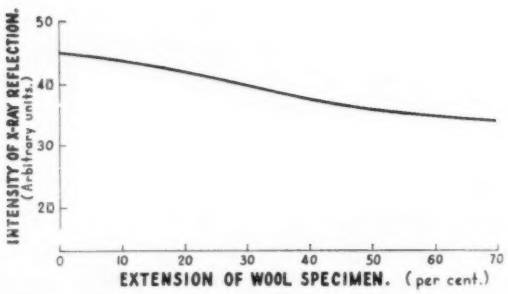

Fig. 3. The true intensity variation of a disappearing x-ray reflection (5.1 Å) during the α–β transformation, obtained by plotting the difference between Curves C and D (Figure 2) against extension.

intensities for variations in specimen thickness during stretching, curves corresponding to that shown in Figure 3 were also obtained by a more direct method in a number of cases. This method rests on the assumption that at Bragg angles well removed from that of actual reflections, the intrinsic intensity remains constant during the α–β transformation. The experimental traces at the various extensions, after correction for counting loss and background, were therefore normalized to the trace at zero extension in the vicinity of $2\theta = 30°$. After this normalization, the peak height variation of the reflections was again drawn as a function of extension; the resulting curves differed little from those obtained with the correction procedure outlined above.

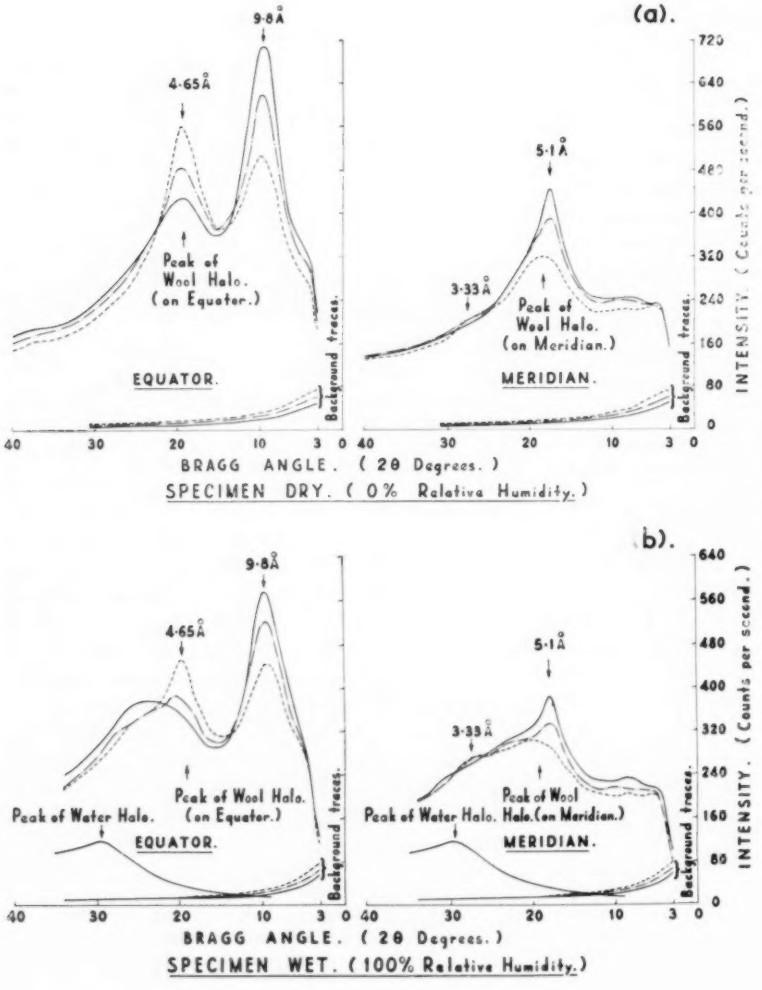

Figure 4. Uncorrected experimental Geiger counter traces of Lincoln wool during the α–β transformation. Unfiltered copper radiation at 35 kV and 13 mA. Sample of about 1000 fibers stretched in water at 50° C. X-ray diagrams obtained in air at 50° C. with specimen dry (over P_2O_5) and wet (over H_2O). Full lines: α-pattern at 0% extension, dotted-dashed lines: pattern at 30% extension, dashed lines: β-pattern at 60% extension.

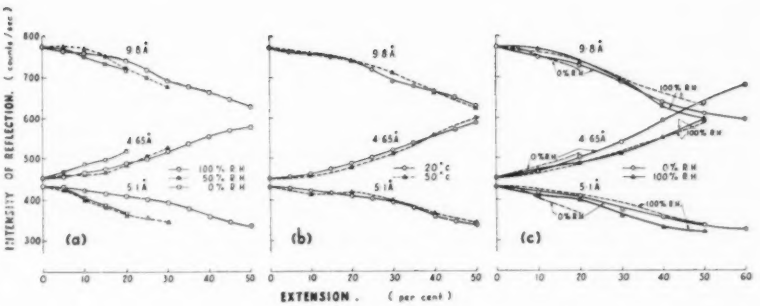

Figure 5. (a) Effect of humidity on the α–β transformation. Stretching and x-ray diagram in air at about 20° C. Curves for 0% RH (over P_2O_5) at 50° C. (b) Effect of temperature on the α–β transformation. Stretching and x-ray diagram in air at 100% RH (over H_2O). (c) Effect of stretching in water at 50° C. on the α–β transformation. X-ray diagrams taken in air at 0% RH (over P_2O_5) and 100% RH (over H_2O). Corresponding curves obtained when stretching in air at 0% RH and 100% RH are shown dotted (taken from Figure 5a).

Results

Typical equatorial and meridional scans of wool specimens, both dry and wet, during the α–β transformation are shown in Figure 4. These traces are not corrected in any way, but the background due to air scatter and scattering at the apertures is shown. Figure 4b also shows the water halo at 30° C. as reported by James [13]; this curve has been normalized to show very approximately the relative intensities of the wool and water diffraction patterns.

Ideally, the variation of the total integrated intensity of a reflection should be plotted against extension to give a true representation of the change in the x-ray diagram. This method involves plotting the entire x-ray diagram for each extension, which is not only very time-consuming but also raises the problem of damage due to long irradiation (see below). Furthermore, even when the complete x-ray diagrams have been obtained, integration of intensities is largely guesswork, not only because the extent of the reflections along the azimuth is ill-defined, but also because it is difficult to decide what to choose as base line in each case. (The base line is the hypothetical x-ray diagram without characteristic reflections.) The difficulty of a satisfactory base line applies particularly to those tests in which the α–β transformation cannot be taken to completion on account of fiber breakage.

The next best method is to plot integrated intensity under the traces (i.e., radially integrated intensity) against extension during the α–β transformation, but this also has the limitation of uncertain base lines.

It was therefore decided to use variations of peak intensity of the reflections as the most satisfactory measure of the change in x-ray diagrams during extension. In certain cases, however, it was possible to confirm that the variation of radially integrated intensity was substantially the same as the peak intensity variation.

The graphs of peak intensity against extension, corrected as indicated above, were drawn for the 9.8 Å, 4.65 Å, and 5.1 Å reflections under a variety of conditions to test the effect of different parameters on the α–β transformation. In most cases more than one curve for each reflection appears on the figures; these curves are normalized at 0% extension to permit comparisons among the different conditions under which the α–β transformation was obtained (e.g., different relative humidities, temperatures, etc.).

Effect of Humidity

Samples were stretched in air at controlled humidity and temperature; the x-ray diagrams were taken under the same conditions (Figure 5a). It can be seen that the α–β transformation proceeds more rapidly at low than at high relative humidities and that under all humidity conditions the intensity of the three reflections starts to change at very low extensions (5% extension or less). (Throughout this report the term "rapid" in connection with the α–β transformation refers to the rate of change of the intensity of the characteristic reflections with extension and not with time.) A noticeable feature of this test is the rapid decrease of intensity of the 5.1 Å reflection at 50% RH in contrast to the gentle and almost linear decrease at 100% RH, while no corresponding difference is observed for the appearing 4.65 Å reflection at these two relative humidities.

The intensity variations of both α- and β-reflections at 0% RH are very marked. This result is in conflict with the findings of Peters and Woods [19], who report that the x-ray diagram of dry fibers,

although progressively more diffuse as the fibers are stretched, is always of the α-type even up to the maximum extension of about 20%.

Effect of Temperature

Samples were stretched in air at 100% RH at different temperatures (Figure 5b). There is little, if any evidence of a temperature effect on the α–β transformation in the range of 20° C. to 50° C.

Effect of Stretching in Water

Samples were stretched in water at 50° C. and the x-ray diagrams at the various extensions were taken in air at 0% RH and 100% RH (Figure 5c). The 4.65 Å reflection appears more rapidly at 0% RH than at 100% RH, while the 5.1 Å reflection disappears more slowly at 0% RH than at 100% RH. This shows that drying of the fibers affects these two reflections differently. Further evidence of difference in behavior of these reflections is provided by a comparison between the curves obtained when stretching in water and testing in air at 100% RH and those obtained when stretching and testing in air at 100% RH (shown dotted in Figure 5c); the α–β curves of the 4.65 Å reflection are practically identical while those of the 5.1 Å reflection differ considerably.

Effect of Relaxing Stretched Fibers in Water

The x-ray diagrams of extended fibers change very little if examined at any given extension over a period of days in air, but when fibers are given an extension in air at room temperature and humidity and are then allowed to relax at that extension in

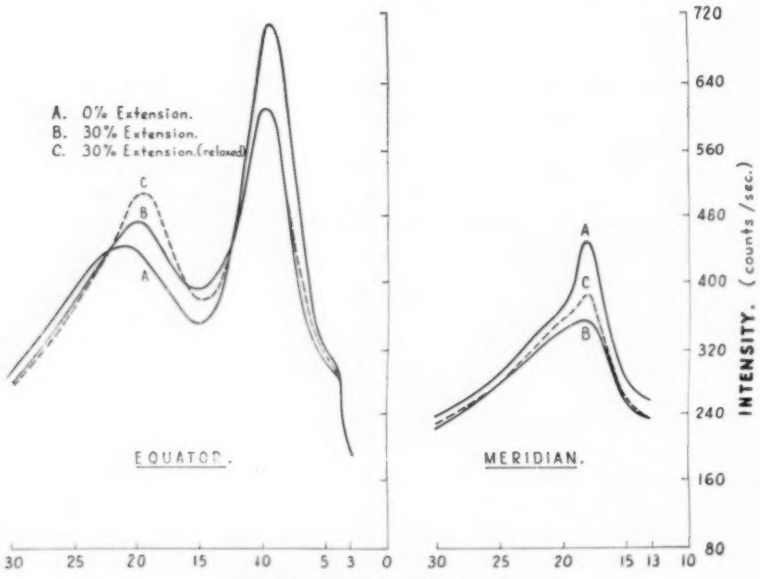

Fig. 6. The effect of relaxation in water on the x-ray diagram of wool fibers stretched in air at 20° C. and 50% RH. Recorder traces at 0% extension (Curve A), 30% extension (Curve B), and at 30% extension after relaxation in water at 50° C. for 10 min. (Curve C).

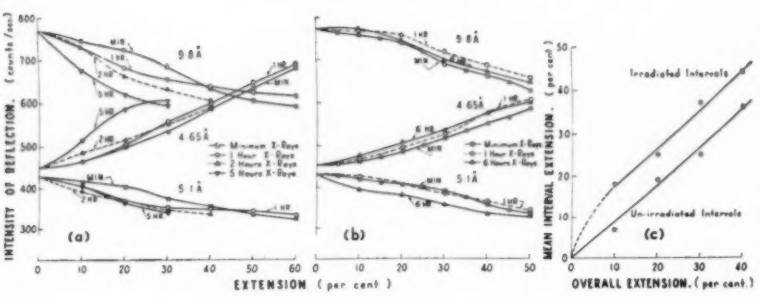

Fig. 7. Intensity-extension curve of wool fibers exposed (in the unstretched state) to unfiltered copper radiation at the window of the x-ray tube. Irradiation at 35 kV, 15 mA, dose rate about 40 r./sec. 2 mm. central region irradiated in all cases. Minimum x-rays refers to the dose received by the fibers during testing in the specimen position, and corresponds to a few minutes irradiation at the window of the x-ray tube. (a) Specimen stretched in water at 50° C., x-ray tests in air at 0% RH (over P_2O_5). (b) Specimen stretched in air at 100% RH (over H_2O) and 20° C.; x-ray diagrams taken under the same conditions. (c) Effect of exposure to x-rays on the extension of wool fibers. Alternate 2-mm. intervals irradiated for 6 hr. at the window of the x-ray tube.

hot water for a few minutes, the x-ray diagrams before and after relaxation are very different (Figure 6).

It is seen that both the characteristic β-reflection (4.65 Å) and the characteristic α-reflection (5.1 Å) increase in intensity after relaxation at 30% extension. Similar results were obtained at other extensions but, whereas the 4.65 Å reflection always considerably increases in intensity, the increase in the case of the 5.1 Å reflection is frequently only small. In every case, however, there is a lack of correspondence between the intensity variations of these two reflections.

Radiation Damage

It was apparent from early tests that the rate of the α–β transformation depends on the amount of radiation received by the fibers during experiments, and it was decided to investigate this effect.

The irradiation was carried out near the window of the x-ray tube, where the intensity was found to be about 40 r./sec., as measured with a ferrous sulfate dosemeter [6]. This compares with a primary beam intensity of about 4 r./sec. at the normal specimen position for diffraction tests. Only the central 2-mm. portion of the specimen was exposed to x-rays. The fiber bundles were stretched in water at 50° C. and the diffraction patterns at the various extensions were obtained in air either at 0% RH or at 100% RH.

Figure 7 shows that wool fibers whose central portions have been exposed to x-radiation exhibit a more rapid α–β transformation and that, in general, the rate of the transformation increases with x-ray dosage. The effect is most marked in the case of dry fibers (Figure 7a). (The terms "dry" and "wet" refer to the condition of the specimen under which the x-ray diagrams are taken and not to the condition during the long initial exposure to x-rays. The effect of moisture content during the initial exposure on the rate of the α–β transformation was investigated, and was found to be insignificant.) Except at high x-ray dosages, the curves in the case of wet fibers are not very different from those of unexposed specimens (Figure 7b).

It was also found that if the entire length of the specimen is exposed to x-radiation, the resulting curves (not shown) differ little from those of unexposed specimens, even at high x-ray dosages. It therefore appears that irradiation weakens the fiber and that, if only part of the fiber is exposed, that part extends more during subsequent extensions than the rest of the fiber. This was tested by placing equally spaced marks along the length of the fiber and irradiating alternate intervals. The fibers were then extended in air at 100% RH and the strain of these intervals measured. The mean percentage extensions of the irradiated and unirradiated intervals were plotted against over-all extension of the fiber (Figure 7c). The test confirms that irradiation causes increased extensibility, particularly in the first 10% over-all extension, after which the extension of the two regions proceeds at an approximately equal rate. The additional extension of the exposed intervals, which is of the order of 10% extension, agrees fairly well with the difference in the intensity–extension curves of unexposed and 6-hr. exposed wet fibers.

Azimuthal Intensity Variation of the X-Ray Diagrams

When peak height intensity is plotted as a function of specimen orientation (Figure 8), it is found that the equatorial reflections are not very sharp azimuthally and that the inner spot at 9.8 Å is considerably sharper at 0% extension than at 70% extension. Similarly, the 4.65 Å β-reflection at 70% extension, which is of course absent at 0% extension, falls off more gradually along the azimuth than is indicated by x-ray photographs of keratin.

Variation of Bragg Angle of Peak Intensities with Extension and Relative Humidity

The angular peak position of the 9.8 Å reflection was measured at various extensions under humidity conditions varying from 0% RH to 100% RH. It was found that the peak angle always increases in an approximately linear manner with extension of the fiber bundle, the total shift at 50%–60% extension corresponding to a decrease in the 9.8 Å spacing of about 0.4 Å. Attempts to carry out similar measurements for the other two prominent reflections (4.65 Å and 5.1 Å) were unsuccessful, because the former is largely merged with the amorphous halo at the lower extensions, while the latter merges with the halo at the higher extensions (see Figure 4).

At any given extension, the peak position of the 9.8 Å reflection is constant at humidities in the range 0%–50% RH, but at 100% RH the peak position

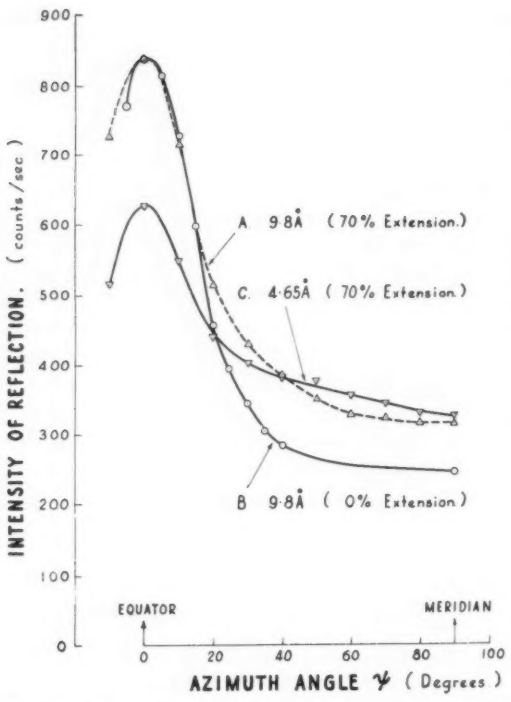

Fig. 8. Variation of azimuthal intensity of the x-ray diagrams of wool. Specimen at 0% RH (over P_2O_5). Curve A normalized to agree with the peak of Curve B at $\psi = 0°$.

corresponds to an increase in spacing of about 0.5 Å. No significant change in the spacing was observed for the 4.65 Å or 5.1 Å reflections under these conditions.

Discussion

It has been generally accepted, on the basis of photographic evidence [2, 19], that no marked changes occur in the x-ray diagram of keratin at extensions below about 20%. This result has been correlated (e.g., Peters and Woods) with the stiffening of wool fibers in the extension range 20%–30%, and it has been suggested that the first 20% extension does not involve the stretching of crystallites (which give rise to the α-pattern), but is due to chain unfolding in the less ordered regions of the fiber. The author's observation that the α–β transformation starts at very low extensions (5% or less) under practically all conditions is therefore in conflict with the photographic evidence and does not permit of a direct linking of the change in the x-ray diagram with the load–extension curve. It is, however, in line with the hypothesis [8, 9, 14] that keratin has a two-phase structure (crystalline microfibrils embedded in an amorphous matrix) because this structure would be expected to give rise to a change in the x-ray diagram even at low extensions [11].

In the above tests, some lack of correspondence is sometimes noted between the disappearing α-reflection and the appearing β-reflection. This might suggest, at first sight, that the classical picture of the α- and β-patterns arising from the same crystalline region requires revision. However, in this connection, the inherent difficulty of correlating the intensity of an x-ray reflection with the amount of the particular phase giving rise to it should be noted. It is possible, for example, that during stretching some slight disordering of a crystalline phase takes place, which could give rise to a quite disproportionate weakening of the reflections associated with this phase. Or again, as the 5.1 Å (α) reflection is composite, but not resolved in these tests, the intensities of some of the individual reflections comprising this group could vary in a manner not directly related to extension, and comparison of the total intensity with that of another reflection might be misleading. Another source of uncertainty is the weakening of the meridional reflections which occurs when the orientation of crystallites in the fiber is changed, as could happen during stretching. Despite these remarks, the simultaneous increase in both α- and β-reflections during the relaxation of stretched fibers in water may be regarded as evidence for two separate crystalline phases, although here again an explanation can be given in terms of the classical picture: stretching initially causes decrystallization, while subsequent relaxation in water causes recrystallization, partly as α- and partly as β-material.[1] Such a process would probably involve a phase intermediate between α and β, such as that postulated by Skertchley [20].

It was observed that irradiation with x-rays weakens the fibers, an effect which has previously been reported by Astbury and Woods [2] in connection with supercontraction tests on wool. The damage, which becomes apparent when only part of the fiber is irradiated and this part is used for subse-

[1] The alternative interpretation in terms of the classical picture was pointed out to the author by Mr. H. J. Woods, of the Textile Physics Laboratory, University of Leeds.

quent diffraction tests, gives rise to a pronounced change in the x-ray diagram of wool even at low extensions. This effect may cause uncertainty when the α–β transformation is followed by a photographic technique requiring long exposures.

Some reference must be made to the fact that, at a given strain up to 20% extension, the α–β transformation has proceeded further with dry than with wet fibers. This suggests that water-accessible material, which is weak when wet, is in series with the nonaccessible material. The former need become accessible only during straining, and might be identified with the X-zones in the microfibrils postulated by Feughelman and Haly [10], while the latter might be identified with the Y-zones which do not open out until the post-yield region (30% extension) is reached.

Acknowledgments

The author is indebted to Professor C. J. Milner, head of the School of Applied Physics at the University of New South Wales, Sydney, for the use of the Norelco Geiger-counter x-ray diffractometer and many other facilities extended during the investigation, and to two members of his staff, Associate Professor J. F. McConnell and Mr. A. Schwartz, for valuable discussions. During the manuscript stage critical and valuable comments were made by Mr. H. J. Woods of the Textile Physics Laboratory, University of Leeds. Thanks are also due to Mr. D. Ross, of the author's laboratory, for assistance in carrying out part of the experimental and computational work.

Literature Cited

1. Astbury, W. T. and Street, A. *Phil. Trans. Roy. Soc.* **A230**, 75 (1931).
2. Astbury, W. T. and Woods, H. J. *Phil. Trans. Roy. Soc.* **A232**, 333 (1933).
3. Astbury, W. T. and Sisson, W. A., *Proc. Roy. Soc.* **A150**, 533 (1935).
4. Astbury, W. T., *Proc. Roy. Soc.* **B141**, 1 (1953).
5. Bendit, E. G., *Nature (London)* **179**, 535 (1957).
6. Cottin, J. and Lefort, M., *J. Chim. Phys.* **53**, 267 (1956).
7. Crick, F. H. C., *Nature (London)* **170**, 882 (1952).
8. Farrant, J. L., Rees, A. L. G., and Mercer, E. H., *Nature (London)* **159**, 535 (1947).
9. Feughelman, M., Textile Research Journal **29**, 223 (1959).
10. Feughelman, M. and Haly, A. R., *Biochim. et Biophys. Acta* **32**, 596 (1959).
11. Feughelman, M. and Haly, A. R., *Kolloid Z.* (to be published).
12. Huggins, M. L., *Proc. Nat. Acad. Sci., U.S.A.* **43**, 204 (1957).
13. James, R. W., "The Crystalline State. Vol. II: The Optical Principles of the Diffraction of X-Rays," London, G. Bell and Sons Ltd., 498 (1954).
14. Jeffrey, G. M., Sikorski, J., and Woods, H. J., *Proc. Int. Wool Text. Res. Conf. Aust.* **F**, 130 (1955).
15. Klug, H. P. and Alexander, L. E. "X-Ray Diffraction Procedures for Polycrystalline and Amorphous Materials," New York, John Wiley and Sons Inc., 281 (1954).
16. Pauling, L., Corey, R. B., and Branson, H. R., *Proc. Nat. Acad. Sci. U.S.A.* **37**, 205 (1951).
17. Pauling, L. and Corey, R. B., *Proc. Nat. Acad. Sci. U.S.A.* **37**, 729 (1951).
18. Pauling, L. and Corey, R. B., *Nature (London)* **171**, 59 (1953).
19. Peters, L. and Woods, H. J., in "Mechanical Properties of Textile Fibres," edited by Meredith, Amsterdam, North-Holland Publishing Co., Chapters VIII and X (1956).
20. Skertchley, A. R. B., *Nature (London)* **181**, 639 (1958).

Manuscript received March 28, 1960.

The Log-Normal Distribution of the Diameter of Wool Fibers in Top Slivers as Studied by R. Henon and J. Ott

Franz Monfort

Peltzer et Fils, Verviers, Belgium

Abstract

The object of this article is to explain some little known work which has been done in France by Professor R. Henon and Mr. J. Ott on the log-normal distribution of the diameter of wool fibers in top sliver. A critical examination is made of the American Society for Testing Materials (ASTM) and the Agricultural Marketing Service (AMS) classifications.

Introduction

Professor R. Henon of the Statistical Institute of Paris and Mr. J. Ott have presented to the Technical Committee of the International Wool Federation several extremely original contributions which together comprise a study of the distribution of the diameter of fibers in a wool top sliver, and these studies [1–6] have covered the following topics:

1. The log-normal distribution of fiber diameter.
2. An examination of the ASTM classification.
3. A study of the natural regression of mean fiber diameter and its standard deviation.
4. An examination of the AMS classification.
5. A nomogram for the classification of wool tops.

It is our opinion that this work has not become sufficiently well known; the present paper presents a summary of it. Further details and discussion are available [7].

Log-Normal Distributions in General

If Y is any variable which is said to be distributed according to a log-normal law, then we understand that the natural logarithm, ln Y, is normally distributed. If we use the notation ln b and c to indicate respectively the average and the standard deviation of ln Y, we can show that

$$\bar{Y} = b \exp (c^2/2) \tag{1}$$

$$CV^2 (Y) = \exp (c^2) - 1 \tag{2}$$

From this we can deduce the values of the parameters b and c, from the mean and the coefficient of variation (CV) of Y thus:

$$b = \bar{Y} / \sqrt{1 + CV^2(Y)} \tag{3}$$

$$c = \sqrt{\ln [1 + CV^2(Y)]} \tag{4}$$

The Log-Normal Distribution of the Diameters of Wool Fibers in Combed Tops

R. Henon has shown that in general the diameter distribution of the fibers in a top can be represented as a log-normal distribution with two parameters; i.e., the log of the median of the diameters and the standard deviation of the logarithms of the diameters [1]. The measurements of fiber diameter used by R. Henon were carried out using the projection microscope method approved by the I.W.T.O.; it will be recalled that this gives a length-biased result. The corresponding graphic adjustments carried out on log-probability paper led to an excellent fit, especially with Merino wool. The chi-square test applied to the different cases examined showed that the hypothesis of a normal distribution was not acceptable from the point of view of significance, whereas the assumption of a log-normal distribution could be accepted.

For cross-bred wool types of approximate mean diameter 30μ, the graphs showed a tendency to diverge from the straight line form into the shape of an open V.

Ordinary fiber diameter measurement leads directly to the calculation of the mean $\bar{d}$ and to the coefficient of variation of diameter $CV(d)$; from Formulas 3 and 4 we can calculate the parameters

ln b and c for the normal distribution in the form

$$b = \bar{d} / \sqrt{1 + CV^2(d)} \quad (5)$$

$$c = \sqrt{\ln [1 + CV^2(d)]} \quad (6)$$

and taking into account the convergent series involved, for a coefficient of variation falling between 0.18 and 0.30, this can be written more simply as

$$c \simeq CV\,(d) \quad (7)$$

$$b \simeq \bar{d} \left[1 - \frac{CV^2(d)}{2} \right] \quad (8)$$

If, therefore, we have available an ordinary estimation of the diameter of a wool top, and thus know $\bar{d}$ and $CV(d)$, we can very easily calculate the two parameters b and c of the log-normal distribution.

For example, if $\bar{d} = 20.50\mu$ and $CV(d) = 0.251$ (25.1%), Formulas 5 and 6 will give $b = 19.88\mu$ and $c = 0.247$.

On the other hand, the approximate Formulas 7 and 8 will give $c = 0.251$ and $b = 19.85\mu$.

An Examination of the American Classification for the Fineness of Tops

ASTM Classification

The ASTM Classification (described on page 449 of the 1951 edition and reproduced in Table I) makes use of 13 classes between 80's (18.8μ) and 36's (40μ). For each of these classes, the specification imposes two limits for the mean diameter, two minimum values for the percentages of fibers falling between two named pairs of limits, and two maxi-

TABLE I. Requirements for Wool Tops *

Grade	80's	70's	64's	62's	60's	58's	56's	50's	48's	46's	44's	40's	36's
Fineness range, μ													
Min.	18.1	19.6	21.1	22.6	24.1	25.6	27.1	29.1	31.6	33.3	34.8	36.6	38.8
Max.	19.5	21.0	22.5	24.0	25.5	27.0	29.0	31.5	33.2	34.7	36.5	38.7	41.3
Fibers, percent													
10–20 μ incl., min.	60	50	36	27	18	16	9	4					
10–25 μ incl., min.	92	84											
10–30 μ incl., min.			94	88	83	74	64	45	34	26	22	16	12
10–40 μ incl., min.									77	70	63	55	44
25.1–30 μ incl., max.	8												
25.1–40 μ incl., max.		16											
30.1–40 μ incl., max.	0.25 (0.5)†	2	6	12	17								
30.1–50 μ incl., max.						26	36	55					
40.1–50 μ incl., max.		0.25 (0.5)	0.33 (1)	0.50 (1)	0.50 (1)	2	5	10					
40.1–70 μ incl., max.									23	30	37	45	56
50.1 and over μ, max.						0.75 (1.5)	1 (2)	1.25 (2.5)					
60.1–80 μ incl., max.									2	2	3	4	4
Min. no. of fibers required for test, per sample	400	400	600	600	800	800	1000	1000	1600	1600	1600	1600	1600

* The requirements for grades 80's to 50's incl. conform to the U. S. Government Requirements for Wool Tops promulgated January 1, 1940.

† Numbers in parentheses represent maximum percentage of fibers of that range permissible in substandard grades.

mum values for the percentages falling between two other limits. Altogether, therefore, six conditions are imposed. These limitations on the frequencies can be thought of as representing a somewhat special way of describing the dispersion of the diameters. The analysis of a batch of wool is carried out using the projection microscope, though the method used differs slightly from that used by the I.W.T.O., and the number of fibers to be measured is also indicated in Table I.

Example. For the 64's class the mean diameter of a wool top is allowed to vary from 21.0 to 22.5μ. A minimum of 36% of its fibers must fall between 10 and 20μ, a minimum of 94% between 10 and 30μ, a maximum of 6% between 30 and 40μ, and a maximum of 0.33% between 40 and 50μ. All these conditions refer to a sample with a minimum of 600 fibers. It may be noted that these limitations on the proportions comprise two *minimum* limitations (36 and 94%) and two *maximum* limitations (6% and 0.33%); we shall return to this distinction below.

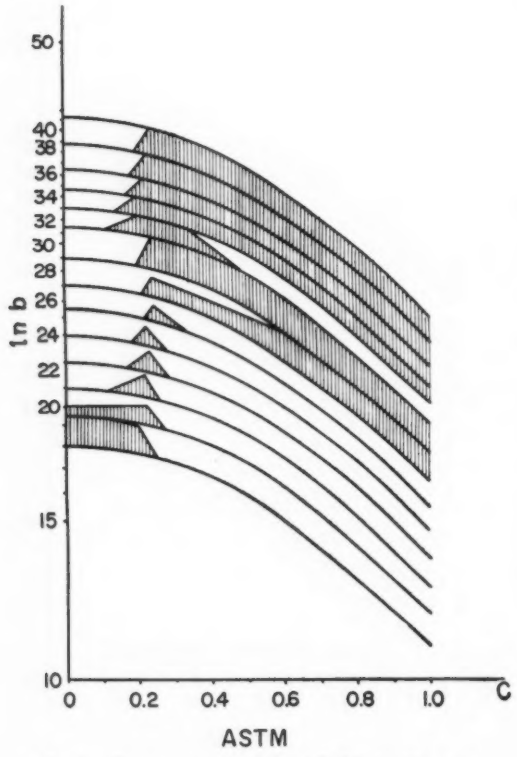

Fig. 1. Representation of the ASTM classifications on the (c, ln b) diagram.

In order to reveal clearly the arbitrary and discontinuous nature of the ASTM classification, Henon plotted the classification conditions used in it in the form of a diagram using special coordinates.

He makes use of two hypotheses:

1. that the distribution of diameter is log-normal and
2. that every class limit also corresponds to a log-normal distribution of diameter.

We must now consider the form taken in this Henon diagram by the various ASTM limits.

The Two Limits on Fiber Mean Diameter

We can rewrite Expression 1 in the form

$$\bar{d} = b \exp (c^2/2) \tag{9}$$

or again

$$\ln b = \ln \bar{d} - \frac{c^2}{2} \tag{10}$$

This equation relates the parameters $\bar{d}$, b, c, of any given distribution, arising, for example, from the diameter analysis of a lot of wool. Thus every such distribution is represented on the (c, ln b) diagram by a point. But if we suppose $\bar{d}$ to be fixed, we can then imagine a whole series of distributions with this particular value of the mean $\bar{d}$ but with differing values for their standard deviations, and there will correspond to them a series of values for c and for ln b. The location of the corresponding points in the (c, ln b) diagram will be a parabola represented by Equation 10 relating ln b and c to a fixed value of $\bar{d}$.

The limits on the mean diameter for each ASTM class will correspond to two extreme values of $\bar{d}$, which may be represented in the (c, ln b) diagram by the region contained between the two parabolas corresponding to the two values of $\bar{d}$. The different parabolas may be interconverted by a vertical displacement. We thus arrive at the 13 contiguous areas represented in Figure 1.

The Two Minimum Fiber Percentage Limits

The two imposed minimum limits on fiber percentages mark out a still narrower region within the band already permitted by the limitations on the mean fiber diameter for any class.

Representation on the ($ln\, b, z$) *diagram.* Let us first of all reconsider the diagram in which ln d is plotted as abscissa and z as ordinate, z being the standardized variable. Then every distribution of

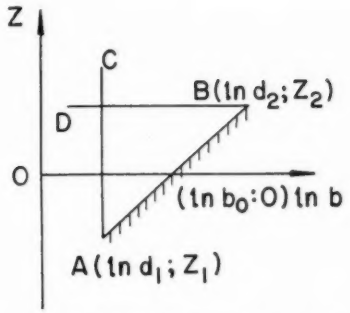

Fig. 2. Plot of minimum percentage limitations on the (ln b, z) diagram.

diameter y is represented on it as a straight line (as a result of Henon's first hypothesis) and in each ASTM class, for every limit of fiber percentage, there corresponds a point on the (ln d, z) diagram. For example, for the 64's class the first limitation on minimum fiber percentage is that, for all lots of wool falling within this class, the proportion of fibers with diameters between 10 and 20μ shall be not less than 36%. In fact, the limits could have been fixed at 0–20μ since in practice no fibers are found in wool tops with diameters below 10μ. Thus if we use the distribution function in the form

$$F(z_1) = 0.36 \quad \text{and} \quad z_1 = \frac{\ln 20 - \ln \bar{d}}{c}$$

we can obtain a value from the normal tables $z_1 = -0.3585$. The coordinates of the point which we are therefore looking for are $\ln d_1 = \ln 20$ and $z_1 = -0.3585$.

By applying the arguments enunciated above, we see that the distribution line must lie above the point (ln 20, -0.3585), which we have just obtained, or in the limiting case must pass through it. For, if the line passed *below* this point we would have for the value ln 20 an ordinate of $z < z_1$, and in consequence the distribution would contain less than 36% of the fibers between 0 and 20μ.

Another point (ln d_2, z_2) on the diagram will correspond to the second limitation on minimum fiber percentage. For example, in the 64's class the second limitation is that such wools must have at least 94% of their fibers between 10 (or 0) and 30μ. Just as before, we can now find a corresponding value for z_2 by imposing the condition $F(z_2) = 0.94$ from which the tables give us $z_2 = +1.5548$. The second point which we are looking for has as its coordinates (ln 30, $+1.5548$). As before, the distribution line must again fall above this point in the diagram or in the limiting case pass through it. If we now combine together these two conditions on the percentage minima for each class we see that the distribution line must fall above the limiting line which passes through the two points (ln d_1, z_1) and (ln d_2, z_2) or coincides with this line.

The equation for the limiting lines may be written

$$z = \frac{z_2 - z_1}{\ln d_2 - \ln d_1} (\ln b - \ln d_1) + z_1 \qquad (11)$$

This line may be defined by its slope $\left(\frac{1}{\alpha}\right)$

$$\frac{1}{\alpha} = \frac{z_2 - z_1}{\ln d_2 - \ln d_1} \qquad (12)$$

and by its point of intersection with the ln b axis (ln b_0, 0) (we shall discuss the importance of $1/\alpha$ below).

The abscissa of this point, which is the logarithm of the value of the maximum median, may be written

$$\ln b_0 = \frac{z_2 \ln d_1 - z_1 \ln d_2}{z_2 - z_1} \qquad (13)$$

Thus, for the 64's class we have

$$d_1 = 20\mu \qquad F(z_1) = 0.36 \qquad z_1 = -0.3585$$
$$d_2 = 30\mu \qquad F(z_2) = 0.94 \qquad z_2 = +1.5548$$
$$\ln b_0 = 3.0718 \qquad b_0 = 21.58\mu \qquad \frac{1}{\alpha} = 4.7188$$

To summarize, we may say that for every ASTM class the two conditions of a minimum fiber percentage are represented in the (ln d, z) diagram (Figure 2) by a section of a limiting straight line between two given points (ln d_1, z_1) and (ln d_2, z_2). This limiting line may be defined by its slope $1/\alpha$ and its intercept on the ln d axis (ln b_0, 0). The straight line corresponding to any wool falling within the class must be above this limiting line.

The slope $1/c$ of a straight line

$$z = \frac{\ln d}{c} - \frac{\ln b}{c} \qquad (14)$$

which represents a distribution of diameter, cannot be negative. All the distributions which satisfy the two minimum fiber percentage requirements of an ASTM class can be theoretically divided into two sub-groups by considering the slope $1/\alpha$ of the limiting line. These are:

(a) a sub-group I for which

$$\frac{1}{\alpha} \leqslant \frac{1}{c} < \infty$$

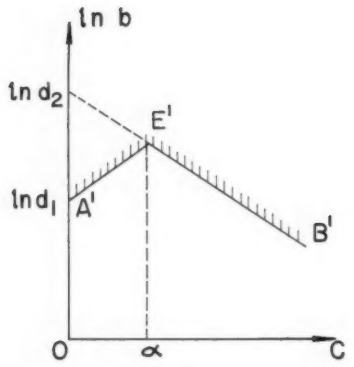

Fig. 3. Plot of minimum percentage limitations on the (c, ln b) diagram.

In Figure 2 this corresponds first of all to the group of straight lines which pass through the point A ($\ln d_1, z_1$) and are contained within the angle BAC; they have the general equation

$$z = \ln d + \left(\frac{z_1}{\beta} - \frac{\ln d_1}{\beta} \right) \qquad (15)$$

and second to the group of straight lines to the left of and parallel to the proceeding ones; their median is less than the value $\ln b = \ln d_1 - \beta z_1$ and

(b) a sub-group II for which

$$0 \leqslant \frac{1}{c} < \frac{1}{\alpha}$$

In Figure 2 this corresponds first to a group of straight lines passing through the point B ($\ln d_2, z_2$) and contained within the angle DBA. They have the general equation

$$z = \frac{\ln d}{\beta} + \left(z_2 - \frac{\ln d_2}{\beta} \right) \qquad (16)$$

and to the group of lines to the left of and parallel to the proceeding ones, for which the median has a value less than $\ln b = \ln d_2 - \beta z_2$.

Representation on the (c, ln b) diagram. So far the frequency limitations have been represented on the ($\ln b, z$) diagram, as in Figure 2. They must now be plotted on the (c, ln b) diagram, just as we have already done for the limitations on mean fiber diameter, in order to bring together on one diagram the whole of the conditions imposed for a particular class.

Corresponding to the limiting line for a class in the ($\ln b, z$) diagram which is defined as passing through the point ($\ln b$, 0) and having a slope $1/\alpha$, we have in the (c, ln b) diagram the point (α, $\ln b_0$).

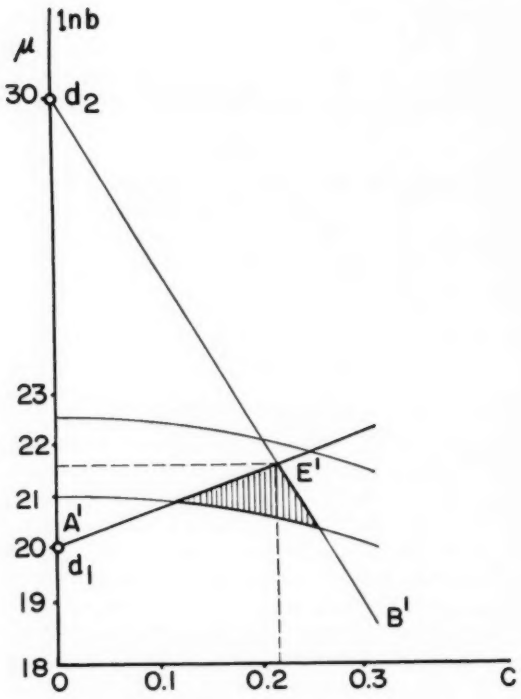

Fig. 4. Representation of the ASTM 64's class on the (c, ln b) diagram.

Similarly, for sub-group I of the distribution defined above we have in the (c, ln b) diagram a limiting straight line passing through the points (0, $\ln d_1$) and (α, $\ln b_0$). In fact a comparison of Equations 13 and 14 gives us the following interrelationship:

$$\beta = c \qquad (17)$$

and

$$\ln b = -cz_1 + \ln d_1 \qquad (18)$$

This last equation represents a linear relationship between c and ln b. Corresponding to it in the (c, ln b) diagram is the straight line A′E′ (Figure 3), which is the trace of the points corresponding to the straight lines of the first group of the subgroup I passing through the point A ($\ln d_1, z_1$) in Figure 2. The points representing the straight lines of the second group will be easily seen to fall below A′E′. In the same way, the sub-group II corresponds to the points of the straight line E′B′ passing through the points (0, $\ln d_2$) and (α, $\ln b_0$) and also to the points falling below this straight line.

To sum up, for every ASTM class, the two limitations on minimum fiber percentages are satisfied in the $(c, \ln b)$ diagram by the area under the two lines passing through the points:

$$[(0, \ln d_1) \text{ and } (\alpha, \ln b_0)]$$

and

$$[(\alpha, \ln b_0) \text{ and } (0, \ln d_2)]$$

The region limited by these two straight lines and by the two axes therefore represents the zone which is permissible for a class; every point within it corresponds to one distribution of the class in question (Figure 3).

The Two Limitations on Frequency Maxima

For every ASTM class there are also two limits on maximum fiber percentages. But it can be immediately seen that such conditions are superfluous. Examples of such limitations for the 64's class are the 6% maximum between 30 and 40μ and the 0.33% maximum for 40–50μ.

The Complete Representation of the ASTM Classes and Conclusions

To every ASTM class there corresponds an area which simultaneously satisfies the limitations both of the means and the frequencies. Thus, Figure 4 shows the area which is appropriate for the 64's class, while Figure 1 represents the whole of the 13 ASTM classes.

In Table II are given the various parameters which could be used to redraw Figure 1. Thus, the coordinates (α, b_0) of the point E′ (see Figure 3) are calculated according to Formulas 12 and 13. The intersections of the straight lines A′E′ with the upper and lower parabolas have been calculated from Equations 11 and 12 and those for E′F′ in an exactly analogous manner. Of course, in every case, the data d_1, d_2, z_1, z_2 can be obtained from Table I.

Figure 1 makes quite clear the discontinuous character and, in consequence, the very arbitrary nature of the ASTM classification. In fact, we have already seen that every point in the $(c, \ln b)$ diagram corresponds to a possible distribution of diameter and therefore to a possible batch of wool. Thus in Figure 1 the permitted regions are shaded while the forbidden regions are shown unshaded. Incidentally, we may point out that Figure 1 differs very slightly from the corresponding cited figure [1] as a consequence of a revision of the calculations.

The natural distribution of wool fiber diameter as determined, for example, by the condition of growth on the sheep, is continuous; this is what would have been expected; moreover, it has been experimentally confirmed in further study (see below). Clearly, this does not mean, however, that for any point taken at random in the $(c, \ln b)$ diagram there will necessarily correspond an actual sample of top, since it is quite possible that, in fact, nature does not produce this particular kind of wool.

TABLE II. General Results for the ASTM Classification

	Intersection points of straight lines A′E′ and E′F′		Intersection of the straight line A′E′ with the				Intersection of the straight line E′F′ with the			
			Lower parabola		Upper parabola		Lower parabola		Upper parabola	
Classes	α	b_0	c^*	b^*	c^*	b^*	c^*	b^*	c^*	b^*
80's	0.1938	19.04			0.137	19.32	0.257	17.42		
70	0.2244	20.00					0.293	18.68		
64	0.2120	21.58	0.1170	20.86			0.250	20.34		
62	0.2268	22.98	0.169	22.18			0.278	21.64		
60	0.2169	24.39	0.182	23.63			0.273	23.12		
58	0.2476	25.58	0.219	24.87			0.345	24.03		
56	0.2386	27.54	0.208	26.43			0.606	24.14		
50	0.2495	30.96	0.242	30.55	0.200	28.39				
48	0.2499	33.26	0.105	31.33	0.198	32.55	0.474	48.15	0.323	31.19
46	0.2464	35.15	0.142	32.87	0.197	34.05				
44	0.2606	36.69	0.170	34.21	0.225	35.69				
40	0.2568	38.73	0.183	35.99	0.229	37.67				
36	0.2809	41.73	0.199	37.90	0.246	40.06				

$c^* = z_1 \pm \sqrt{z_1^2 - 2 \ln (d_1/d)}$ $\quad d_{upper}$: z_1 and d_1

$\text{Log } b^* = -c^* z_1 + \ln d_1$ $\quad d_{lower}$: z_2 and d_2.

On Figure 1 we have also included the limits on the values of c, i.e., 0.188 and 0.284, for the natural continuous distribution of diameter discussed below. We should not expect to encounter tops which fall outside the band enclosed by the dotted lines in the $(c, \ln b)$ diagram. The very curious arrangement of the ASTM classes therefore appears in direct contradiction to the natural distribution of wool fiber diameters.

The Continuous Regression between Mean Diameter and Standard Deviation

Natural Regression

In order to verify whether or not a natural continuous regression existed $(\bar{d}, s_d)$, Henon and Ott have examined over a considerable period of time the results of diameter measurements on some 5,855 wool tops coming from all kinds of sources and divided between countries as follows: Germany 9%, England 17%, Belgium 8%, Spain 3%, France 23%, Holland 4%, Italy 33%, and U.S.A. 2%; these tops were all provided by members of the I.W.T.O. Technical Committee and were measured according to the I.W.T.O. method.

The results of these measurements were recorded in the form of mean diameter $\bar{d}$ and the standard deviation s_d (N.B.: s_d is used and not c). The plotting on a graph of these pairs of points (d, s_d) amounting to almost 6,000 results produced a cloud of points indicating a curvilinear regression, but without any gaps or discontinuity at all. Some idea of the nature of this figure can be seen in Reference 8, Figure 1, and Reference 7, page 191, though these illustrations include only 1,333 samples. We can therefore say that nature produces a complete selection of wools which we here encounter in the form of top slivers, for which the mean diameter varies between 17 and 38μ in a continuous manner, and with a steady progressive increase in the mean standard deviation from 3.9 to 10μ.

Regression Equation

The regression equation deduced from the analysis of 5,855 tops [8] may be written as

$$(s_d)^{\frac{1}{2}} = 1.275\bar{d} - 16.05 \qquad (19)$$

where $\bar{d}$ and s_d are in microns.

The expected value for the regression deviation is 0.55μ.

Table IV (from [8]) summarizes these results for 5,855 tops. The first column there shows the selected classes (except for the last class, they are 1.5μ wide). The second column shows the number of measurements made on the tops available for each class; the third, the mean diameters calculated from the measured means; the fourth, the average standard deviations calculated from the measurements; the fifth, the standard deviations calculated from the regression Equation 19; and the sixth, the deviations (in microns) between the values in the fourth and fifth columns. The agreement is, in fact, excellent except in those extreme classes where the amount of experimental material available was too small.

The regression curve, which is rather flat, can be transformed into a straight line by a change of variable

$$Y = (s_d)^{\frac{1}{2}} \qquad (20)$$

TABLE III. AMS Classification

Class	80's	70's	64's	62's	60's	58's	56's	54's	50's	48's	46's	44's	40's	36's
Class limits, μ	18.1 19.5	19.6 21.0	21.1 22.5	22.6 24.0	24.1 25.5	25.6 27.0	27.1 28.5	28.6 30.0	30.1 31.7	31.8 33.4	33.5 35.1	35.2 37.0	37.1 38.9	39.0 41.2
Fiber diameters	Percentage fibers of diameter shown in left-hand column													
10.0–25 μ incl.	≥91	≥83												
10.0–30 μ incl.			≥92	≥86	≥80	≥72	≥62	≥54	≥44					
10.0–40 μ incl.										≥75	≥68	≥62	≥54	≥44
Above 25.1 μ	<9	<17												
Above 30.1 μ	<1	<3	<8	<14	<20	<28	<38	<46	<56					
Above 40.1 μ			<1	<1	<2					<25	<32	<38	<46	<56
Above 50.1 μ						<1	<1	<2	<2					
Above 60.1 μ										<1	<1	<2	<3	<4
Minimum number of fibers to be examined	400		600		800			1000				1600		

Figure 5 shows this transformation for the 50% line and also indicates the dispersion interval, taking into account the expected value for the regression deviation.

It may be asked why the authors have used the power $\frac{3}{2}$ in Equation 19, and some explanation should perhaps be given. In fact, in his original communication Henon [1] sought to explain the dependence between the parameters by advancing certain theories relating to the formation of the fibers. One of these (which was not acceptable to the I.W.T.O. Technical Committee, however) supposed that the increasing diameters of a wool fiber behave as though they were constituted of successive layers of relatively constant and independent thickness. This is the same as saying that the variable $\Delta d/d$ follows a normal law and that d follows a log-normal law. As a consequence, if we go from a mean diameter d_0 for a batch of wool to a diameter $d_k = k\,d_0$ for one fiber, the relation between the standard deviations s_0 and s_k, corresponding respectively to d_0 and d_k for the log-normal law, can be written

$$s_k = s_0\sqrt{k} \tag{21}$$

In the original untransformed distribution, we obtained as a general expression of standard deviation (σ_k)

$$\sigma_k = s_k d_k = s_0\sqrt{\frac{d_k}{d_0}}\,d_k = \frac{s_0}{\sqrt{d_0}}\,(d_k)^{\frac{3}{2}} \tag{22}$$

The standard deviation will thus be equal to the product of the constant and the diameter raised to the power $\frac{3}{2}$. Henon, in fact, continued to employ this notion, and the more thorough examination of the correlation $(\bar{d}, \sigma_d)$ shows that this particular form of Equation 19 is very appropriate. Reference 7, page 195–196, also refers to the earlier work of Huberty on this regression $(\bar{d}, s_d)$.

Classification of Tops, Nomogram by Ott

By using the expected value for the regression deviation we can draw on the $(\bar{d}, Y)$ diagram (Figure 5) the straight lines:

$$s_d = (1.275\bar{d} - 16.05)^{\frac{1}{2}} \pm 0.55\,n \quad n = 1,2,3 \tag{23}$$

By using the normal distribution tables we can then calculate for each of these lines the mean proportion of tops which will have a standard deviation equal to or smaller than $(\bar{d} \pm 0.55\,n)$. Thus, for example, 84.1% of tops will have a standard deviation of diameter which is less than or equal to $(\bar{d} + 0.55)$.

Figure 5 thus permits the classification of tops on a basis of a knowledge of mean diameter and

TABLE IV. Results of Measurements on 5855 Samples of Tops Supplied by 14 Laboratories

Diameter class	n	$\bar{x}$	$\bar{y}$	σ_y^2	y	$y - \bar{y}$	
15.0/16.5	6	16.06	3.48	0.15	2.70	−0.78	
16.5/18.0	62	17.53	3.83	0.17	3.41	−0.42	
18.0/19.5	754	18.94	4.26	0.15	4.03	−0.23	
19.5/21.0	1664	20.23	4.56	0.21	4.56	0.00	
							$\Sigma(y - \bar{y})$ positive = 1.75
21.0/22.5	1080	21.67	4.99	0.27	5.12	+0.13	
22.5/24.0	596	23.19	5.58	0.45	5.69	+0.11	
24.0/25.5	437	24.69	6.22	0.32	6.20	−0.02	$\Sigma(y - \bar{y})$ negative = −1.79
25.5/27.0	275	26.20	6.73	0.29	6.70	−0.03	
27.0/28.5	271	27.69	7.26	0.32	7.18	−0.08	
28.5/30.0	219	29.16	7.74	0.31	7.64	−0.10	
30.0/31.5	185	30.76	8.22	0.31	8.13	−0.09	
31.5/33.0	158	32.19	8.59	0.29	8.55	−0.04	$\frac{\Sigma(y - \bar{y})}{13} = 0.1$
33.0/34.5	82	33.63	8.96	0.28	8.96	0.00	
34.5/36.0	36	35.16	9.24	0.27	9.39	+0.15	n = number of samples
36.0/37.5	24	36.62	9.46	0.29	9.79	+0.35	$\bar{x}$ = mean diameter
37.5/39.0	5	38.11	9.48	0.64	10.19	+0.71	$\bar{y}$ = standard deviation
39.0/41.0	1	40.63	10.55		10.85	+0.30	σy^2 = variance
							$y = (1.275 \times -16.05)^{\frac{1}{2}}$
	5855						

standard deviation, without involving any recourse whatever to the conventional or arbitrary top classifications. Every top is represented by a point whose coordinates are $\bar{d}$ and $Y = (s_d)^{\frac{1}{2}}$.

The location of a point on this diagram allows us to judge of the homogeneity of diameter of the corresponding top when compared with the bulk of tops of the same mean diameter. It can be very easily shown that it is simpler to use standard deviations instead of coefficients of variation in such graphs.

Thus Ott [8] has devised a nomogram which can be employed for the classification of tops according to their fineness. This nomogram is reproduced in Figure 6; its shape is not quite what is expected by the experts in the wool trade. The mean diameters are plotted as linear abscissas in microns and the ordinates are graduated according to the scale $F(z)$ or $F(n)$ in percent.

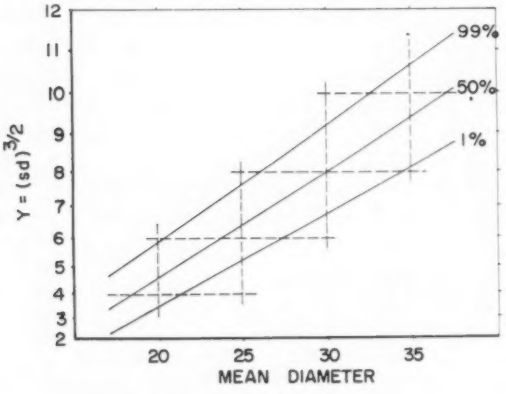

Fig. 5. The $Y = (s_d)^{\frac{1}{2}}$ transformation.

The nomogram also carries a network of curves corresponding to constant values of s_d. The locus of these curves has been calculated point by point using the methods described above. We can, for example, calculate the ordinate for the curve $s_d = 5\mu$ for $\bar{d} = 23\mu$ by applying Equation 23 as follows:

$$5 = [(1.275 \times 23) - 16.05]^{\frac{1}{2}} \pm 0.55\, n$$

from which

$$n = -1.11 \quad F(n) = 13.35\%$$

from which the ordinate we want is 13.4%. What then, is the value of such a diagram?

Suppose we have measured the mean diameter of a wool and obtained $\bar{d} = 22.6\mu$ and standard deviation 5.6μ. If we compare this data with the nomogram we obtain an ordinate corresponding to 60%. The result can therefore be interpreted as follows: among all tops having the same diameter 22.6μ there will on the average be 60% which will have a standard deviation smaller than 5.6μ so there will be 40% which have a higher standard deviation or, as Ott puts it, such a top will be 60th out of a class of 100.

Evidently, this is not a method of judging tops which is very commonly employed by wool experts, and probably it is not one to be recommended. Remembering our own school results, we recall that to be 60th out of a class of 100 was not a very brilliant result. On the other hand, a standard deviation of 5.6μ for a mean diameter of 22.6μ is quite a good result. In fact, according to the nomogram in Figure 6, 22.6μ tops will on the average have a standard deviation of 5.5μ. The top which we are discussing therefore falls into the

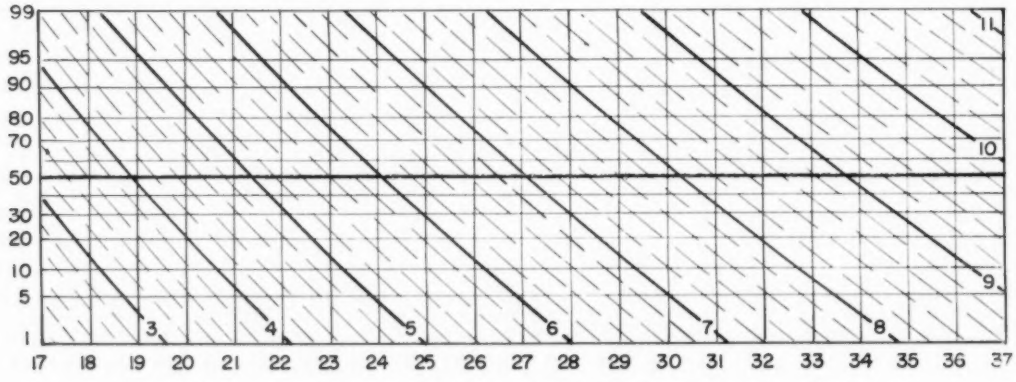

Fig. 6. Ott's nomogram for the classification of tops. Horizontal axis: mean diameter, μ; vertical axis: $F(y)$; diagonal curves: s_d, μ.

group which is 0–10% *above* the average and cannot therefore be truly designated as being heterogeneous. We must, in fact, not forget that the *average* top is in fact the *most probable* top.

The curves for constant standard deviation in the nomogram are rather flat and no great error will therefore be committed if they are treated as straight lines making use of the normal distribution law. We can then fix a probability level, for example, considering as acceptable the 60% of tops which fall around the mean, i.e., in an interval of -30% to $+30\%$. Those from -30% to -45% can be designated as very homogeneous, those from $+30\%$ to $+45\%$ as rather heterogeneous. Below -45% could be considered as exceptionally homogeneous, and those above $+45\%$ as very heterogeneous.

This classification would be indicated on the graph by horizontal lines separating the zones. What we have just suggested is, of course, put forward only as an example. It is very probable that such zones would never be fixed officially and every top-maker would draw the limits according to his own commercial experience. It is, however, quite certain that the employment of such a nomogram would allow a top maker to make a very good estimate of the relative heterogeneity in fineness of any given wool top by comparing it with the collection of standard deviations coming from all other tops of the same mean diameter. For research purposes, of course, the value of Ott's nomogram is obvious. Other details of such classification of tops are dealt with elsewhere [8, 9], in particular concerning the risk of a misclassification.

The New AMS Classification

In January 1954 the Agricultural Marketing Service of Washington published a new classification of tops which came into use as of January 1955 and which will be designated in what follows as the AMS classification.

Table III shows the new specification. In it there are 14 classes; 8 of them are 1.5μ wide (18–30μ), 3 are 1.7μ wide (30–35.1μ), 2 are 1.9μ wide (35.1–38.9μ), and 1 is of 2.3μ width (38.9–41.2μ).

The differences between the AMS classification and that described previously as the ASTM can be indicated briefly as follows:

1. There are 14 instead of 13 classes.
2. The class interval increases from one group of classes to another.
3. The interval for the 54's class is better established.
4. The conditions for maximum frequencies are applied above a certain limit and not at intervals.
5. Three limiting conditions on the frequencies and two minimum limitations are used, as before.

This new classification has also been examined by Henon [4]. He points out that the AMS classification can be subjected to the same criticisms as have already been used for the ASTM. In order to put the matter very briefly he indicated that he would describe these new criticisms by a new method which leads us to suppose that both the theories and the reasoning which have been used in examining the ASTM classification can once again be applied.

The new method consists of

a. calculation for each class of the slope $1/\alpha$ of the limiting straight line,
b. calculation of α,
c. consideration of α (which is a value $c \simeq CV_d$) as the maximum of CV_d, and
d. deducing the maximum value for the standard deviation s, according to the relation $s_{max} = \alpha \bar{d}_{sup}$.

The values of s_{max} are calculated and comprise a diagram in the form of a staircase $(\bar{d}, s)$. Every AMS class is represented there by a rectangle of which the base is the permitted interval for the mean and the height is the value of s_{max}.

The scale used for the abscissas is linear but that for the ordinates is defined by the change of variable $Y = s^{\frac{1}{2}}$ in order to be able to use the results from the natural regression. This staircase-like diagram reveals that the AMS classification is also discontinuous and this, once again, is in contradiction to the continuous natural regression of $(\bar{d}, s)$.

It is, however, possible to examine the AMS classification by use of the same arguments used in the examination of the ASTM classification. In this way, we avoid the necessity for supposing that α is a maximum value of c (Figure 3) and for considering the standard deviation as being constant between the limits of the upper and lower class (mean diameter).

Thus, following exactly the same method of calculation and in particular using the formulas shown in Table I as well as the analogous expressions, we

TABLE V. General Results of the AMS Classification

Classes	Intersection points of straight lines A′E′ and E′F′		Intersection of the straight line A′E′ with the Lower parabola		Intersection of the straight line A′E′ with the Upper parabola		Intersection of the straight line E′F′ with the Lower parabola		Intersection of the straight line E′F′ with the Upper parabola	
80's	0.1851	19.51	—	—	—	—	0.231	17.54	0.193	19.15
70	0.1968	20.72	—	—	—	—	0.245	18.93	0.199	20.63
64	0.3123	19.34	0.282	20.18	0.222	21.95	—	—	—	—
62	0.2309	23.37	—	—	0.231	23.37	0.262	21.75	0.231	23.37
60	0.2373	24.57	—	—	0.223	24.88	0.266	23.16	0.233	24.79
58	0.2930	25.30	—	—	0.224	26.33	0.310	24.31	—	—
56	0.2528	27.77	—	—	—	—	0.281	26.01	0.255	27.63
54	0.2615	29.22	—	—	0.— / 0.201	30.— / 29.40	0.295	27.21	0.266	28.96
50	0.2317	31.07	0.—	30.—	0.214	30.98	0.266	28.95	0.236	30.80
48	0.2455	33.90	—	—	—	—	0.292	30.42	0.267	32.24
46	0.2182	36.12	—	—	—	—	0.267	32.24	0.243	34.09
44	0.2319	37.26	—	—	—	—	0.281	33.69	0.251	35.83
40	0.2277	39.01	—	—	—	—	0.278	35.57	0.247	37.70
36	0.2132	41.31	—	—	0.135	40.83	0.268	37.53	0.230	40.11

TABLE VI. Calculation of s_{max} in $\mathfrak{y}$ for AMS Classification

Classes	$\alpha\bar{d}_{exp.}$	Straight line A′E′ and Lower parabola	Straight line A′E′ and Upper parabola	Straight line E′F′ and Lower parabola	Straight line E′F′ and Upper parabola
80	3.61			4.05	3.70
70	4.13			4.64	4.11
64	7.03	5.69	4.87		
62	5.54			5.70	5.40
60	6.05		5.54	6.16	
58	7.91		5.85	7.54	
56	7.20			7.31	7.05
54	7.85		5.90	8.03	7.70
50	7.34		6.62	7.70	7.27
48	8.20			8.88	8.61
46	7.66			8.61	8.28
44	8.58			9.47	8.99
40	8.86			9.89	9.31
36	8.78			10.06	9.23

have determined the permitted zones in the AMS classification and indicated them on the ($\ln b$, c) diagram. The numerical results have been included in Columns 4–11 of Table V, and the graphic results are shown in Figure 7.

The introduction of the AMS classification has produced some rather astonishing changes (with the exception of the 80's class). This change may be seen by comparing Figure 1 with Figure 7. Apparently, the AMS classification is much more continuous than the ASTM one. Only for the 50's class do we have one continuous solution between 48's and 50's and another (very short) between 54's and 50's. But this general continuity arises only in the region $c < 0.2$, i.e., outside the range of ordinary tops. The discontinuity reappears in the region $0.188 < c < 0.284$.

The modifications in Figure 7 as compared with Figure 1 are due in large part to the high values for d_2 given in the AMS classification. In consequence the angle A′E′F′ nearly always has its summit above the upper parabola and in the greater proportion of cases only the intersections of the parabolas with the straight line E′F′ have to be considered (see Table V). A curious exception is that of the 64's class, where the angle A′E′F′ has its apex depressed below the lower parabola. These geometric details can be very well appreciated from the graph and also from the discussion of the coordinates of the points of intersection given in Table V.

In order to determine the values of s_{max} for each class by use of the graphic method it is necessary to examine the various possible values of s_{max} which are given by the points of intersection by the straight line A′E′ or E′F′ with the limiting parabolas (see Table VI). The values are given in Figure 7. The greater part of the classes is situated within the acceptance interval 1–50% of the natural regression; this is a little unrealistic. Only the classes 58's and 64's are better distributed, while the 64's class is probably too big. If we take account of all the values given in Columns 3–6 of

Table VI the steps of the staircase are seen to lean from the left towards the right. This result is clearly in contradiction with the ideas already deduced from the study of the natural regression, where in general the standard deviation of the diameter increases as the mean increases. This result could also be deduced by examining Figure 7.

Briefly, then, we may say that the AMS classification represents a considerable improvement compared with the ASTM, but it is in no way a step towards a more rational classification.

Conclusion

The work of Henon and Ott suggests that we should abandon the old commercial European classifications such as those of Bradford, Roubaix, Germany, etc.—classifications which are, moreover, often very different from one another. The American classifications given by the ASTM and the AMS are equally subject to doubt.

The rational classification of any batch of wool should be based on the examination of the position of the point $(\bar{d}, s_d)$ on the Ott nomogram or the position of the point $(\bar{d}Y = s_d^{\frac{1}{3}})$ in the $(\bar{d}, y$ diagram.

Acknowledgment

The author wishes to thank Dr. E. G. Carter (I.W.S., London) for his kindness in translating this long text from French into English.

Literature Cited

1. Henon, R., Contribution statistique aux méthodes de classification des finesses de laine. (Journal de la Société de Statistique de Paris, avril-mai-juin 1952. 120–133; également C.T. de la F.L.I. Londres, juin 1952, rapport no. 15.)
2. Henon, R., Recherche des caractéristiques de finesse d'un peigné théoriquement parfait du point de vue de la régularité de la finesse. (C.T. de la F.L.I. Paris, janvier 1954, rapport no. 8 non publié.)
3. Henon, R., Contribution statistique aux méthodes de classification des finesses de la laine. (C.T. de la F.L.I. Paris, janvier 1956, rapport no. 13 non publié.)
4. Henon, R., Etude de la classification des peignés de l'Agricultural Marketing Service U.S.A. (C.T. de la F.L.I. Paris, janvier 1956, rapport no. 14 non publié.)
5. Henon, R. and Ott, J., Etat actuel de la recherche d'une corrélation entre les diamètres moyens et les écarts-types (rubans de peigné). (C.T. de la F.L.I. Zürich, juin 1956, rapport no. 14, non publié.)
6. Henon, R. and Ott, J., Enquête sur la corrélation diamètre moyen-écart-type. Comparaison des résultats de 128 analyses U.S.A. à 5.450 analyses européennes. (C.T. de la F.L.I. Zürich, juin 1956, rapport no. 15, non publié.)
7. Monfort, F., Aspects scientifiques de l'Industrie Lainière (Editions Dunod, Paris, 1960).
8. Ott, J., Etude d'une nouvelle classification des laines. (B.I.T.F. no. 77, octobre 1958.)
9. Ott, J., Identifications des échantillons de laine (B.I.T.F., no. 79, fevrier 1959).

Manuscript received December 28, 1959.

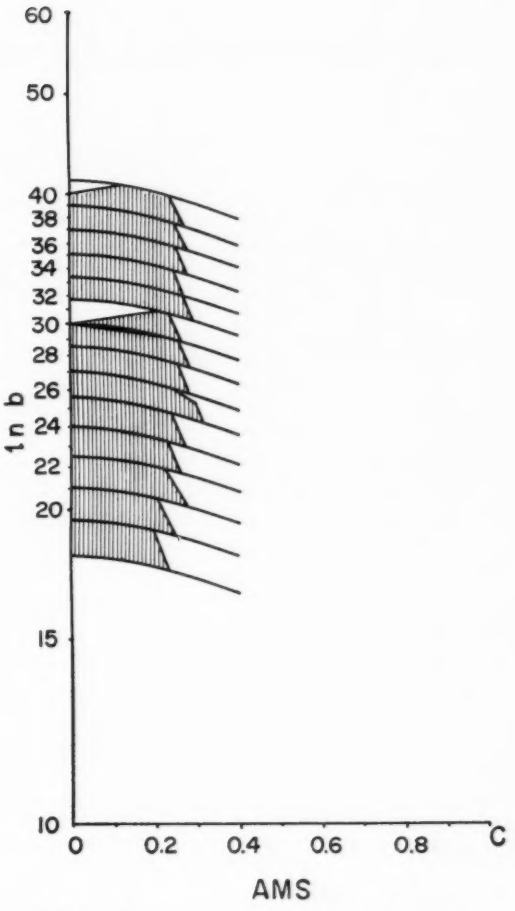

Fig. 7. Representation of the AMS classification on the $(c, \ln b)$ diagram.

Load–Deflection Analysis of Fibers with Plane Crimp

R. Chicurel[1] and E. Suppiger

Textile Research Institute, Princeton, New Jersey

Abstract

An analysis is presented for the change in shape, due to bending and stretching, of a coplanar crimped fiber subjected to static loading. For a fiber of given original configuration and specific loading, one may obtain the deformed configuration from the solution of two nonlinear differential equations. The load–deflection relations are calculated for a fiber with semicircular crimp and for three fibers with sine-wave crimps of different amplitude–wave length ratios. Reported also is an experimental verification of the results for two of the sine-wave crimps, using thin wire test specimens.

Introduction

A knowledge of the mechanical behavior of a single crimped fiber is basic in the study of textile structures. Since an analytical approach to this problem is complicated by the complex nature of real fibers, one conceives a model fiber in which the most pertinent parameters are incorporated but which is amenable to mathematical treatment. Such a model of a crimped fiber serves as the basis for the work reported in this paper; the following conditions are imposed:

1. The axis of the fiber is coplanar.
2. The material is linearly elastic and homogeneous.
3. The cross section is circular and of constant diameter and this diameter is small compared to the smallest radius of curvature, and length, of the fiber axis.
4. Shear deformations are negligible.

If one ignores the stretching of the fiber (or filament) axis, so that the deformations are due to bending alone, one has the classical problem of the "elastica" first examined by L. Euler [3] some years ago; an alternative formulation of this was made by J. L. Lagrange [5]. Kirchhoff [4] and Clebsch [2] extended the "elastica" to a tortuous curve in space and obtained a set of six differential equations governing the deformed shape thereof.

Method of Analysis

Figure 1 shows an elastic filament which conforms to the requirements of the model, or ideal, fiber. The broken curve represents the filament when loaded at one end by a force P and a bending couple T; the other end is constrained at O and is chosen as the origin of the xy-axes. Q_0 and Q represent the same point on the filament axis—before and after the loads are applied. Since we are including the stretching of the filament axis, the distance s_0 from O to Q_0 is not the same as the distance s from O to Q. The x-axis is chosen parallel to the force P, and $(L - L_0)$ is the extension as usually measured.

If the loads P and T are known, as well as the manner of constraint at O, then the deformed shape is determinate. For each s_0 there corresponds an s and θ, i.e.,

$$s = s(s_0) \quad \text{and} \quad \theta = \theta(s_0)$$

and these functions may be found from the equilibrium condition for minimum potential energy of the system.

The potential energy is (1) the strain energy of the filament plus (2) the potential energy of the loads. The strain energy of the filament is due to bending and to stretching; the component due to bending is obtained first.

The well known relation [8] between the change in curvature of the filament axis and the bending moment is

$$\Delta\kappa = \kappa - \kappa_0 = \frac{M}{EI}$$

where the initial and final curvatures are κ_0 and κ, the bending moment is M, and the flexural rigidity is EI.

[1] Present address: Virginia Polytechnic Institute, Blacksburg, Va.

The strain energy of bending, per unit length, is

$$\frac{dU_b}{ds} = \frac{M}{2}\,\Delta\kappa = \frac{M^2}{2EI} = \frac{EI}{2}\,(\kappa - \kappa_0)^2 \qquad (1)$$

If $\frac{ds}{ds_0} \equiv 1$ then $\frac{d\theta}{ds} \equiv \frac{d\theta}{ds_0}$. Thus if we assume that the bending energy depends only on $\theta(s_0)$ but not on $s(s_0)$ we may write

$$\kappa = \frac{1}{\rho} = \frac{d\theta}{ds} \cong \frac{d\theta}{ds_0} = \theta'$$

and Equation 1 becomes, after integration [1]

$$U_b = \int_0^{S_0} \frac{EI}{2}\,(\theta' - \kappa_0)^2\,ds_0$$

The strain energy due to stretching, per unit length, is

$$\frac{dU_t}{ds_0} = \frac{AE\epsilon^2}{2}$$

where A is the cross-sectional area, E is Young's modulus, and the unit strain

$$\epsilon = \frac{ds - ds_0}{ds_0} = \frac{ds}{ds_0} - 1 = s' - 1$$

$$\therefore \frac{dU_t}{ds_0} = \frac{AE}{2}\,(s' - 1)^2$$

and this becomes, after integration [1]

$$U_t = \int_0^{S_0} \frac{AE}{2}\,(s' - 1)^2\,ds_0$$

If one considers the load P as a weight attached to the lower end of the filament, the potential energy of P is evidently

$$-P(L - L_0)$$

Since $\frac{dL}{ds} = \frac{dL}{ds_0}\frac{ds_0}{ds} = \cos\theta$,

$$\frac{dL}{ds_0} = s'\cos\theta$$

and the potential energy of P becomes

$$-P\int_0^{S_0} s'\cos\theta\,ds_0 + PL_0$$

The potential energy of the bending couple T need not be considered (see below). Thus the total energy of the system is

$$\int_0^{S_0}\left[\frac{EI}{2}\,(\theta' - \kappa_0)^2 + \frac{AE}{2}\,(s' - 1)^2 - Ps'\cos\theta\right]ds_0 + PL_0$$

which may be written as

$$U = \int_0^{S_0} \psi\,(\theta, \theta', s')\,ds_0 + PL_0$$

The usual methods of the calculus of variations [6] allow us to find the variation of U in terms of arbitrary variations of θ and s. Thus, since $\delta(PL_0) = 0$, we have

$$\delta U = \delta\int_0^{S_0} \psi\,(\theta, \theta', s')\,ds_0$$

$$= \int_0^{S_0}\left\{\left[\frac{\partial\psi}{\partial\theta} - \frac{d}{ds}\left(\frac{\partial\psi}{\partial\theta'}\right)\right]\delta\theta + \frac{\partial\psi}{\partial s'}\,\delta s'\right\}ds_0 \qquad (2)$$

wherein $[\delta\theta]_{s=0,S_0} = [\delta s']_{s=0,S_0} = 0$ since the variation is between definite limits.

The variation in the potential energy of the two end moments T is the negative of the work done by these moments, i.e.,

$$[T\,\delta\theta]_{s=0} - [T\,\delta\theta]_{s=S_0} = 0$$

Thus, for minimum U, we may write

$$\delta U = \delta\int_0^{S_0} \psi(\theta, \theta', s')\,ds_0 = 0 \qquad (3)$$

It is evident from Equation 2, since $\delta\theta$ and $\delta s'$ are arbitrary, that the integral in Equation 3 can vanish only for

$$\frac{\partial\psi}{\partial\theta} - \frac{d}{ds_0}\left(\frac{\partial\psi}{\partial\theta'}\right) = 0 \quad \text{and} \quad \frac{\partial\psi}{ds'} = 0,$$

for all $0 \leqslant s_0 \leqslant S_0$

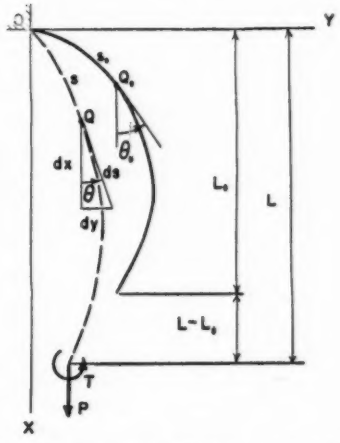

Fig. 1. Arbitrary coplanar filament. ——, unloaded filament; - - - loaded filament.

or

$$\left.\begin{aligned} \frac{P}{EI}\, s' \sin\theta - \theta'' + \theta_0'' &= 0 \\ (s' - 1) - \frac{P}{AE}\cos\theta &= 0 \end{aligned}\right\} \tag{4}$$

and these Equations 4 may be rewritten as

$$\frac{ds}{ds_0} = \frac{P}{AE}\cos\theta + 1 \tag{5}$$

$$\frac{P}{EI}\left(\frac{P}{AE}\cos\theta + 1\right)\sin\theta - \frac{d^2\theta}{ds_0^2} + \frac{d^2\theta_0}{ds_0^2} = 0 \tag{6}$$

If a solution of Equation 6—which contains only the one unknown $\theta(s_0)$—can be found for a specified crimp and loading, then the stretching $s(s_0)$ is given by Equation 5.

For cases in which the stretching of the filament axis is negligible, the term $P/AE\cos\theta \ll 1$ and Equations 5 and 6 reduce to

$$\frac{ds}{ds_0} = 1 \tag{7}$$

$$\frac{P}{EI}\sin\theta - \frac{d^2\theta}{ds_0^2} + \frac{d^2\theta_0}{ds_0^2} = 0 \tag{8}$$

Filament with Unloaded Shape a Circular Arc

An exact solution of Equations 7 and 8 is possible for $\frac{d^2\theta_0}{ds_0^2} \equiv 0$. This is the case of a filament in the shape of a circular arc before the application of any loading. A solution follows for a semicircle with diameter on the x-axis and with $\theta_0(0) = \frac{\pi}{2}$. If the ends are free to rotate, this case may be solved in much the same manner as outlined by Mitchell [7]. If the ends are not permitted to rotate, the problem is simplified. Both cases will be analyzed here.

Equation 7 states that $s = s_0$; no distinction between the two is necessary, and Equation 8 becomes

$$\theta'' - m\sin\theta = 0 \tag{9}$$

where $m = P/EI$. Equation 9 may be rewritten as

$$\frac{1}{\theta'}\left(\tfrac{1}{2}\theta'^2 + m\cos\theta\right)' = 0$$

Since $1/\theta' \neq 0$, it follows that

$$\left(\tfrac{1}{2}\theta'^2 + m\cos\theta\right)' = 0$$

upon integration with respect to s, we obtain

$$\theta'^2 + 2m\cos\theta = a, \quad a \neq a(s)$$

$$\therefore \frac{d\theta}{ds} = \theta' = \kappa = -\sqrt{a - 2m\cos\theta} \tag{10}$$

wherein the negative sign is used since $\theta' < 0$ for all values of s. Thus

$$ds = \frac{-\,d\theta}{\sqrt{a - 2m\cos\theta}} = \frac{-\,d\theta}{\sqrt{(a - 2m) + 4m\sin^2\frac{\theta}{2}}}$$

Let: $\phi = \frac{\pi}{2} - \frac{\theta}{2}$ $\therefore \cos\phi = \sin\frac{\theta}{2}$, $-\frac{\pi}{4} \leqslant \frac{\theta}{2} \leqslant \frac{\pi}{4}$

$$\therefore ds = \frac{2\,d\phi}{\sqrt{a + 2m}\,\sqrt{1 - K^2\sin^2\phi}} \tag{11}$$

where $K^2 = \frac{4m}{a + 2m}$ and $K^2 < 1$.

Ends Not Allowed to Rotate

The boundary conditions are

$$\left.\begin{aligned} \theta = \frac{\pi}{2},\ \phi = \frac{\pi}{4} \quad &\text{for} \quad s = 0 \\ \theta = -\frac{\pi}{2},\ \phi = \frac{3\pi}{4} \quad &\text{for} \quad s = S \end{aligned}\right\} \tag{12}$$

From Equation 11 and the first of Equations 12 we have

$$s = \frac{2}{\sqrt{a + 2m}}\int_{\pi/4}^{\phi} \frac{d\phi_1}{\sqrt{1 - K^2\sin^2\phi_1}}$$

wherein the subscript 1 is used to denote the dummy variable ϕ_1. Thus

$$s = \frac{2}{\sqrt{a + 2m}}\left[F\left(K, \phi\right) - F\left(K, \frac{\pi}{4}\right)\right] \tag{13}$$

where $F(K, \phi)$ is an elliptic integral of the first kind. Since the filament is symmetrical, we have

$$\theta = 0, \phi = \frac{\pi}{2} \quad \text{for} \quad s = \frac{S}{2} = \frac{\pi R}{2}$$

with R = radius of the unloaded filament. It follows from Equation 13 that

$$\frac{\pi R}{2} = \frac{2}{\sqrt{a + 2m}}\left[F\left(K, \frac{\pi}{2}\right) - F\left(K, \frac{\pi}{4}\right)\right]$$

$$\therefore \sqrt{a + 2m} = \frac{4\left[F\left(K, \frac{\pi}{2}\right) - F\left(K, \frac{\pi}{4}\right)\right]}{\pi R} \tag{14}$$

and, from the definition of K, we have

$$m = \frac{K^2(a + 2m)}{4} \tag{15}$$

Combining Equations 14 and 15

$$m = \frac{4K^2}{\pi^2 R^2}\left[F\left(K, \frac{\pi}{2}\right) - F\left(K, \frac{\pi}{4}\right)\right]^2 \tag{16}$$

Solving Equation 14 for a, and using Equation 16

$$a = \frac{8}{\pi^2 R^2}\left[F\left(K, \frac{\pi}{2}\right) - F\left(K, \frac{\pi}{4}\right)\right]^2 (2 - K^2) \tag{17}$$

Evidently

$$x = \int_0^s \frac{dx}{ds_1}\, ds_1 = \int_0^s \cos\theta\, ds_1$$

and from Equation 10

$$\cos\theta = \frac{1}{2m}(a - \theta'^2)$$

$$\therefore x = \frac{1}{2m}\int_0^s (a - \theta'^2) ds_1$$

$$= \frac{a}{2m}\int_0^s ds_1 - \frac{1}{2m}\int_0^s \theta'\theta' ds_1 \tag{18}$$

The second of these two integrals reduces to

$$\int_0^s \theta'\theta' ds_1 = -\int_0^s \sqrt{a - 2m\cos\theta}\,\theta' ds_1$$

$$= -\int_{\pi/2}^{\phi} \sqrt{(a+2m) - 4m\sin^2\phi}\, d\theta_1$$

$$= -\sqrt{a+2m}\int_{\pi/4}^{\phi} \sqrt{1 - \frac{4m}{(a+2m)}\sin^2\phi_1}\,(-2d\phi_1)$$

$$= 2\sqrt{a+2m}\int_{\pi/4}^{\phi} \sqrt{1 - K^2\sin^2\phi_1}\, d\phi_1$$

$$= 2\sqrt{a+2m}\left[G(K, \phi) - G\left(K, \frac{\pi}{4}\right)\right]$$

where $G(K, \phi)$ is an elliptic integral of the second kind.

Equation 18 now becomes

$$x = \frac{as}{2m} - \frac{\sqrt{a + 2m}}{m}\left[G(K, \phi) - G\left(K, \frac{\pi}{4}\right)\right]$$

Substituting for s the value from Equation 13

$$x = \frac{a}{m\sqrt{a + 2m}}\left[F(K, \phi) - F\left(K, \frac{\pi}{4}\right)\right] - \frac{\sqrt{a + 2m}}{m}\left[G(K, \phi) - G\left(K, \frac{\pi}{4}\right)\right]$$

Combining the above with Equations 14, 15, and 17

$$\frac{x}{R} = \left\{\pi\left\{(2 - K^2)\left[F(K, \phi) - F\left(K, \frac{\pi}{4}\right)\right] - 2\left[G(K, \phi) - G\left(K, \frac{\pi}{4}\right)\right]\right\}\right\} \div 2K^2\left[F\left(K, \frac{\pi}{2}\right) - F\left(K, \frac{\pi}{4}\right)\right] \tag{19}$$

To determine y, we write

$$y = \int_0^s \frac{dy}{ds_1}\, ds_1 = \int_0^s \sin\theta\, ds_1$$

and from Equation 9

$$\sin\theta = \frac{\theta''}{m}$$

$$\therefore y = \frac{1}{m}\int_0^s \theta'' ds_1 = \frac{1}{m}[\theta'(s) - \theta'(0)]$$

Substituting θ' from Equation 10, and using the first of Equations 12

$$y = \frac{1}{m}[-\sqrt{a - 2m\cos\theta} + \sqrt{a}]$$

In terms of ϕ, this becomes

$$y = \frac{1}{m}[-\sqrt{(a + 2m) - 4m\sin^2\phi} + \sqrt{a}]$$

$$= \frac{\sqrt{a}}{m} - \frac{\sqrt{a + 2m}}{m}\sqrt{1 - K^2\sin^2\phi}$$

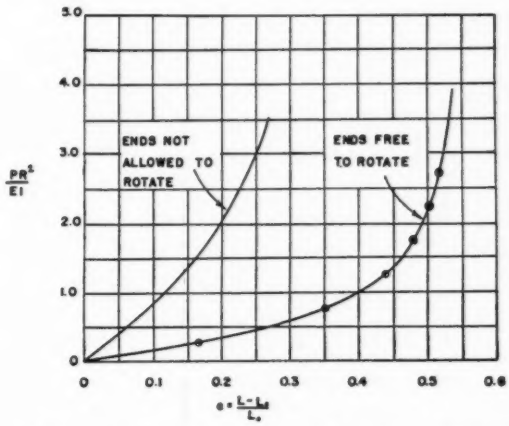

Fig. 2. Load-extension diagrams for filaments with semicircular crimp. Effect of bending alone: solid lines from exact solution; points enclosed in circles from the numerical solution.

Using Equations 14, 15, and 17 to eliminate a and m

$$\therefore \frac{y}{R} = \frac{\pi\{\sqrt{4 - 2K^2 - 2\sqrt{1 - K^2 \sin^2\phi}}\}}{2K^2\left[F\left(K, \frac{\pi}{2}\right) - F\left(K, \frac{\pi}{4}\right)\right]} \quad (20)$$

The increase in length, per unit of original length of filament, is

$$e = \frac{L - 2R}{2R} = \frac{2(x)_{\phi=\pi/2} - 2R}{2R}$$

Using Equation 19

$$e = \frac{\pi}{2K^2}\left\{2 - K^2 - 2\frac{\left[G\left(K, \frac{\pi}{2}\right) - G\left(K, \frac{\pi}{4}\right)\right]}{\left[F\left(K, \frac{\pi}{2}\right) - F\left(K, \frac{\pi}{4}\right)\right]}\right\} - 1 \quad (21)$$

Since $m = P/EI$ we may obtain the load P, in dimensionless form, from Equation 16

$$\frac{PR^2}{EI} = \frac{4K^2}{\pi^2}\left[F\left(K, \frac{\pi}{2}\right) - F\left(K, \frac{\pi}{4}\right)\right]^2 \quad (22)$$

Equations 21 and 22 give the relation between e and PR^2/EI in terms of the parameter K. By assuming values of K (a load factor) between 0 and 1, we obtain corresponding e and PR^2/EI values. The results of such calculations are plotted in Figure 2.

If the configuration of the loaded filament is also required, one may obtain the values of $x(\phi)$ and $y(\phi)$ from Equations 19 and 20 for each assumed K value; i.e., x and y are given in terms of the parameter ϕ (or θ).

Ends Free to Rotate

If the end moments $T = 0$, the boundary conditions for the semicircular filament are

$$M = EI(\theta' - \theta_0') = 0 \quad \text{for} \quad s = 0, S \quad (23)$$

Combining Equation 10 with the first of Equations 23, and with $\kappa_0 = \theta_0' = 1/R$, we obtain

$$\sqrt{a - 2m\cos\theta(0) - \frac{1}{R}} = 0$$

$$\therefore \cos\theta(0) = \frac{1}{2m}\left(a - \frac{1}{R^2}\right)$$

or

$$\frac{a}{2\cos\theta(0)} - m = \frac{1}{2R^2\cos\theta(0)} \quad (24)$$

from the definition of K

$$a + \left(2 - \frac{4}{K^2}\right)m = 0 \quad (25)$$

and from the solution of Equations 24 and 25

$$a = \frac{1}{R^2}\frac{K^2 - 2}{K^2[1 + \cos\theta(0)] - 2}$$

$$m = -\frac{1}{2R^2}\frac{K^2}{K^2[1 + \cos\theta(0)] - 2}$$

thus

$$(a + 2m) = \frac{1}{R^2}\frac{2}{2 - K^2[1 + \cos\theta(0)]} \quad (26)$$

Equation 14 was obtained for the case of ends fixed. However, if in the derivation of this equation we hold $\phi(0)$ unknown instead of using the condition that $\phi(0) = (\phi)_{s=0} = \pi/4$, we may obtain the following relation valid for any end condition

$$\sqrt{a + 2m} = \frac{4\left[F\left(K, \frac{\pi}{2}\right) - F(K, \phi(0))\right]}{\pi R} \quad (27)$$

Squaring both sides of Equation 27 and combining with Equation 26

$$\frac{1}{2 - K^2[1 + \cos\theta(0)]} = \frac{8}{\pi^2}\left[F\left(K, \frac{\pi}{2}\right) - F(K, \phi(0))\right]^2 \quad (28)$$

and from the definition of ϕ

$$\phi(0) = \frac{\pi}{2} - \frac{\theta(0)}{2} \quad (29)$$

Equations 28 and 29 contain the unknowns $\theta(0)$ and $\phi(0)$; from their solution one may obtain $\phi(0)$ in terms of the load factor K. The results are shown in Figure 3.

The expressions for x/R, y/R, e, and PR^2/EI for the case of ends free to rotate are the same as those for fixed ends except that $G(K, \pi/4)$ and $F(K, \pi/4)$ should be replaced by $G(K, \phi(0))$ and $F(K, \phi(0))$. The procedures for finding the relations between e and PR^2/EI and between x/R and y/R are the same as before except that now for each chosen K, the value of $\phi(0)$ must be obtained from Figure 3 and used in the expressions for x/R, y/R, e, and PR^2/EI. The lower curve in Figure 2 was so obtained. The load–extension values for this case of free ends were also determined by a numerical inte-

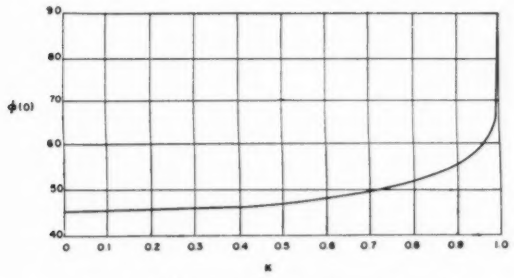

Fig. 3. Relation between $\phi(0)$ and K from Equations 28 and 29.

gration procedure, using a digital computer. These values are the encircled points in Figure 2; they fall on the curve plotted from the exact solution.

Numerical Solutions

A program was developed [1] for an IBM 650 digital computer in order to obtain numerical solutions of Equations 5 and 6 for arbitrary original configurations. The boundary conditions for this program are those for ends free to rotate; however, modifications of the program for other boundary conditions are possible. The program was designed for shapes symmetrical about the line $x = L/2$; this limitation may also be removed without undue difficulty.

No attempt is made here to describe the computer program in detail. The preliminary steps of reducing Equations 5 and 6 to a suitable form for numerical integration will alone be indicated. Computer routines are available for the numerical integration of a system of equations of the type

$$\frac{df_i}{dt} = g_i(f_1, \cdots, f_n) \qquad i = 1, \cdots, n \qquad (30)$$

where $f_1, \cdots, f_n$ are the unknown functions of the independent variable t.

The first step in designing a program to solve Equations 5 and 6 is to write them in the form of Equations 30. To do this we let $\mu = \theta'$ and write Equation 6 as the two equations

$$\left.\begin{aligned} \mu &= \theta' \\ \mu' &= m(p\cos\theta + 1)\sin\theta + \theta_0'' \end{aligned}\right\} \qquad (31)$$

where $m = P/EI$ and $p = P/AE$.

A solution of Equations 31 yields $\theta(s_0)$. However, θ_0'' is not normally known in terms of s_0 since the shape of the unloaded filament is usually given as $y_0 = y_0(x_0)$. It is also convenient to express the deformed shape as $y = y(x)$. For these reasons we introduce other unknowns (and thereby increase the number of differential equations to be solved).

Using the notation: $\dot{y}_0 = \dfrac{dy_0}{dx_0}$, $\ddot{y}_0 = \dfrac{d^2y_0}{dx_0^2}$, etc., the initial curvature $\theta_0' = \dfrac{d\theta_0}{ds_0}$ may be written as

$$\theta_0' = \frac{\ddot{y}_0}{[1 + \dot{y}_0^2]^{\frac{1}{2}}}$$

thus

$$\theta_0'' = \frac{d\theta_0'}{ds_0} = \frac{d\theta_0'}{dx_0}\frac{dx_0}{ds_0}$$

$$= \frac{[1+\dot{y}_0^2]^{\frac{1}{2}}\dddot{y}_0 - \ddot{y}_0\{3[1+\dot{y}_0^2]^{\frac{1}{2}}\dot{y}_0\ddot{y}_0\}}{[1+\dot{y}_0^2)^3}[1-y_0'^2]^{\frac{1}{2}} \qquad (32)$$

but

$$\dot{y}_0 = \frac{dy_0}{dx_0} = \frac{dy_0}{\sqrt{(ds_0)^2 - (dy_0)^2}}$$

$$= \sqrt{\frac{1}{\dfrac{1}{y_0'^2} - 1}} = \sqrt{\frac{y_0'^2}{1 - y_0'^2}}$$

$$\therefore \quad y_0' = \frac{dy_0}{ds_0} = \sqrt{\frac{\dot{y}_0^2}{1 + \dot{y}_0^2}}$$

substituting this in Equation 32, and simplifying

$$\theta_0'' = \frac{[1 + \dot{y}_0^2]\dddot{y}_0 - 3\ddot{y}_0^2\dot{y}_0}{[1 + \dot{y}_0^2]^3} \qquad (33)$$

If $y_0 = y_0(x_0)$ is differentiable three times, then the right side of Equation 33 may be written in terms of x_0. For an example, let $y_0 = A_0 \sin \dfrac{\pi x_0}{L_0}$. Equation 33 yields

$$\theta_0'' = \left\{\left[1 + \left(\frac{A_0\pi}{L_0}\right)^2 \cos^2\left(\frac{\pi x_0}{L_0}\right)\right] A_0\left(\frac{\pi}{L_0}\right)^3 \cos\frac{\pi x_0}{L_0} - 3\left(\frac{A_0\pi^2}{L_0^2}\right)^2 \sin^2\left(\frac{\pi x_0}{L_0}\right)\frac{A_0\pi}{L_0}\cos\frac{\pi x_0}{L_0}\right\} \div \left[1 + \left(\frac{A_0\pi}{L_0}\right)^2 \cos^2\left(\frac{\pi x_0}{L_0}\right)\right]^3$$

Since, in general, θ_0'' is some known function of x_0, we write

$$\theta_0'' = h(x_0)$$

and

$$\frac{dx}{ds} = \cos\theta, \qquad \frac{dy}{ds} = \sin\theta, \qquad \frac{dx_0}{ds_0} = \cos\theta_0$$

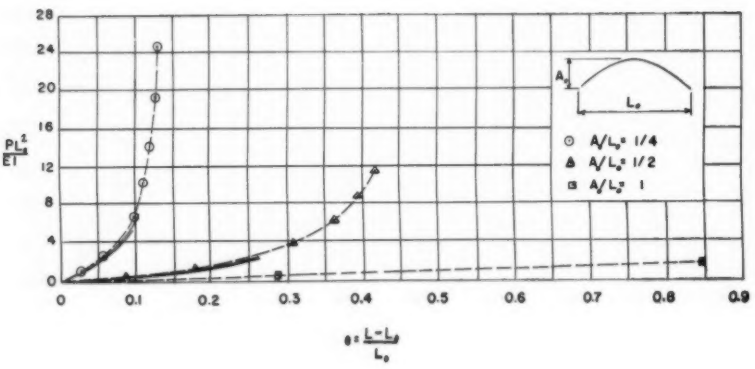

Fig. 4. Load–extension diagrams for half-sine wave filaments with ends free to rotate. Effects of bending and stretching: dashed curves and points refer to computed values; the solid curves are experimental (upper curve = loading, lower curve = unloading).

From Equation 5 and the above

$$\left.\begin{aligned} x' &= \frac{dx}{ds_0} = \frac{dx}{ds}\frac{ds}{ds_0} = \cos\theta(p\cos\theta + 1) \\ y' &= \frac{dy}{ds_0} = \frac{dy}{ds}\frac{ds}{ds_0} = \sin\theta(p\cos\theta + 1) \\ x_0' &= \frac{dx_0}{ds_0} = \cos\theta_0 \end{aligned}\right\} \quad (34)$$

Equations 31 may now be rewritten as

$$\left.\begin{aligned} \mu &= \theta' \\ \mu' &= m(p\cos\theta + 1)\sin\theta + h(x_0) \\ \mu_0 &= \theta_0' \\ \mu_0' &= h(x_0) \end{aligned}\right\} \quad (35)$$

wherein $h(x_0) = \theta_0''$ as given by Equation 33, and the new variable μ_0 is added. Considered as a single group, Equations 34 and 35 form a system of equations exactly like Equation 30.

In addition to the semicircular shape discussed above, three half-sine waves of different amplitude–wave length ratios were investigated by the computer method. For the sine-wave shapes, the effect of the stretching of the filament axis was considered. The results of the machine computations for the load–extension values are shown as the plotted points in Figure 4 for the sine wave shapes; the curves shown as solid lines were determined experimentally.

Experimental Verification

In order to provide a check on the analysis, and on the correctness of the computer program, the load–extension curves for two of the three half-sine wave filaments were obtained experimentally. Specimens were made of spring steel wire and tested in an Instron machine. The dimensions of the test specimens were:

Specimen	Diameter, d	Length, L_0	Amplitude, A_0
1	.021 in.	3.00 in.	0.75 in.
2	.021	3.00	1.50

Various factors were weighted in the selection of the relative dimensions of the specimens. To keep the ratio d/R small, the diameter d should be as small as feasible. However, the deformation of a specimen due to its own weight increases as d/L_0 decreases since the moment of inertia I (and thus the flexural rigidity EI) varies as d^4 while the loading due to the weight of the filament varies as d^2. Hence there exists a practical lower limit for d for a specimen of given length L_0. The effect of the stretching of the filament is difficult to ascertain experimentally since this becomes significant only for large deformations, and for comparable large deflections the stresses in wire of large d exceed the elastic limit sooner than do the stresses in wire of small d.

The preceding discussion is based on a specimen of given original shape and length. The size effect should be considered in comparing the tests here reported with test data of textile fibers, since the latter are usually much finer than the wire specimens here described.

The wire specimens were placed, with both ends free to rotate, in the Instron testing machine. These boundary conditions were realized by fitting the ends of the specimens with steel balls and then holding these balls in special grips so as to give a spherical-seated bearing. In order to attach the balls to the ends of the specimens, a diametral hole was drilled through each ball and the specimen end inserted and secured by soldering. A drop of light

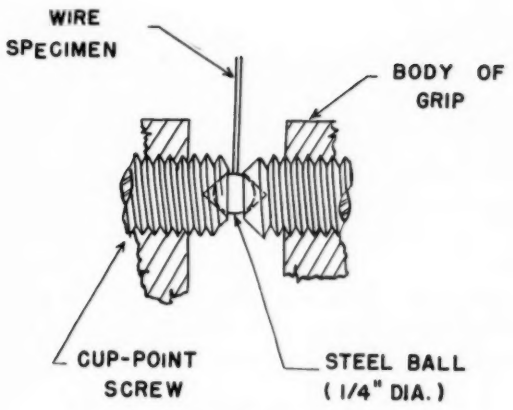

Fig. 5. Method of holding the specimen in testing machine.

machine oil was applied to each ball to minimize the frictional moment. A sketch of the specimen end and grip is given in Figure 5.

The results of the tests are the load–extension curves shown by the solid lines in Figure 4. A comparison with the broken lines drawn through the computed points, in the same Figure 4, shows very satisfactory agreement; no adjustment of parameters is involved here.

Conclusions

The model of a crimped fiber, as used in the analysis of this paper, appears to possess the principal characteristics governing the mechanical behavior of an actual fiber under static loading. The applicability of this study to the performance of actual textile fibers has not been verified.

As stated, this analysis is limited to coplanar filaments; studies are now underway in which this restriction is removed. Further complications arise if one attempts to include viscous effects in addition to those of linear elasticity, even assuming the simplest type of visco-elasticity.

The foregoing theory may be applied in the study of the influence of artificial crimp in man-made fibers on the load–extension characteristics of such fibers. Perhaps in this way a rational procedure may be developed to design crimp shapes associated with specified mechanical textile behavior.

Literature Cited

1. Chicurel, R., Dissertation, Princeton University (1959).
2. Clebsch, A., "Theorie der Elasticität Festerkörper," Leipzig (1862).
3. Euler, L., "De Curvis Elasticis," Additamentum I, Methodus Inveniendi Lineas Curvas Maximi Minimive Proprietate Gaudentes, Geneva (1744); "Elastic Curves," translated and annotated by W. A. Oldfather, *Isis* **20**, 72–160 (1933).
4. Kirchhoff, G. R., "Vorlesungen über Math. Physik, Mechanik," 3rd Edition, Leipzig (1883).
5. Lagrange, J. L., "Sur la Force des Ressorts Pliés," Vol. 3, Oeuvres de Lagrange, Paris, J. A. Serrett, 77 (1869).
6. Lanczos, C., "The Variational Principles of Mechanics," Toronto, U. of Toronto Press, 57–60 (1949).
7. Mitchell, T. P., "The Nonlinear Bending of Thin Rods," *J. App. Mech.*, Trans. of the ASME, Paper No. 58-A50 (1958).
8. Timoshenko, S., "Strength of Materials," Part II, 2nd Edition, Princeton, N. J., D. Van Nostrand Co., 68 (1941).

Manuscript received March 10, 1960.

Durability of Oleophobicity of Cotton Fabrics Imparted by Fluorochemicals

Ralph J. Berni, Ruth R. Benerito, and Frederick J. Philips[1]

Southern Regional Research Laboratory,[2] *New Orleans, Louisiana*

Abstract

Durability of oleophobicity imparted to cotton fabrics by additive finishes (perfluorometallic complexes and perfluoro-acrylate) and by the incorporation of fluorochemicals into the cellulose molecule by means of an ether linkage has been investigated. Studies on the relative effectiveness of additive finishes in maintaining oleophobicity on weathering have been made. Results of soil burial tests involving the use of aluminum triacetate and perfluorooctanoic acid on various fabric constructions are reported. Various techniques used in efforts to improve durability of the latter finish to aqueous launderings are described. Data are presented to explain losses in oleophobic properties when fabrics treated with perfluorooctanoic acid complex of chromium or aluminum are subjected to aqueous launderings. The preparation of 1,1-dihydroheptafluorobutoxyhydroxypropyl and 1,1-dihydropentadecafluorooctoxyhydroxypropyl ethers of cellulose which possessed hydrophobic and oleophobic properties durable to alkaline aqueous washings and commercial drycleaning solutions are described. The preparation of 1,1,7-trihydrododecafluoroheptoxyhydroxypropyl ether of cellulose which possessed only a small degree of oil repellency due to the presence of an omega-hydrogen atom is also given.

Introduction

Various methods have been used for the treatment of cotton with fluorochemicals. Some of these applications have been the subject of previous reports [6, 7, 8] establishing the relative effectiveness of several classes of fluorocarbon compounds in imparting satisfactory oleophobic and hydrophobic surface characteristics to cotton fabrics. The preparation and properties of partial esters of cotton cellulose and perfluoro acids, as well as the rates of hydrolysis of cellulose-perfluorooctanoate, have also been investigated and reported [2]. This report is concerned with further evaluation of previously reported finishing methods involving the use of fluorochemicals and certain modifications of these previously reported applications; it discusses limited investigations concerned with new chemical compounds of cellulose—the fluoroalkoxyhydroxypropyl ethers of cellulose. Previously investigated treatments imparted excellent oil and water repellent properties in many instances, but the linkages between cellulose and fluoro moieties were hydrolyzed, particularly in the presence of alkaline soap washes and, therefore, were not durable to conventional aqueous launderings or commercial drycleaning processes. In this investigation, modifications of effective fluorochemical surface treatments have been made in attempts to make those finishes with available fluorochemicals more durable to aqueous media containing detergents. The preparation of a chemical compound in which the perfluoro moiety is attached to cellulose through an ether linkage which should be stable to alkaline hydrolysis and, consequently, to commercial launderings or drycleanings has been undertaken.

[1] Deceased.

[2] One of the laboratories of the Southern Utilization Research and Development Division, Agricultural Research Service, U. S. Department of Agriculture.

Materials and Methods

Fabric Description

Cotton fabrics employed in most of the treatments were a 48 × 48 sheeting weighing 4.18 oz./sq. yd. and an 80 × 80 print cloth weighing 3.12 oz./sq. yd. Both fabrics were desized, scoured, and then processed in commercial peroxide bleaching equipment. Some experiments were also performed on an 8.5-oz. sateen and on cotton-rayon oxford whipcord which had been desized and scoured.

Chemicals

Analytical reagent grade aluminum sulfate and lead acetate were used to prepare aluminum triacetate solutions which were used as a mordant in the *in situ* formation of an aluminum complex of perfluorooctanoic acid.

Aluminum complex of perfluorooctanoic acid was prepared especially for this investigation by E. I. du Pont de Nemours & Co. Inc.[3]

The chromium complex of perfluorooctanoic acid was furnished under the trade name FC-805 by the Minnesota Mining and Manufacturing Co.[3] as a 30% solution of the complex in 95% isopropanol. Its chromium : acid mole ratio was 3.5 : 1.

A fluorine-containing acrylic polymer, Poly F B A, (F.C.401—Latex) was commercially available from Minnesota Mining and Manufacturing Co.[3] and contained 35% solids.

Rhoplex B-15, an unfluorinated acrylic polymer emulsion of the nonionic type, was commercially available from Rohm and Haas Co.[3]

The 1,1-dihydroheptafluorobutanol and 1,1-dihydropentadecafluorooctanol were reagent grade chemicals obtained from Columbia Organic Chemicals Co., Inc.[3] The 1,1,7-trihydrododecafluoroheptanol was a reagent grade chemical obtained from E. I. du Pont de Nemours & Co. Inc.[3] All fluorinated alcohols were used as obtained in the preparation of glycidyl ethers. Epichlorohydrin was a commercial product of the Shell Development Co.[3]

Oils used for testing were white mineral oil, S.A.E. No. 10 lubricating oil, paraffin oil, a refined cottonseed oil, and a refined olive oil.

A sulfonated castor oil (Turkey-red oil) was obtained from the Matheson, Coleman, and Bell Co.[3]

Weathering Tests

Weather exposure tests were conducted in an unshaded location particularly free from airborne industrial contaminants. All samples were exposed on open-backed wooden racks which face south at an angle of 45° from the vertical, at a minimum distance of 30 in. above the ground. Samples were removed for oil repellency and breaking strength tests after 2 weeks and thereafter every 4 weeks up to a total of 22 weeks of exposure.

[3] Use of a company and/or product named by the Department does not imply approval or recommendation of the product to the exclusion of others which may also be suitable.

Rot Resistance Tests

A soil burial method was used in testing rot resistance of samples. The soil was a specially prepared mixture which was placed in a wooden drawer in a closed cabinet at 90° F. ±2° F. The moisture content was 28–30% and the pH was 6.5–7. Rot resistance tests were followed for a period of six weeks. Five strips (1 × 6 in.) of each fabric were removed at one-week intervals for testing.

Textile Testing

The ASTM or Federal Specifications standard methods were used for the following textile testings: breaking strengths by the strip method (80 thread count width) on a Scott Tester[3] [1a], tear strengths by the Elmendorf Method [1b], and crease recovery angles by the Monsanto Method [5] with a 500-g. weight. Values reported are the averages of five test samples.

Oil and water repellency values were determined according to a previously published method [6].

Experimental

Treatment with Chromium Complex

The application of the chromium complex of perfluorooctanoic acid and/or acrylic lattices to cotton fabrics to obtain oil and water repellent surfaces was carried out according to previously published procedures [6, 7].

Treatments with Aluminum Triacetate and Perfluorooctanoic Acid by Mordant Method

The application of perfluorooctanoic acid to cotton fabrics pretreated with aluminum triacetate solutions as a mordant to produce oleophobic surfaces has also been published previously [7, 8]. Modifications of this method have been used in this investigation in attempts to produce a more effective mordant surface of basic aluminum acetate or aluminum oxides. The following four methods of pretreatment with 0.5 *M* aluminum acetate solutions have been investigated: (a) fabric padded with acetate solution and then air dried; (b) fabric padded with acetate solution, steamed for 2 hr. at atmospheric pressure, and then air dried; (c) fabric padded with a 10% aqueous solution of a sulfonated castor oil, commonly known as Turkey-red oil, and oven dried at 110° C. for 2 hr. before being treated with acetate solution and then air dried; (d) fabric treated as in (c) but

steamed after application of acetate solution. After all four methods of pretreatment, the fabric was air dried for 16 hr., padded with a 5% alcoholic solution of perfluorooctanoic acid to a 100% wet pickup, and then dried in an oven at 110° C. for 30 min.

Preparation of Samples with Aluminum Complex of Perfluorooctanoic Acid

Aqueous and methanolic solutions containing both 3% and 5% by weight of a specially prepared aluminum complex of perfluorooctanoic acid were used in padding solutions. In the aqueous solutions, it was necessary to add 2% formic acid, based on the weight of solid complex, to maintain a clear solution. Samples of 48 × 48 sheeting, 80 × 80 print cloth, an 8.5-oz. sateen, and a cotton-rayon oxford whipcord were padded to 100% wet pickup and then air dried for approximately 16–20 hr.

Preparation of Fluoroglycidyl Ethers

$$(R_FCH_2—O—CH_2—\underset{\diagdown\,O\,\diagup}{CH}—CH_2)$$

The 1,1-dihydroheptafluorobutyl, 1,1-dihydropentadecafluorooctyl, and 1,1,7-trihydrododecafluoroheptyl glycidyl ethers were prepared essentially according to the method of Brey and Tarrant [3] from epichlorohydrin and 1,1-dihydroheptafluorobutanol,

TABLE I. Time in Hours Required for Test Oils to Wet 80 × 80 Fabric vs. Weeks of Weathering

Finishing compound	Total solids in bath, %	Test oils	Weeks of exposure 0	2	6	10	14	18	22
Chromium complex (FC 805)	1.5	SAE No. 10	NW*	NW	NW	NW	NW	NW	>168†
		Paraffin	NW	NW	NW	NW	NW	NW	NW
		Olive	NW	NW	NW	NW	NW	NW	NW
		Cottonseed	NW	NW	NW	NW	NW	NW	>168
Chromium complex (FC 805)	1.0	SAE No. 10	NW	NW	NW	>168	NR‡	NR	NR
		Paraffin	NW	NW	NW	NR	NR	NR	NR
		Olive	NW	NW	NW	>168	>168	NR	NR
		Cottonseed	NW	NW	NW	>168	>168	NR	NR
Chromium complex (FC 805)	0.5	SAE No. 10	NW	NW	>168	NR	NR	NR	NR
		Paraffin	NW	NW	0.2	NR	NR	NR	NR
		Olive	NW	NW	0.5	NR	NR	NR	NR
		Cottonseed	NW	NW	0.1	NR	NR	NR	NR
Perfluoro acrylate (Poly FBA-FC 401)	10.0	SAE No. 10	NW	>168	>168	>168	>168	24	>168
		Paraffin	NW	>168	>168	>168	>168	48	>168
		Olive	NW	>168	24	>168	>168	4	24
		Cottonseed	NW	>168	>168	48	24	4	>168
(Acrylate (Rhoplex B-15))**	5.0	SAE No. 10	NW	>168	NR	NR	NR	NR	NR
(Chromium complex)	0.5	Paraffin	NW	NR	NR	NR	NR	NR	NR
		Olive	NW	>168	NR	NR	NR	NR	NR
		Cottonseed	NW	>168	NR	NR	NR	NR	NR
(Aluminum triacetate)	0.5	SAE No. 10	NW	NW	>168	>168	>168	>168	>168
(Perfluorooctanoic acid)††	5.0	Paraffin	NW	NW	NW	>168	>168	>168	NW
		Olive	NW	NW	NW	>168	>168	>168	NW
		Cottonseed	NW	>168	>168	>168	>168	>168	100
Untreated control	0	SAE No. 10	NR						
		Paraffin	NR						
		Olive	NR						
		Cottonseed	NR						

* Denotes no wetting or penetration of fabrics by test drops during 168-hr. test period.

† > 168 denotes partial oil repellency resulting in partial wetting of undersurface of fabric due to penetration without disappearance of test liquid.

‡ NR denotes complete wetting in less than 1 min. (no repellency).

** One-step process.

†† Two-step process.

1,1-dihydropentadecafluorooctanol, and 1,1,7-trihydrododecafluoroheptanol, respectively, in the presence of sodium hydroxide.

Oxirane oxygen contents of the gylcidyl ethers were determined titrimetrically with hydrobromic acid in glacial acetic acid solvent according to the method of Durbetaki [4].

Preparation of Fluoroalkoxyhydroxypropyl Ethers of Cellulose

The following is given as typical of the procedures used to prepare fluoroalkoxyhydroxypropyl ethers of cellulose by base catalysis. A 1.75-g. sample of a desized, scoured, and bleached 80 × 80 cotton fabric was impregnated with a 15% by weight aqueous solution of sodium hydroxide by immersing the fabric in an excess of base solution for 15 min. and then centrifuging the fabric to a 100% wet pickup. The fabric was then immersed in approximately 20 ml. of fluoroalkoxy glycidyl ether and allowed to react for 6 hr. at 60–80° C. for the preparation of 1,1-dihydroheptafluorobutoxyhydroxypropyl ether. For the preparation of longer chain fluoroalkoxy ethers (1,1-dihydropentadecafluorooctoxyhydroxypropyl and 1,1,7-trihydrododecafluoroheptoxyhydroxypropyl ethers of cellulose) the reaction time was extended to 16 hr. at 95° C. During the entire reaction time, the reaction flask was shaken. The resultant etherified fabric was washed free of excess etherifying agent with methanol, then acetone, and then ironed dry at 180° C.

A typical procedure for the acid-catalyzed preparation of fluoroalkoxyhydroxypropyl ethers of cellulose is as follows. The fabric was padded twice to a 70% wet pickup in a methanol solution containing 30% by weight of fluoroalkoxy glycidyl ether and 4% by weight of zinc fluoborate catalyst. The wet fabric was placed between glass plates and cured for 6 min. at 125° C. The dried fabric was washed in acetone and then water before being ironed dry at 180° C.

Results and Discussion

Weathering Studies

An evaluation of resistances offered by various perfluoro finishes to adverse effects of weathering was made over a period of 22 weeks. Samples of 80 × 80 fabric were treated with solutions containing 0.5%, 1.0%, and 1.5% of the chromium complex of perfluorooctanoic acid, and others were made oleophobic by treatment with a Poly FBA solution containing 10% solids. Both of these treatments have been described previously [6]. A modified emulsion containing Rhoplex B-15 in combination with a 0.5% solution of chromium complex of perfluorooctanoic acid, as well as a solution of 5% perfluorooctanoic acid by a mordant method, were applied as previously reported [7, 8]. The finished fabrics from all six treatments were exposed to the weather and tested periodically for oil repellency and breaking strengths. Results of oil repellency tests are given in Table I.

Data in Table I show that all treatments resulted in excellent oleophobic properties originally. However, the best oil repellency to four test oils after weathering was exhibited by fabric which had been treated with 1.5% solution of the chromium complex of perfluorooctanoic acid, as this sample retained its oil repellency even after 22 weeks of exposure. When less concentrated solutions of the same chromium complex were used in the treating bath, the oleophobicity was not as durable to weathering. For example, use of a 1.0% solution of chromium complex resulted in an oleophobic finish which was still excellent after 6 weeks of exposure, but lost some of its repellency to paraffin oil after 10 weeks of exposure. When the percentage of solids in the treating bath was reduced to 0.5%, the excellent oleophobic properties were durable to only 2 weeks of exposure; some repellent properties were present after 6 weeks of exposure only in the case of the SAE No. 10 oil, and all oil repellency was lost after 10 weeks of exposure.

Data in Table I show that the aluminum triacetate–perfluorooctanoic acid mordant method imparted oil repellent properties which were maintained to some degree even after 18 weeks of exposure, but did not impart a finish that was as oleophobic as the chromium complex finish of the same perfluorooctanoic acid.

When a 0.5% solution of chromium complex was applied alone, it produced a more durable oleophobic finish than when it was applied in conjunction with Rhoplex B-15. Data in Table I show that, in the latter case, the oleophobicity was reduced during 2 weeks of exposure and completely disappeared at 6 weeks of exposure. This phenomenon might be attributed to the nonionic emulsifier present in the Rhoplex B-15. Even traces of the nonionic emulsifier adsorbed on the surface of the finished fabric could act as a wetting-back agent to oil.

In the instance of an oleophobic finish produced by the use of perfluorobutyl acrylate (Poly FBA), data in Table I show that excellent original oil repellency was reduced after only two weeks of weathering, after which time some wetting due to penetration of oils occurred.

In addition to imparting the best oleophobicity to cotton fabric, the chromium complex of perfluorooctanoic acid also resulted in the best breaking strength retention after 22 weeks of weathering, as evidenced by data in Table II. However, none of the treatments resulted in excessive loss in breaking strength after weathering, and even the best treatment resulted in strength retentions only slightly greater than that of untreated cloth after 22 weeks of exposure. All breaking strengths recorded in Table II are the averages of 5 breaks.

Rot Resistance Tests

Earlier work [7] in this laboratory had shown that samples of 80 × 80 print cloth treated with either perfluorooctanoic acid chrome complex or with Poly FBA were completely disintegrated after one week of burial in a biologically active soil, whereas those samples which had been subjected to the aluminum triacetate–perfluorooctanoic acid mordant treatment showed no signs of attack during a similar period. Since there was apparently a high retention of breaking strength in the latter treatment, further investigations were undertaken with the mordant method applied to various types of fabrics. Table III contains breaking strengths, reported as percentages of original breaking strengths retained, of samples which were removed after one-week intervals of burial for a period of six weeks. While percentage of strength retained after one week of burial was high, as reported previously [7], with all types of treated fabric it can be seen that breaking strengths decreased rapidly after one week of burial in all cases except that of cotton-rayon oxford whipcord, which maintained approximately 50% of its strength after six weeks of burial. Oil repellency tests on all

TABLE II. Breaking Strength Retention*, %, vs. Weeks of Weathering

Finishing compound	Total solids in bath, %	Original breaking strength, lb.	Weeks of exposure 2	6	10	14	18	22
Chromium complex (FC 805)	1.5	51.6	96.9	88.2	83.9	80.8	76.6	76
Chromium complex (FC 805)	1.0	50.6	97.8	91.1	80.4	81.6	77.7	79.6
Chromium complex (FC 805)	0.5	51.0	98.2	82.7	84.7	76.7	77.3	77.3
Perfluoro acrylate (Poly FBA-FC 401)	10.0	51.2	88.1	73.4	72.3	63.5	60.7	61.1
(Acrylate (Rhoplex B-15))	5.0	52.4	100.0	81.3	76.7	70.8	70.2	68.3
(Chromium complex)†	0.5							
(Aluminum triacetate)	0.5	48.4	99.6	81.8	72.3	71.1	66.7	65.7
(Perfluorooctanoic acid)‡	5.0							
Untreated control (80 × 80)	0	50.6	91.1	83.4	74.1	67.6	76.5	72.7

* All strengths were calculated as a percentage of the original breaking strengths of treated fabric before weathering.
† One-step process.
‡ Two-step process.

TABLE III. Breaking Strength Retention*, %, vs. Weeks in Soil Burial

Fabrics	Breaking strength, lb.	Weeks in soil bed 1	2	3	4	5	6
Untreated 48 × 48 sheeting	61.6	0	—	—	—	—	—
Treated† 48 × 48 sheeting	61.8	77.3	34.0	21.4	16.8	10.2	6.3
Untreated 80 × 80 print cloth	50.5	0	—	—	—	—	—
Treated† 80 × 80 print cloth	51.0	63.5	17.1	10.6	5.3	3.1	3.1
Untreated 8.5-oz. sateen	121.0	9.8	0	—	—	—	—
Treated† 8.5-oz. sateen	126.4	78.7	30.0	12.5	8.5	6.2	4.5
Untreated cotton rayon-oxford whipcord	95.2	15.2	3.9	0	—	—	—
Treated† cotton rayon-oxford whipcord	94.4	79.0	78.9	60.6	65.8	62.8	51.4

* All strengths were calculated as a percentage of the original strength before soil burial.
† Treatment was a two-step process: fabric was padded with 0.5 *M* aluminum triacetate, air dried, padded with 5% alcoholic perfluorooctanoic acid, and then oven dried at 110° C. for 30 min.

TABLE IV. Time in Hours Required for Test Oils to Penetrate Fabrics Treated with Aluminum Complex of Perfluorooctanoic Acid

Fabric	Total solids in bath, %	Solvent	Test oils			
			SAE No. 10	Paraffin	Olive	Cottonseed
48 × 48 Sheeting	3	Methanol	>168*	NW†	>168	>168
48 × 48 Sheeting	5	Methanol	>168	NW	>168	>168
48 × 48 Sheeting	3	Water	>168	>168	>168	>168
48 × 48 Sheeting	5	Water	>168	NW	NW	>168
80 × 80 Print cloth	3	Methanol	>168	NW	>168	>168
80 × 80 Print cloth	5	Methanol	>168	NW	>168	>168
80 × 80 Print cloth	3	Water	>168	>168	>168	>168
80 × 80 Print cloth	5	Water	>168	NW	>168	>168
8.5-Oz. sateen	3	Methanol	>168	NW	>168	144
8.5-Oz. sateen	5	Methanol	>168	NW	>168	144
8.5-Oz. sateen	3	Water	3	48	1	3
8.5-Oz. sateen	5	Water	48	>168	48	48
Cotton rayon-oxford whipcord	3	Methanol	>168	NW	>168	>168
Cotton rayon-oxford whipcord	5	Methanol	>168	NW	>168	>168
Cotton rayon-oxford whipcord	3	Water	1	24	24	1
Cotton rayon-oxford whipcord	5	Water	1	24	24–72‡	24

* >168 denotes partial oil repellency resulting in partial wetting of the undersurface of fabric due to penetration without disappearance of test liquid.

† NW denotes no wetting or penetration of fabric by test drops during 168-hr. test period.

‡ Drops wet fabric completely over weekend.

samples removed after one week of burial indicated that, although the drops remained on the surface, there was penetration of the fabrics by all oils tested. After two weeks of burial, the whipcord showed a slight degree of oil repellency, but the oleophobicity of all fabric samples was destroyed for all practical purposes.

Figure 1 shows changes in breaking strengths during soil burial tests of whipcord samples which had been treated with 0.5 *M* aluminum triacetate and 5% perfluorooctanoic acid solutions individually, as well as with both chemicals by the two-step mordant method. It can be seen that both aluminum triacetate and perfluorooctanoic acid are required, since neither chemical alone offered good resistance to degradation in soil burial tests.

Aluminum Complex Treatment

All fabrics treated with both 3% and 5% aqueous and alcoholic solutions of an aluminum complex of perfluorooctanoic acid possessed some degree of oleophobicity, as shown by data in Table IV. In general, alcoholic solutions at 3% solid concentration imparted better oil repellency than did aqueous solutions, but at 5% concentration, both aqueous and alcoholic solutions imparted a fair degree of oleophobicity. Better oil repellency was obtained with 48 × 48 and 80 × 80 cloths than with sateen and whipcord for a given treatment. The use of aluminum complex of perfluorooctanoic acid was not as effective a treatment as was the use of chromium complex of perfluorooctanoic acid. Not only was initial oil repellency of the former less effective than that imparted by the chromium complex, but it was also less effective than that imparted by the mordant treatment, in which perfluorooctanoic complex is supposely formed *in situ* on cloth which is first covered with an active aluminum oxide and then treated with perfluorooctanoic acid solution.

Both oil and water repellent properties of fabric treated with an aluminum complex of perfluorooctanoic acid were lost when the fabrics were immersed in an aqueous solution of Fab[3] detergent at 60° C., rinsed in tap water, and oven dried at 105° C.

Microscopical Examination

Electron micrographs of 48 × 48 sheeting which had been treated with a 10% solution of Poly FBA revealed the presence of a material which covered much of the original fiber surface detail. The treatment was uneven from fiber to fiber, and treated fibers attracted extraneous soil particles which were

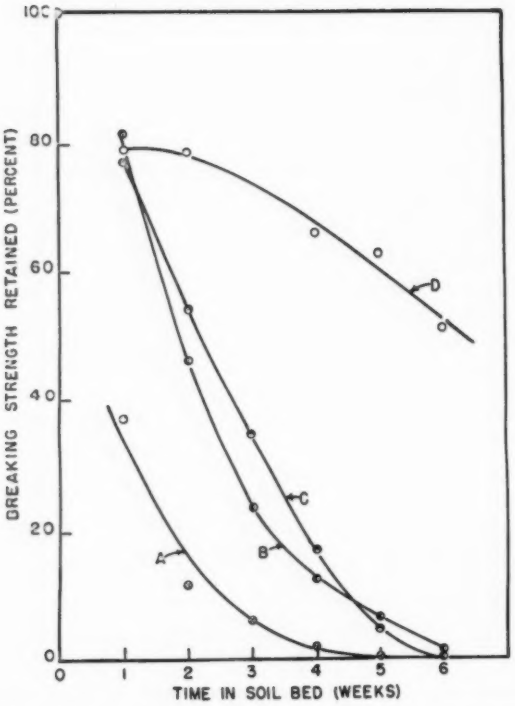

Fig. 1. Breaking strength, % retained, of rayon-oxford whipcord as a function of time in soil bed. (A) Untreated control; (B) treated with 0.5 *M* aluminum acetate; (C) treated with 5.0% alcoholic perfluorooctanoic acid; (D) treated with 0.5 *M* aluminum acetate and 5.0% perfluorooctanoic acid.

obvious on the electron micrographs in Figure 2a. After five dry cleanings, Poly FBA was still present, but extraneous soil particles had been removed, as shown in Figure 2b.

Electron micrographs were made of fibers from 48 × 48 fabric which had been treated in the following ways: (a) fabric padded with a 5% alcoholic solution of perfluorooctanoic acid and then oven dried at 110° C. for 30 min., (b) fabric padded with a 0.5 *M* solution of aluminum acetate and then oven dried for 30 min. at 110° C., (c) fabric padded with 0.5 *M* solution of aluminum acetate and then steamed at atmospheric pressure for 2 hr., and (d) fabric treated with a 0.5 *M* solution of aluminum acetate, oven dried at 110° C. for 30 min., padded with 5% perfluorooctanoic acid solution in ethanol, and dried at 110° C. for 30 min. Treatment (a) resulted in fiber surfaces which were practically indistinguishable from untreated fiber surfaces. Treatment (b) resulted in deposits of small particles of aluminum oxide scattered on the surface and a few smooth glassy areas. Application of the same solution of aluminum acetate by treatment (c) resulted in a fiber surface completely obscured by large masses of aluminum oxide. Surface detail of fabric treated in a two-stage process by method (d) was obscured with large deposits of aluminum oxide, and

Fig. 2. Electron micrographs of surface replicas obtained by the polystyrene-carbon method; platinum (80%)–palladium (20%) shadowing; 8000×. (a) Top: 48 × 48 sheeting treated with 10% Poly FBA (FC 401); (b) bottom: same cloth after five drycleaning cycles.

Fig. 3. Electron micrographs of surface replicas obtained by the polystyrene–carbon method; platinum (80%)–palladium (20%) shadowing; 8000×. (a) Top: 48 × 48 sheeting oven dried at 110° C. for 30 min., after being padded first with 0.5 *M* aluminum triacetate and then with 5% alcoholic perfluorooctanoic acid solution. (b) Bottom: same fabric after being washed in aqueous solution containing 1% Joy detergent at 25° C.

there were few extraneous soil particles present. However, after the last fabric was soaked with an aqueous solution containing 1.0% Joy[3] detergent at 25° C., its electron micrograph showed that it had picked up soil particles. Since artificial soil was not added to the Joy solution, the extraneous soil particles were probably picked up during normal handling of the fabric. Ordinarily, fabrics do not show pickup of soil particles from a detergent solution or during normal handling operations. Typical electron micrographs of fabrics subjected to the aluminum triacetate–perfluorooctanoic acid mordant treatment before and after washings with aqueous solutions of Joy detergent are shown in Figures 3a and 3b.

Although both Poly FBA treatment and aluminum triacetate–perfluorooctanoic acid treatments gave excellent oil repellencies as tested by the liquid drop method, both treatments resulted in surfaces which attracted extraneous soil particles and, therefore, offered little resistance to dry soiling.

Effects of Variation in Method of Application of Mordant

Fabrics pretreated by four methods as outlined under *Experimental* were analyzed for aluminum and acetyl contents before and after washing in distilled water (pH = 5.5), tap water (pH = 9.7), and in aqueous 1% Joy solution (pH = 7.0). Results of these analyses and molar ratios of aluminum: acetyl are given in Table V. It can be seen that steaming of fabric padded with aluminum acetate solution before air drying, either with or without the Turkey-red oil pretreatment, results in a larger percentage of aluminum deposited on the cloth and the least loss in aluminum on washing.

Fabrics mordanted according to four different methods of pretreatment and then padded to 100% wet pickup with 5% alcoholic perfluorooctanoic acid solutions were analyzed for aluminum, acetyl, and fluorine contents before and after washing in distilled water, tap water, and in aqueous solutions of 1% Joy detergent. Analytical results are recorded in Table VI.

Comparison of data in Tables V and VI obtained on unsteamed fabrics indicates that the addition of perfluorooctanoic acid prevents a decrease in aluminum content on washing in aqueous detergent solutions. Data in Table VI also show that steaming produced a much larger uptake of aluminum, but that the use of sulfonated castor oil in pretreatment had little effect. Loss in oil repellency after washing in solutions of neutral detergents such as Joy was probably due either to a change in orientation of perfluoro moieties adsorbed, since there was very little loss in fluorine in any of the fabrics during washings,

or to residual amounts of detergent left in the fabric. Although the fabrics were rinsed extensively in hot water in attempts to wash out the neutral detergent used in the soaking treatment, it is possible that trace amounts of detergent adsorbed on the fabric act as a wetting-back agent to oil. All fabrics, after being soaked in 1.0% aqueous Joy solution at 25° C. and rinsed in water, showed penetration of all test oils in less than 1 min. In no case did it appear that any of the methods of application would make the process durable to aqueous launderings even in the presence of neutral detergents.

TABLE V. Effects of Wash Media on Aluminum and Acetyl Contents of 48 × 48 Fabric Treated in Various Ways with 0.5 *M* Aluminum Triacetate

Method of application	Soaking solution	pH	Weight %		Approximate molar ratios
			Al	Acetyl	Al:acetyl
Pad, air dry	None	—	0.45	1.46	4:3
	Distilled water	5.5	0.15	0.92	2:3
	Tap water	9.7	0.09	1.11	3:10
	1% Joy	7.0	0.06	1.06	2:11
Pad, steam, air dry	None	—	1.38	0.36	17:1
	Distilled water	5.5	1.47	0.46	14:1
	Tap water	9.7	1.45	0.60	11:1
	1% Joy	7.0	1.35	0.40	17:1
Pretreat with TRO*, pad, air dry	None	—	0.19	1.80	1:2
	Distilled water	5.5	0.14	1.42	1:3
	Tap water	9.7	0.16	1.28	1:2
	1% Joy	7.0	0.09	1.43	1:5
Pretreat with TRO*, pad, steam, air dry	None	—	1.26	1.00	5:1
	Distilled water	5.5	1.44	1.11	5:1
	Tap water	9.7	1.51	0.84	6:1
	1% Joy	7.0	1.42	0.92	6:1

* Turkey-red oil (sulfonated castor oil) pretreatment consisted of padding and oven drying at 60° C. for 2 hr. before application of aluminum triacetate.

TABLE VI. Effect of Wash Media on Aluminum, Acetyl, and Fluorine Contents of 48 × 48 Fabric Treated with Modifications of the Aluminum Triacetate–Perfluorooctanoic Acid Method *

Method of application of aluminum triacetate	Soaking solution	pH	Weight %			Approximate molar ratios
			Al	Acetyl	Fluorine	Al : Acetyl : Fluorine
Pad, air dry	None	—	1.00	1.70	2.36	2 : 1 : 4
	Tap water	9.7	0.94	1.60	2.31	2 : 1 : 4
	1% Joy	7.0	1.06	1.40	1.47	2 : 1 : 2
Pad, steam, air dry	None	—	1.01	0.94	3.76	4 : 1 : 10
	Tap water	9.7	1.02	0.90	2.48	5 : 1 : 7
	1% Joy	7.0	1.01	0.86	3.30	5 : 1 : 9
Pretreat with TRO†, pad, air dry	None	—	0.61	1.81	2.88	1 : 1 : 4
	Tap water	9.7	0.86	1.92	2.67	2 : 1 : 4
	1% Joy	7.0	1.00	1.71	2.44	2 : 1 : 4
Pretreat with TRO†, pad, steam, air dry	None	—	0.93	1.45	2.82	3 : 1 : 5
	Tap water	9.7	1.32	1.28	2.57	5 : 1 : 5
	1% Joy	7.0	1.21	1.35	2.13	4 : 1 : 4

* Every method was a two-stage operation which differed in the first stage involving application of aluminum triacetate; second stage in all methods consisted of padding with 5% alcoholic perfluorooctanoic acid to a 100% wet pickup and oven drying at 110° C. for 30 min.

† Turkey-red oil (sulfonated castor oil) pretreatment consisted of padding to 100% wet pickup and oven drying for 2 hr. at 60° C. before application of aluminum triacetate.

Durability of Chromium Complex of Perfluorooctanoic Acid in Aqueous Media

Samples of 80 × 80 fabric treated with a chromium complex of perfluorooctanoic acid to give excellent oil repellency were analyzed for chromium and fluorine before and after being soaked in aqueous media of various pH values, since earlier work [6, 7] had shown that oleophobic properties imparted by this chrome complex were lost in aqueous detergent solutions. Results of analyses are recorded in Table VII. These results show that chromium is not lost, but that the fluorine content decreases even in acidic media and is almost completely lost in basic media. Loss in fluorine correlates with loss in oil repellency, which is fair after soakings in acid media but which disappears after soakings in basic media.

TABLE VII. Effects of pH on 80 × 80 Fabric Finished with Chromium Complex of Perfluorooctanoic Acid *

Sample	Weight %†	
	Cr	F
Original	0.31	0.40
After neutral soak (pH = 7)	0.44	0.21
After acidic soak (pH = 3)	0.35	0.24
After basic soak (pH = 9)	0.47	0.10
After soak in Fab detergent (pH = 8)	0.38	0.01

* Fabrics padded to 100% wet pickup with 1.5% solution of the chromium complex of perfluorooctanoic acid (FC-804) and dried in oven at 110° C. for 30 min.

† Average of duplicate samples.

Glycidyl Ethers

The glycidyl ethers, as prepared, had oxirane oxygen contents which were 75–80% of the theoretical values of 6.2 for 1,1-dihydroheptafluorobutyl, 3.5 for 1,1-dihydropentadecafluorooctyl, and 4.1 for 1,1,7-trihydrododecafluoroheptyl glycidyl ether. The byproduct in every case was a diether, $R_FCH_2OCH_2$-$CHOHCH_2OCH_2R_F$.

Of the three glycidyl ethers, only 1,1-dihydroheptafluorobutyl has been previously reported by Brey and Tarrant [3], who reported a 23% yield of glycidyl ether (b.p. 79° C. at 49 mm.; η_D^{25}, 1.3350) and a 24% yield of diether (b.p. 112–115° C. at 15 mm.; η_D^{25}, 1.3338). In this investigation, the crude 1,1-dihydroheptafluorobutyl glycidyl ether was fractionally distilled. Fraction 1 (b.p. 55–63° C. at 78 mm., η_D^{25}, 1.3315) had an oxirane oxygen content of 4.7%; Fraction 2 (b.p. 63–120° C. at 240 mm.) had an oxirane oxygen content of 5.1%; and Fraction 3 (b.p. 120° C. at 240 mm.; η_D^{25}, 1.3454) had an oxirane oxygen content of 3.02%. A second fractional distillation resulted in the following: Fraction 1 (b.p. 79° C. at 49 mm.; η_D^{25}, 1.3309), Fraction 2 (b.p. 79–90° C. at 49 mm.; η_D^{25}, 1.3365), and Fraction 3 (b.p. 90–105° C. at 15 mm.; η_D^{25}, 1.3480).

Fluoroalkoxy Substituted Ethers of Cellulose

Both acid and base catalysts effected the introduction of fluorinated moiety into cellulose by means of an ether linkage. Fluorinated glycidyl ethers could be used alone and in conjunction with suitable solvents when sodium hydroxide was the catalyst. When zinc fluoborate was the catalyst, the glycidyl ethers were always dissolved in methanol.

The 1,1-dihydroheptafluorobutoxyhydroxypropyl ether of cellulose, corresponding to a degree of substitution of 0.05, as determined by weight increase and fluorine analyses, was prepared under conditions of base catalysis. The resultant product had the color, tear strength, hand, structure, and general appearance approximately that of the original fabric. In addition, it possessed some degree of resistance to penetration of oil and water. This repellency was durable to 20-min. boils in aqueous alkaline soap solutions. As was to be expected, the dry crease recovery angle was the same as that of the untreated fabric (188° w + f), but its wet crease recovery angle was 277° (w + f).

The alkali-catalyzed method with the longer chain perfluoro glycidyl ether yielded products with excellent oil and water repellent finishes. With 1,1-dihydropentadecafluorooctoxyhydroxypropyl ethers of cellulose, excellent oil and water repellent finishes which were durable to 20-min. boils in alkaline soap solutions and to 30-min. boils in aqueous soap-soda solutions were obtained at a degree of substitution as low as 0.01. The oleophobic and hydrophobic properties were also durable to soakings in drycleaning solutions of Stoddard's[3] solvent which contained an alkaline drycleaning soap.

The 1,1,7-trihydrododecafluoroheptoxyhydroxypropyl ethers of cellulose, prepared by basic catalysis, showed good water repellency and some degree of resistance to penetration by oil. However, these ethers containing the omega-hydrogen did not possess the excellent oleophobic properties of the shorter chain 1,1-dihydroheptafluorobutoxyhydroxypropyl ethers of cellulose, which did not contain a terminal hydrogen atom.

Smaller weight gains were obtained with zinc fluoborate-catalyzed reactions with all three fluoroglycidyl ethers used in this investigation. However, excellent oil and water repellent properties were obtained in the instance of 1,1-dihydropentadecafluorooctoxyhydroxypropyl ether of cellulose. In fact, better oil and water repellent finishes were obtained on acid catalysis with shorter chain 1,1-dihydroheptafluorobutoxyhydroxypropyl ether than on base catalysis, and even after a 2-hr. soap-soda boil, the fabric still possessed improved oil repellency compared to the control fabrics.

Conclusions

Of all additive finishes investigated, the chromium complex of perfluorooctanoic acid offered the best oil repellency after exposure to weathering tests. However, this finish was not durable to aqueous launderings or to drycleanings in the presence of alkaline detergents and offered no protection against degradation of fabrics in soil burial tests. Perfluorobutyl acrylate used in at least 10% by weight in the padding bath gave an oleophobic finish which was maintained after a few aqueous launderings with mild detergents. Disadvantages of this finish were its poor resistance to dry soiling as compared to the perfluoro-metallic finishes and its lack of protection against degradation of fabric in soil burial tests. Best resistance to degradation of fabric in soil burial tests resulted from finishes applied through the use of aluminum triacetate and perfluorooctanoic acid, but these were not durable to aqueous launderings. All efforts to modify the aluminum-perfluorooctanoic acid finishing method to produce oleophobicity which was stable to aqueous launderings were to no avail.

None of the additive finishes evaluated in this investigation or the perfluorooctanoic ester of cellulose evaluated previously were durable to alkaline washes or drycleanings and, therefore, could not be used on fabrics which are to be subjected to commercial launderings or drycleaning cycles.

This report calls attention to the durability of oleophobic and hydrophobic finishes applied to cotton cellulose when the perfluoro moiety is linked to cellulose by an ether linkage. It is to be noted that only a very low degree of substitution is needed to provide desired repellencies, and that only a short perfluorinated chain is needed to impart hydrophobicity and oleophobicity. When the fluoro moiety contains an omega-hydrogen atom, only a small degree of resistance to wetting by oil and water is obtained, but the finish is durable to alkaline washes. A complete evaluation of fabric properties of the perfluoroalkoxy substituted propyl ethers of cellulose was not obtained at this time because of the high prices of perfluorinated alcohols used as reagents and lack of availability of perfluoro glycidyl ethers at this time. Further treatments, particularly with perfluoro diglycidyl ethers, are needed to complete a fundamental study of surface energies of fluorinated cellulose and to completely evaluate fabric properties.

Acknowledgments

The authors wish to express their appreciation to Mr. Paul J. Murphy for the fluorine and aluminum analyses, Mr. Harold P. Pastor for the acetyl analyses, Miss Dorothy C. Heinzelman for the spectroscopic chromium analyses, Mr. Verne W. Tripp and Miss Anna T. Moore for the electron micrographs, Miss Hilda M. Ziifle for the preparation of the graph, and members of the Textile Testing Investigations for physical testings.

Literature Cited

1. American Society for Testing Materials, (a) D39-59 (b) D1424-59, Philadelphia, Pennsylvania.
2. Benerito, Ruth R., Berni, R. J., and Fagley, T. F., TEXTILE RESEARCH JOURNAL **30**, 393–9 (1960).
3. Brey, Mary and Tarrant, P., *J. Am. Chem. Soc.* **79**, 6533–36 (1957).
4. Durbetaki, A. J., *Anal. Chem.* **28**, 2000–01 (1956).
5. Federal Specification CCC-T-191b, Method 5212, U. S. Govt. Printing Office, Washington, D. C. (1951).
6. Philips, F. J., Segal, L., and Loeb, L., TEXTILE RESEARCH JOURNAL **27**, 369–78 (1957).
7. Segal, L., Philips, F. J., Loeb, L., and Clayton, R. L., Jr., TEXTILE RESEARCH JOURNAL **28**, 233–41 (1958).
8. Tripp, V. W., Clayton, R. L., and Porter, Blanche R., TEXTILE RESEARCH JOURNAL **27**, 340–42 (1957).

Manuscript received March 18, 1960.

The Determination of Moisture in Wool with Karl Fischer Reagent

John R. Wilson and M. M. Sandomire

Western Regional Research Laboratory,[1] Albany, California

Abstract

A rapid method for determination of moisture in wool with the Karl Fischer reagent has been developed and tested. This method offers the advantages of precision, accuracy, and speed.

The ASTM convection oven method [1] and a vacuum oven method (70° C. for 40 hr. at 5 mm. Hg or less) were used for comparative purposes.

Formamide was used as the water-extracting solvent in the Fischer method. It is a powerful dehydrating agent capable of dehydrating activated alumina, silica gel, and other such desiccants. In addition, with direct titrations, formamide gives a more stable endpoint than methanol.

Apparatus and Reagents

A Senior Model Fisher titrimeter[2] qualitative unit was used for detection of the endpoint. Formamide and Fischer reagent were the same as those previously described [2]. Ground-glass-stoppered 250-ml. Erlenmeyer flasks were used for the Fischer moisture determinations [3]. Glass dishes with ground-glass covers were used for all oven moisture determinations [1].

Procedure

All wool samples were equilibrated for a minimum of 72 hr. at standard conditions [1]. Ground samples were equilibrated after grinding and all moisture values represent equilibrium moistures. For each material, triplicate determinations on each of two portions were made. Method 1 denotes the ASTM procedure, Method 2 the vacuum oven method used for comparison, and Method 3 the Karl Fischer method described.

Samples for all three moisture methods were weighed consecutively, with care to protect the material against moisture change. Sample weights ranged from 2.0 to 5.0 g. for the oven methods and from 0.3 to 1.5 g. for the Fischer method.

The samples for the Fischer method were covered with 20 ml. of formamide, stoppered, and placed in a forced-draft oven preheated to 70° C. Heating the sample for 15 min. gave a maximum moisture value. The samples were removed from the oven, stirred with a magnetic stirrer until cooled to room temperature, and immediately titrated in a sealed system to prevent contamination by atmospheric moisture. The endpoint was considered stable when it persisted for 30 sec.

Materials and Methods of Preparation

The following materials were prepared in two ways: by cutting into 1-in. squares (Preparation A) or by grinding in a Wiley mill to pass an 8-mesh screen (Preparation B). Both preparations were used on Samples 1 through 7; Preparation B only for Samples 8 through 13.

1. Wool-nylon flannel (20% nylon) dyed olive green
2. Yellow wool flannel
3. Wool flannel
4. Wool flannel, bleached (H_2O_2)
5. Wool flannel, severely bleached (H_2O_2)
6. Wool flannel, 1% modified epoxy resin
7. Wool flannel, 3% modified epoxy resin
8. Wool in grease, Rambouillet
9. Mohair in grease, Oregon Kid
10. Top Wool, ½ blood
11. Card sliver wool, from Columbia-Southdale ewe

[1] A laboratory of the Western Utilization Research and Development Division, Agricultural Research Service, U. S. Department of Agriculture.

[2] Mention of specific products does not imply recommendation by the Department of Agriculture over those of a similar nature not mentioned.

TABLE I. Average Moisture (for Two Portions in Triplicates) in Cloth and Nonwoven Wool, Obtained by Different Moisture Methods and Methods of Preparation (Units: Percentage Moisture)

Material	Moisture Method 1		Moisture Method 2		Moisture Method 3	
	Prep. A	Prep. B	Prep. A	Prep. B	Prep. A	Prep. B
			Cloth			
1	8.51	9.01	8.60	9.07	8.87	9.24
2	10.52	11.03	10.47	10.91	10.71	11.30
3	11.42	11.37	11.15	11.17	11.61	11.60
4	11.98	11.57	11.72	11.32	12.12	11.87
5	12.05	11.60	11.88	11.42	12.23	11.86
6	11.84	11.21	11.84	11.26	12.01	11.42
7	11.72	11.09	11.64	11.19	11.78	11.30
All cloth	11.15	10.98	11.04	10.91	11.33	11.23
			Nonwoven wool			
8	—	12.88	—	13.14	—	13.14
9	—	10.47	—	10.67	—	10.67
10	—	11.30	—	11.33	—	11.60
11	—	11.45	—	11.46	—	11.69
12	—	11.34	—	11.30	—	11.53
13	—	11.40	—	11.24	—	11.60
All wool		11.47		11.52		11.70

TABLE II. Standard Deviations for Triplicate Moisture Determinations (Units: Percentage Moisture) for Seven Types of Woven Cloth and Six Types of Nonwoven Wool

Moisture method	No. portions	Range of values of standard deviations with		Average standard deviation
		Prep. A	Prep. B	
		Cloth		
1	14	.031–.133	.021–.151	.082
2	14	.006–.085	0 –.072	.045
3	14	.012–.092	.020–.100	.065
		Nonwoven wool		
1	12	—	.026–.115	.079
2	12	—	0 –.125	.055
3	12	—	.006–.130	.064

12. Mohair scoured, Texas adult
13. Clean loose wool, Rambouillet

Results

Table I shows the average moisture values experimentally determined. Each average represents triplicate determinations on two portions of material. Statistical analysis of these data for each of the three methods was carried out to study relative precision of the methods (Tables II–III), to study relative accuracy of the methods (Tables IV–VI), and to determine the relative number of portions needed to provide a given level of precision for the average moisture of material pieces (Table VII).

Statistical Study

A standard deviation was computed for each set of triplicates and tabulated according to moisture method, material, method of preparation, and portion (Table II).

After conversion of standard deviations to logarithms, an analysis of variation was carried out to determine whether the set of data was homogeneous or differed significantly according to moisture method and other methods used. The analysis of variance for each moisture method is given in Table III for the cloth and in Table IV for the nonwoven wool. From these, no significant variation in the standard deviations may be ascribed to the different materials used or to the method of preparation of the cloth.

From the combined results for all moisture methods, in the lower part of Tables III and IV, the interpretation is similar for these factors. However, a significant difference is found among the average standard deviations obtained for the three moisture methods. That is, the *variability of Method 1* is significantly greater than for the other methods, while Method 3 just borders being significantly higher in variability at the 5% probability level than Method 2. Thus, the data for the different methods should not be pooled in obtaining average standard deviations. The average given separately in Table II for each moisture method was obtained by pooling

values for the different materials as well as for the methods of preparation in the case of the cloth.

An analysis of variance of the data of Table I for each method is given in Table V. It may be noted that the square root of the mean square for determinations agrees with the average standard deviation in Table II. The variation between duplicate portions is significantly greater than among triplicate

TABLE III. Analysis of Variance of Standard Deviations for Triplicate Moisture Determinations (in Logarithmic Units) for Seven Types of Woven Cloth, in Squares and Ground

Each moisture method

Source of variation	Degrees of freedom	Mean squares for Method 1	Method 2	Method 3
Materials (M)	6	.0400	.1484	.0449
Preps (P)	1	.0176	.1013	.2967
MP interaction	6	.0281	.1062	.0648
Portions	14	.0669	.0790	.1078
Total	27			

All moisture methods

Source of variation	Degrees of freedom	Mean square
Materials (M)	6	.0712
Preps (P)	1	.1777
MP interaction	6	.0211
Methods (Me)	2	.7980*
Me × M interaction	12	.0811
Me × P interaction	2	.1190
Me × MP interaction	12	.0890
Portions	42	.0845
Total	83	

* Significant at 1% probability level.

TABLE IV. Analysis of Variance of Standard Deviations for Triplicate Moisture Determinations (in Logarithmic Units) on Seven Types of Cloth and Six Types of Wool, Prepared by Grinding Only (Prep. B)

Each moisture method

Source of variation	Degrees of freedom	Mean squares for Method 1	Method 2	Method 3
Materials (M)	12	.0253	.1205	.0766
Portions	13	.0695	.0700	.1111
Total	25			

All moisture methods

Source of variation	Degrees of freedom	Mean square
Material (M)	12	.0676
Methods (Me)	2	1.0153*
Me × M interaction	24	.0773
Portions	39	.0835
Total	77	

* Significant at 1% probability level.

TABLE V. Analysis of Variance of Moisture Determinations (Units: Percentage Moisture)

For seven types of woven cloth, in squares and ground, by each moisture method

Source of variation	Degrees of freedom	Mean squares for Method 1	Method 2	Method 3
Materials (M)	6	13.84	11.98	12.95
Preps (P)	1	.5767	.3814	.2294
MP interaction	6	.7493*	.5934*	.5890*
Portions	14	.0339*	.0303*	.0265*
Determinations	56	.0067	.0021	.0041
Total	83			

For six types of wool, ground only, by each moisture method

Source of variation	Degrees of freedom	Mean squares for Method 1	Method 2	Method 3
Materials	5	3.66	4.21	6.04
Portions	6	.0410*	.0303*	.0535*
Determinations	24	.0063	.0030	.0043
Total	35			

* Significant at 1% probability level.

TABLE VI. Variance Components of Moisture Determinations of Cloth, in Squares (Prep. A)

Moisture method	Source of variation	Mean square, s^2	Variance component, σ^2	Estimated no. of determinations per portion, k
1	Portions	.0418	.0120	
	Determinations	.00566	.0057	<1
			.0177	
2	Portions	.0265	.0079	
	Determinations	.00274	.0027	<1
			.0106	
3	Portions	.0345	.0093	
	Determinations	.00654	.0065	<1
			.0158	

values from the same portion; the interaction of Materials and Method of Preparation is significantly greater than the variation ascribed to duplicate portions.

This inconsistency may be noted by inspection of the averages in Table I. Thus, depending upon the material involved, grinding of the cloth yielded either a higher or lower moisture than when whole cloth was used. For any material, this relation is repeated with all three moisture methods. For this reason statistical study of the data for the nonwoven wool, prepared by grinding, was not continued.

Because of the differences in variability of the different methods, a comparison of the method averages may not be precise, in terms of probabilities. But, since such a combined analysis revealed a very large difference among the averages obtained with the three methods, the fact of the differences should not be overlooked. From Table IV it is found that for cloth with Preparation A, Method 1 resulted in an average increase of 0.1% moisture, and Method 3 resulted in an average increase of about 0.3% moisture. This analysis suggested, further, the existence of a Method–Material interaction. That is to say, the difference obtained with the two moisture methods is not constantly 0.1 or 0.3 for all materials, but fluctuates significantly from these for different materials.

It was noted above that preparing cloth by grinding did not improve the precision of the moisture determination, while at the same time it led to a difference in the average moisture obtained. This relation between results obtained by the two methods of preparation was similar, irrespective of which of the three moisture methods was used. For this reason, an estimate of the number of measurements required to obtain a desired precision was made with data obtained for squares of cloth only (Prep. A), by the following method.

The general formula for estimating number of measurements required on a single type of cloth to obtain a preselected measure of precision (expressed as a standard deviation) is:

$$s^2 = \frac{\sigma^2(p)}{n} + \frac{\sigma^2(d)}{nk}$$

where $\sigma^2(p)$ = estimated variance component for portions, $\sigma^2(d)$ = estimated variance of determinations, s^2 = square of required standard error of an average moisture, n = number of portions required, and k = number of determinations per portion required.

There is, thus, one equation with two unknown values, n and k. It may be shown that the total number of determinations, nk, is minimized when k is estimated first so as to bring about the following relation:

$$\frac{\sigma^2(d)}{k} \sim \sigma^2(p)$$

The variance components required were computed in Table VI from the analysis of variance of the data for Prep. A only. It was found that the value of k need not exceed one.

Then by selection of a series of values of s, as listed in Table VII, the number of portions, n, of a material to be taken to assure the desired precision was computed by arranging the first equation in the form

$$n = \frac{\sigma^2(p) + \sigma^2(d)}{s^2}$$

The values of n are the number of portions required with one determination per portion.

TABLE VII. Number of Portions in Squares (Prep. A) Required to Assure the Indicated Precision of the Average Moisture of Material Pieces, With One Determination per Portion

Standard error of an average of nk determinations (in original units of percentage moisture)	No. portions of a material, n, according to moisture method used		
	Method 1	Method 2	Method 3
.04	11	7	10
.05	7	5	7
.06	5	3	5
.07	4	2	3
.08	3	2	3
.09	2	2	2
.10	2	1	2
.11	2	1	2
.12	1	1	1

Summary and Discussion

The Fischer method has several advantages over oven methods. It is rapid; on a routine basis it requires 10–15 min./sample. The value determined represents water, not a loss in weight. The method is calibrated against a weighed amount of water.

A precision of ±0.1% is attained with 2 portions; 7 portions will give a precision of ±0.05%. Increasing the size of the portion in the Fischer determination also increases the precision. The volume of formamide used will also have to be increased in proportion to the increase in sample size. The volume of formamide used must be large enough to cover the sample completely.

The use of formamide in the Fischer method assures a complete extraction of water with a minimum of heating. Interfering substances give little or no trouble.

It was found that the moisture in woven wool should be determined with squares of cloth rather than ground material. Grinding changes moisture content in an irregular manner which cannot be predicted. Further, precision is not improved by grinding.

Preliminary work has been done on a large sample of material (20–30 g.) in 200 ml. of formamide, and aliquots were taken for the determination of moisture.

This method should prove valuable as a calibration method for physical determinations of moisture in wool.

Literature Cited

1. American Society for Testing Materials. Part III, 1952, 4 (a) (1944).
2. McComb, E. A. and McCready, R. M., *J. Assoc. Offic. Agr. Chemists* **35**, 437 (1952).
3. McComb, E. A. and Wright, H. M., *Food Technol.* **8**, No. 2, 73 (1954).

Manuscript received April 4, 1960.

Some Observations on Kinetic Friction of Jute

A. C. Chakravarty

Technological Research Laboratories, Indian Central Jute Committee, Tollygunge, Calcutta 40, India

Abstract

A horizontally rotating flat surface and a pair of fiber pads, suspended from a torsional system, sliding over it were used to measure the coefficient of kinetic friction, μ_k, of jute. μ_k of jute sliding over glass ranged between 0.20 and 0.35. It was dependent upon (a) normal load, (b) speed of sliding, (c) moisture content, and (d) physical and chemical treatment of the fiber. Values obtained with porcelain, stainless steel, and wood surfaces were nearly equal to that obtained with glass. Interfiber friction using a fiber felt as the sliding surface was found to be considerably higher than these values.

Introduction

Friction between fiber and other surfaces as well as interfiber friction play an important part during processes involved in the conversion of a mass of textile fiber into finished products. The kind of friction that comes into play is primarily kinetic. Most of the past studies were based on the "stick-slip" method where single filaments were used and the relative motion stopped after very small traverses. While such studies were undoubtedly of importance, the experimental techniques, as was pointed out by Lord [10], were often difficult and tedious. He showed that, in general, the measurement of frictional forces using fiber assemblies rather than single filaments offered possibilities of obtaining representative and reproducible results because many of the effects of large variation in the surface characteristic of individual filaments were reduced. This observation is applicable to multicellular vegetable fibers like jute whose individual filaments vary widely in their physical properties. Therefore it was considered worthwhile to study some aspects of the kinetic friction of jute using an assembly of individual filaments that slid continuously for any length of time over a standard surface. The rotating disc and the slider method of Bowden and Tabor [3] used in their studies of metallic friction readily suggested itself. However, the apparatus actually used retained only the rotating disc to provide a continuously moving surface and instead of their cantilever and spring assembly, the torsional displacement of a steel wire was utilized for measuring the frictional force. Previous investigations by other workers [5, 6, 8, 9, 13, 14] were mostly aimed at the verification and/or modification of the well-known Amonton's law of friction when applied to fibers. We were primarily concerned with the study of the frictional forces of jute as they were affected by the various physical and chemical agencies that were expected to be commonly met in the industry.

Experimental Procedure

A heavy aluminum disc A, as shown in Figure 1, was axially rotated by means of an electric motor. Several speeds of rotation were obtained through a suitable gear assembly. The rubbing surface B, in the form of a disc, was rigidly fixed upon A. A steel wire S was clamped at one end to the heavy frame E of the apparatus. The lower end of the wire was secured to I, which consisted of a heavy cylindrical mass at the center and two light but rigid arms of equal lengths. The suspended system was adjustable to lie coaxial with A. The two arms had two double-tiered perforations on each side, equally spaced from the center. Two wooden yokes CC, shaped like a π, were inserted through these holes to stand freely and vertically upon the rotating surface B. The filaments under test were mounted on two identical pads FF, each of which consisted of a small rectangular piece of light wood topped with a strip of plastic. Two slots were punched into the other side of the wooden block so that, when properly placed, the two legs of the yokes CC fitted loosely into them. The two pads FF were placed with the mounted filaments touching the rubbing surface B. Suitable loads W, in addition to the

constant weight of the yokes and the pads, could be placed on the latter as shown in the figure. As B rotated, it dragged the pads FF along with it due to frictional forces which, transmitted through the freely fitted yokes, formed a couple giving rise to a torsional displacement of the steel wire S. An angular measure of this displacement could be obtained with the help of two pointers attached at the two ends of the arms of I and a scale pasted outside G. G was a rectangular chamber with glass sides that covered the whole apparatus, making it practically air-tight. The moment of inertia of I was so chosen, by adjusting the central mass, as to avoid resonance of torsional oscillations of the suspension with the stick-slip frequencies of the sliding system. As our object was to obtain an average value of the frictional forces over a length of time, the torsional system was further damped by incorporating two dampers DD fixed at the ends of the two arms of I. The lower ends of DD, consisting of two fiber brushes, were suspended in a viscous mineral oil contained in a suitable vessel V at the base.

The relative humidity of the air inside the glass chamber was controlled by placing appropriate solutions in two flat-bottomed glass dishes, HH, within E and periodically forcing air of the required humidity through G. All wooden parts of the apparatus were thoroughly impregnated beforehand with paraffin wax to render them moistureproof. Each test sample was allowed to remain overnight inside the chamber at a particular humidity. Sulfuric acid and its solutions of different strengths were used to provide the required moisture content of the air inside the chamber.

Theoretical Considerations

The equation of motion of a similar system has been considered by Guthrie and Oliver [7], who showed that if k_1 is a constant of the apparatus, and the kinetic frictional force F_k be assumed constant

$$F_k = \tfrac{1}{2}k_1(\phi_s + \phi_b)$$

where ϕ_s = angular deflection of the wire at the instant slip occurs (i.e., corresponding to static friction) and ϕ_b = the same when the slip stops (i.e., braking friction). Thus an average of the oscillatory deflections may be considered to give a fair index of the kinetic friction developed during the slip. As has already been stated, this averaging was done very satisfactorily by suitably choosing

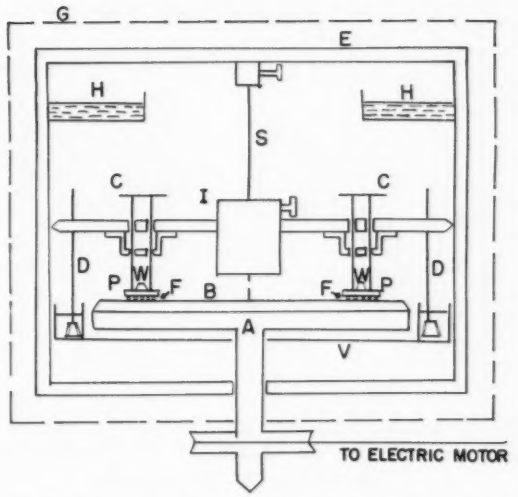

Fig. 1. Apparatus for measuring kinetic friction of jute.

the moment of inertia of the torsional system and introducing suitable damping so that the deflection at any particular speed of rotation remained practically constant. As a check, oscillatory deflections of the torsion wire when the dampers were inoperative were plotted on a graph; the mean curve was approximately linear and parallel to the time axis; it followed very closely the curve obtained with the values of deflections when the dampers were operative. However, discrepancies appeared at higher values of relative humidity of the air inside the chamber. For this reason, all observations, except where moisture content was the variable factor, were made at zero percent relative humidity.

The modulus of rigidity of the steel wire was determined by the torsional oscillation method. Mean distance of the pads from the center of rotation as well as the length and diameter of the steel wire being known, the constant of the apparatus could easily be calculated. Effective weight of each of the pads was the normal load, R, acting on the fibers; therefore, the coefficient of friction $\mu_k = F_k/R$ for a particular set of observations.

Results and Discussion

Twenty-five jute filaments were mounted equally spaced over the plastic strip. Ten varieties of jute of different Quality Ratios[1] and five pairs of pads

[1] $\text{Q.R.} = \dfrac{\text{Breaking strength (lb.)}}{\text{Grist (lb.)}} \times 100.$

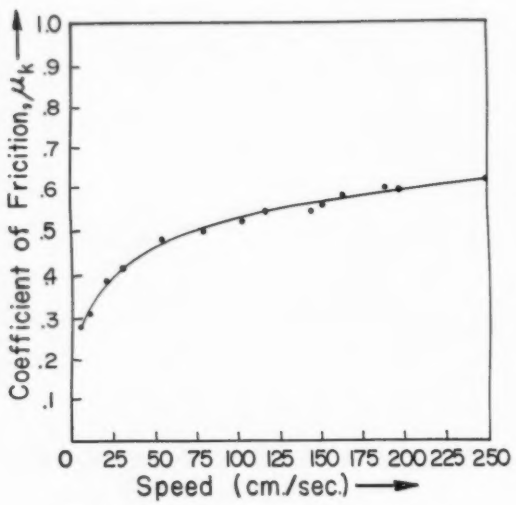

Fig. 2. Kinetic friction of jute at different speeds of sliding.

for each sample were used to arrive at a mean result. A disc of plate glass formed the standard sliding surface. The glass surface was cleaned by benzene and then polished with a grease-free chamois leather before each test. No extra load was placed on the filament pads, each of which had an effective weight of 2.20 g. The constant speed of rotation gave a linear speed of 4.96 cm./sec.

Effect of Time, Mounting, and Direction of Sliding

In a preliminary test two samples of jute were tested for any possible time effect. Sliding, both ways, was carried on for periods up to 1.75 hr. No significant effect was encountered. No significant results were obtained for (a) difference in alignment of mounted filaments (at 0°, 45°, and 90° with the direction of sliding) or (b) difference in the apparent area of contact (assumed to be proportional to the number (2, 3, 5, 10, 25, 50, and 100) of filaments mounted) and (c) fibers from different regions along the plant.

The mean values of μ_k for the ten different samples, with filaments from the middle of the fiber strand, covered a range from 0.20 to 0.35.

Effect of Speed of Sliding

The coefficient of kinetic friction was found to increase with increasing speed, the rate of increase decreasing as speed increases (Figure 2). It was not possible with this instrument to investigate the region between the speeds of 0 and 4.96 cm./sec., but it might safely be stated that the fact that static friction was higher than the kinetic friction would be valid only at low speeds of sliding. As the speed increased, the coefficient of kinetic friction might approach that of static friction, and after overtaking the latter at a certain point might reach a value which would be considerably higher than the coefficient of static friction. Wood [19], studying artificial fibers, found a marked increase in frictional force as speed increased. However, contrary to our results, he found a greater rate of increase at the higher speeds. Results obtained by Röder [15] for cotton, Breazeale [4] for cotton yarn, and Lyne [11], Taylor [18], and K. Schlein [16] for acetate yarn were similar to those reported here. Taylor stated that, for cotton, kinetic friction at carding speeds was greater than static friction. Röder had, on the other hand, indicated that, when kinetic friction was greater than the static friction, it was a general rule that the resultant sliver was poorly carded.

According to Miszkis and Tabor [12], even in the absence of mutual solubility of the rubbing surfaces, adhesion between them plays a fundamental part in friction. This may be true for thermoplastic fibers, which would then show less friction at higher speeds due to softening caused by frictional heat. However, for jute the major contribution to friction would probably be from cohesion between the asperities of

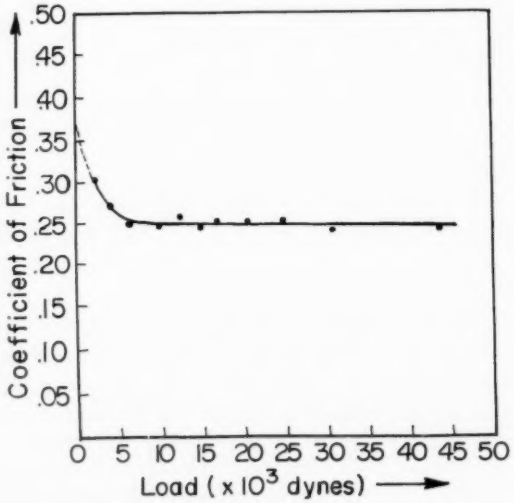

Fig. 3. Kinetic friction of jute at different normal loads.

the two sliding surfaces, i.e., due to roughness alone [2].

Effect of Normal Pressure

Tabor [17] showed that, at high loads, the deformation of solids being more plastic, the area of real contact was roughly proportional to the normal load, so that Amonton's law was obeyed. At light loads, the area of contact was more nearly elastic than plastic and depended on the size and shape of the specimen and on the number of points of contact. Thus μ_k was no longer constant but increased steadily as the load was reduced. Results obtained with jute sliding over glass, as shown in Figure 3, corroborate this view. The extrapolated dotted curve indicates a possible high value of μ_k even at zero load. This is difficult to explain except for a fiber–fiber surface, where the friction at zero load would be due to the residual cohesion between asperities or minute side-branches of the individual filaments.

Effect of Relative Humidity

For jute, hygroscopic as it is, the coefficient of kinetic friction was found to vary almost linearly with the relative humidity of the surrounding air. This is shown in Figure 4, with a plot of the values of μ_k corresponding to the percentage moisture content of jute at different relative humidities. Results of similar nature were also reported by Bandopahdyay [1] for static friction.

Effect of Different Agents

Friction being primarily a property of the surface, any treatment that brings about its modification with or without any chemical change in the fiber substance is expected to influence it. In Table I are given several values of μ_k when jute was treated with different agents. Two different sets of samples were tested for the two different series. It is interesting to note that, except when treated with higher strengths of the agents, the treatments known to produce distinct chemical reaction in the fiber substance do not bring about any marked change in kinetic friction. With the higher strengths, destructive changes are brought about and in the process may obliterate most of the surface irregularities, resulting in a fall in friction, as has been observed.

Removal of fats and waxes from raw jute is likely to expose a greater number of asperities on the surface of the filaments. This was probably the cause

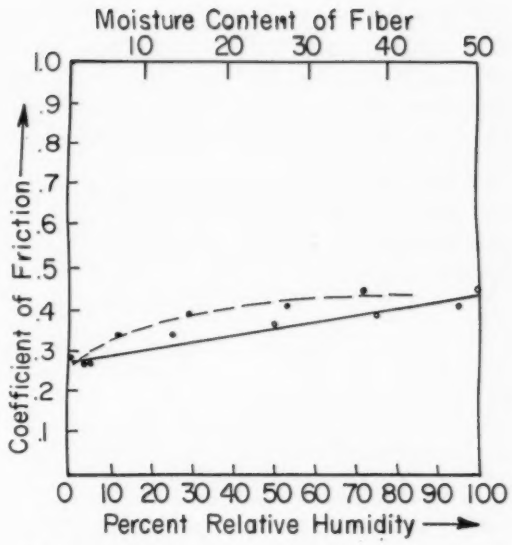

Fig. 4. Kinetic friction of jute versus relative humidity (———) and versus corresponding moisture contents of the fiber (- - - - - -).

of the increase in the value of μ_k for such samples. Fibers treated with a batching emulsion (30% of the fiber wt./wt.) could be expected to contain a very thin layer of mineral oil after moisture was evaporated inside the dry chamber. The low value of μ_k for batched fiber might be due to the lubricating action of this film. However, if the tests were carried out at higher relative humidities, the effect of moisture content would overcome the lubricating action of the oil film and, at ordinary humidity conditions met in the mills, batched fiber might have a tendency to show greater friction than raw jute. Another significant result was that while jute had less friction when treated with batching emulsion, it was considerably higher when it was treated with either the emulsifier or the mineral oil (in proportion to their contents in batching emulsion) separately. Oils of different viscosities, as well as similar emulsions made with them, when added to jute did not produce any conclusive result. However, it appeared that oils of medium viscosities (and not the light mineral oils) were best suited to prepare batching emulsions without unduly increasing kinetic friction at ordinary humidities. Extensive studies with oils of different viscosities in larger number than were available for this test may lead to some conclusive results of great importance for the industry.

Other Fibers

Only one sample of each of several fibers of different origins was available for study. It was thus quite likely that the average values obtained with a larger number might be different from those given in Table II.

If other factors do not intervene, cotton and acetate rayon as well as wool and nylon having the same coefficients may be expected to produce well-blended yarns.

Effect of Different Sliding Surfaces

Samples of jute were also tested against five different surfaces. Though differences in the surface condition in the same substance will influence results, it was interesting to note that coefficients of kinetic friction of jute and substances over which the fiber was most likely to slide along during its manufacture into finished goods were approximately equal to one another. These substances were stainless steel, porcelain, and wood. The set-up of the apparatus did

TABLE I. Coefficients of Kinetic Friction of Jute Treated with Different Agents (Mean Values With their Standard Errors)

Treatment a		Treatment b	
Raw (untreated)	0.26 ± .004	Raw (untreated)	0.28 ± .001
Hemicellulose removed by alkali treatment	0.24 ± .003	Dewaxed and defatted	0.33 ± .001
Delignified	0.26 ± .004	Batched	0.24 ± .001
Treated with 1% H_2SO_4(wt./wt.)	0.24 ± .003	Treated with mineral oils of (i) low viscosity	0.33 ± .002
Treated with 10% H_2SO_4(wt./wt.)	0.20 ± .001	(ii) medium viscosity	0.26 ± .001
Woolenized	0.21 ± .002	(iii) high viscosity	0.52 ± .002
Treated with formaldehyde (37–41%)	0.26 ± .002	Treated with grease	0.62 ± .002
Treated with saturated solution of NaCl	0.25 ± .002	Treated with glycerine	0.66 ± .002
Boiled in water	0.26 ± .001	Treated with jute wax, traces only	0.28 ± .001
		Same, 30% of fiber mass	0.35 ± .001
		Emulsifier treated	0.55 ± .004
		Treated with batching emulsions made with	
		(i) oil of low viscosity	0.41 ± .002
		(ii) oil of medium viscosity	0.28 ± .001
		(iii) oil of high viscosity	0.39 ± .002

TABLE II. Coefficients of Kinetic Friction of Different Fibers and of Jute Sliding over Different Substances

Fiber (In descending order)		Surface	
1. Cuprammonium rayon	0.49 ± .012	1. Glass	0.28 ± .008
2. Sisal (processed)	0.47 ± .001	2. Porcelain	0.31 ± .005
3. Linseed flax	0.46 ± .001	3. Wood	0.32 ± .005
4. Cotton (raw)	0.43 ± .003	4. Stainless steel	0.34 ± .008
5. Acetate rayon (coml.)	0.43 ± .003	5. Jute felt	0.85 ± .021
6. Hemp	0.41 ± .002		
7. Human hair (degreased)	0.38 ± .002		
8. Silk	0.36 ± .005		
9. Coir	0.35 ± .001		
10. Viscose rayon	0.32 ± .008		
11. Nylon	0.29 ± .008		
12. Wool (processed)	0.29 ± .004		

not permit the use of a rotating fiber surface without encountering excessive cohesion and intertwining. Thus no reliable and reproducible result could be obtained for interfiber friction. However, a high value of μ_k was obtained with a rotating pad made of short lengths of jute fiber, chemically treated and heavily pressed to form a feltlike structure. The surface was thus made of randomly oriented filaments with numerous loose ends that got caught into the test filaments. Evidently this was the reason for the high value; actual interfiber friction may be expected to be lower than this value.

Summary

Kinetic friction of jute was determined by sliding an assembly of filaments mounted on pads suspended from a torsional system over the plane surface of a horizontally rotating glass disc. The following results were obtained:

1. Coefficient of kinetic friction, μ_k, was found to be independent of the apparent area of contact, of the direction, and of period (up to 1.75 hr.) of sliding.

2. It increased with increase of speed, at first rapidly and afterwards at a slower rate, with the distinct possibility of overtaking at a certain speed the coefficient of static friction.

3. At higher values of normal load, μ_k was independent of load but at the lower ranges, μ_k increased with decreasing loads.

4. μ_k increased approximately linearly with the increase of relative humidity of the surrounding air.

5. Mild chemical treatments did not affect kinetic friction to any great extent, while drastic treatments reduced it.

6. Removal of wax and fat increased friction.

7. Friction was greater when jute was treated separately with the components of batching emulsion than when it was treated with the emulsion itself. Oils of medium viscosity appeared to be most suitable for batching purpose; they ensured adequate softening without unduly increasing kinetic friction.

8. Values of coefficient of kinetic friction of jute sliding over glass, porcelain, stainless steel, and wood did not differ much from one another, while interfiber friction obtained with a fiber felt surface was much higher.

Literature Cited

1. Bandopadhyay, S. B., Textile Research Journal **21**, 659 (1951).
2. Bikerman, J. J., *J. Appl. Phys.* **30**, 448 (1959).
3. Bowden, F. P. and Tabor, D., "The Friction and Lubrication of Solids," Oxford University Press (1950).
4. Breazeale, F., Textile Research Journal **17**, *27* (1947).
5. Chapman, J. A., Parcoe, M. W., and Tabor, D., *J. Textile Inst.* **46**, P1 (1955).
6. Gralen, N., Olofsson, B., and Lindberg, J., Textile Research Journal **23**, 623 (1953).
7. Guthrie, J. C. and Oliver, P. H., *J. Textile Inst.* **43**, T579 (1952).
8. Howell, H. G., *J. Textile Inst.* **42**, T521 (1951).
9. Howell, H. G. and Mazur, J., *J. Textile Inst.* **44**, T59 (1953).
10. Lord, E., *J. Textile Inst.* **46**, P41 (1955).
11. Lyne, D. G., *J. Textile Inst.* **46**, P112 (1955).
12. Miszkis, K. W. and Tabor, D., "Friction in Textiles," London, Butterworth's Scientific Publications (1959).
13. Olofsson, B., Textile Research Journal **20**, 476 (1950).
14. Postle, L. J. and Ingham, J., *J. Textile Inst.* **43**, T77 (1952).
15. Röder, H. L., *J. Textile Inst.* **46**, P85 (1955).
16. Schlein, K., *J. Textile Inst.* **45**, A61 (1954).
17. Tabor, D., *Nature* **173**, 899 (1954).
18. Taylor, D. S., *J. Textile Inst.* **46**, P59 (1955).
19. Wood, C., *J. Textile Inst.* **42**, T338 (1951).

Manuscript received March 14, 1960.

Studies of the Movement of Wool Fibers in Fabrics During Felting, with Particular Reference to the Permanency of Pleats

Part III: Felting in a Woolen Fabric[1]

K. Rachel Makinson

C.S.I.R.O. Wool Research Laboratories, Division of Textile Physics, Ryde, N.S.W., Australia

Abstract

The changes of configuration and the movements of fibers in a woolen fabric during washing have been studied by the use of red-dyed tracer fibers and a pattern of printed lines. The behavior of isolated fibers and of yarns when wetted has also been studied. The dominant mechanism of felting has been found to be one for which the name "release" mechanism is proposed: rootward migration of some fibers releases interfiber constraints and allows short lengths of many fibers to untwist from their helical shape to a limited extent. This is associated with very rapid shrinkage of the fabric. This mechanism is present but is usually much less important in worsteds.

Pleats are even more rapidly spoiled by washing when this mechanism of felting is dominant than when Shorter's mechanism (see Part II) is dominant.

The definition of felting is discussed.

Materials and Methods

The woolen fabric used had the following construction:

Fiber diameter (mean)	19.7 μ
Coefficient of variation of diameter	30.9%
Yarn linear density	89 tex
Twist	11 turns/in.
Ply	Single
Weave	Plain
Ends	26/in.
Picks	24/in.

The fabric was received in the unfinished (grey) state as it came from the loom, and was given no setting treatment other than that received incidentally when it was printed (q.v.).

The techniques employed were essentially the same as described in Parts I and II. The undyed wool used to make the fabric was blended with 0.5% of red-dyed wool of the same quality. The paths of the red fibers, made visible by immersion of the fabric in *o*-dichlorobenzene, were recorded photographically. Part of a set of photographs, taken at various stages of washing, is reproduced in Figure 1. The fiber paths shown in Figure 2 were traced from this set at a magnification of 7×, and are reproduced here at 1.3×.

The fabric was printed as required with patterns of fine black lines, which were used to detect small displacements of individual fibers, as described in Part I, and to provide a scale for the determination of fabric shrinkage. Usually the printing paste contained benzyl alcohol and the print was fixed by steaming the fabric for a few minutes at 121° C.; sometimes a paste was used in which formic acid [4] was the solvent instead of water, and in these cases the fabric was not steamed. The formic acid was rinsed out with water. There was no noticeable difference in the behavior of samples printed by the two techniques.

Samples of fabric were felted in either of two ways: they were rubbed in warm alkaline soapsuds on a scrubbing board or they were milled with soap in laboratory-scale stocks. Felting was much slower in the stocks, but there were no obvious differences between the final felts.

[1] Parts I and II appeared in TEXTILE RESEARCH JOURNAL **29**, 432, 439 (1959).

Results

Conspicuous Differences between this Woolen Fabric and the Worsted Studied Previously

Shrinkage.—When this woolen fabric is washed it shrinks and felts faster, and under smaller forces, than the worsted whose behavior was described in Parts I and II. Even during a very light wash (20 rubs on the scrubbing board or 5 min. in the stocks), and even at the smallest detectable level of microfelting (0.1 mm.), the fabric shrinks appreciably. During prolonged milling the rate of shrinkage of the woolen has never been found to be less than that of the worsted, and is usually greater, so that the

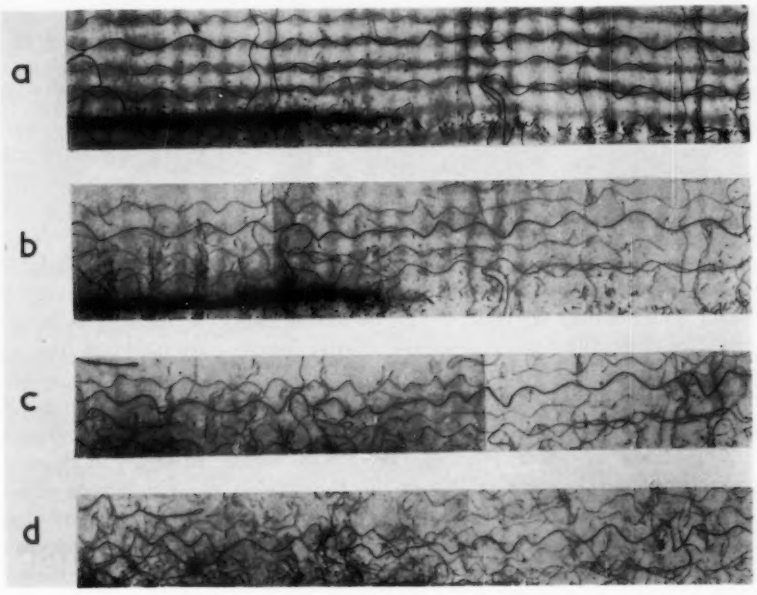

Fig. 1. A region of woolen fabric (a) before washing; (b), (c), (d) at successive stages of washing. Magnification 4×.

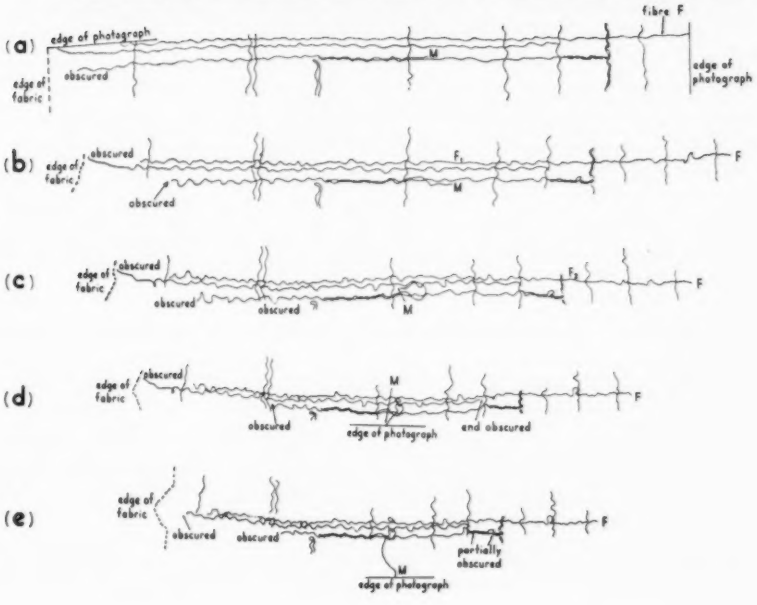

Fig. 2. Tracings of fibers in woolen fabric (a) before washing; (b), (c), (d), (e) at successive stages of washing. These fibers pass through the region shown in Figure 1. Magnification 1.3×.

total felting shrinkage for any time of milling up to several hours is greater in the woolen.

In the worsted an induction period, during which there was little or no shrinkage, was observed at the beginning of felting, as described in Part II. During this period microfelting occurred, the fibers undergoing small rootward migrations. An induction period has not usually been observed in the woolen; work in progress suggests that the conditions of milling determine whether it occurs. In contrast, it has been observed in the worsted under all conditions so far studied.

The shrinkage corresponding to any particular degree of microfelting is very much greater in the woolen than in the worsted; Table I illustrates this. To obtain the data for this table the observer estimated the "degree of microfelting" by eye as the mean displacement of those fibers which had migrated. This is satisfactory for the present purpose. Exact measurement would not only be difficult but would be of doubtful value, since the relative importance of distance moved, number of fibers moving, and variation in the distance moved by individual fibers has not yet been determined.

Appearance of felted fabric.—There is a more conspicuous development of "cover" in the woolen than in the worsted.

Shapes of fibers in the fabric.—When the woolen fabric is washed, the helices formed by individual fibers contract in length and increase in diameter. This effect is observable also in the worsted fabric, but it is very much less marked there. It is illustrated for the woolen in Figure 2, which shows the projected paths of four neighboring fibers before and at various stages of washing. The positions of some transverse fibers have also been indicated, as markers. It is noticeable that all the helices have contracted considerably and fairly uniformly on washing; so has the whole fabric, as is shown by the spacings of the transverse fibers. The helices have increased in diameter, and in the later stages of washing have become irregular. Only one of the fibers (M) has migrated any considerable distance.

The relatively taut lengths of fiber observed in the worsted after washing (region BC of Figure 2 in Part II) are rarely seen in the woolen fabric, and they do not persist from wash to wash as in the worsted. The regions F1 and F2 of the long fiber F in Figures 2b and 2c respectively are typical of the "taut" fibers observed in the woolen.

Behavior of pleats.—The wet fabric was folded along either the warp or the weft, held between glass plates under moderate pressure and steamed at 121° C. for 5 or 10 min. The pleats so formed were not perceptibly spoiled if the fabric was dropped into initially boiling water and left undisturbed while the water cooled. They were rapidly and completely destroyed by very light hand washing, even without scrubbing; washing so light that it did little damage to pleats in the worsted fabric almost obliterated pleats in the woolen. The associated microfelting was less than $\frac{1}{4}$ mm. In contrast, microfelting of about 1 mm. was necessary to cause equal damage to pleats in the worsted fabric.

The shapes of fibers at the pleats and in the unpleated regions of the woolen fabric were examined by cutting snippets of yarn and teasing them out, as described for the worsted in Part I. Samples were taken from unwashed fabric and from fabric washed until the pleats were almost undetectable. There were no conspicuous differences in the shapes of fibers from the woolen and the worsted after similar treatment, except that the effect of washing was produced more rapidly in the woolen. In both fabrics the pleated shape, described in Part I, of fibers from the unwashed sample was largely destroyed in fibers from the washed sample, but it could be restored to a considerable extent by relaxation of the indi-

TABLE I. Comparison of Shrinkage of Woolen and Worsted Fabrics at Comparable Levels of Microfelting

Number of washes		Microfelting, mm.		Shrinkage of woolen, %		Shrinkage of worsted, %	
Woolen	Worsted	Woolen	Worsted	Warp	Weft	Warp	Weft
1	2	$\frac{1}{2}$–1	$\frac{1}{2}$–1	3.9	2.7	1.8	0.0
2	3	1	$1\frac{1}{4}$	6.4	6.2	1.8	0.7
3	4	2	2	10.0	9.6	3.0	2.0

The mean degree of microfelting was estimated by eye (see text). All shrinkages were measured from the relaxed state. The samples were conditioned at 68° F., 65% RH for 4 days before each measurement. Each wash consisted of 100 rubs along the warp and 100 rubs along the weft in hot soap suds on a scrubbing board.

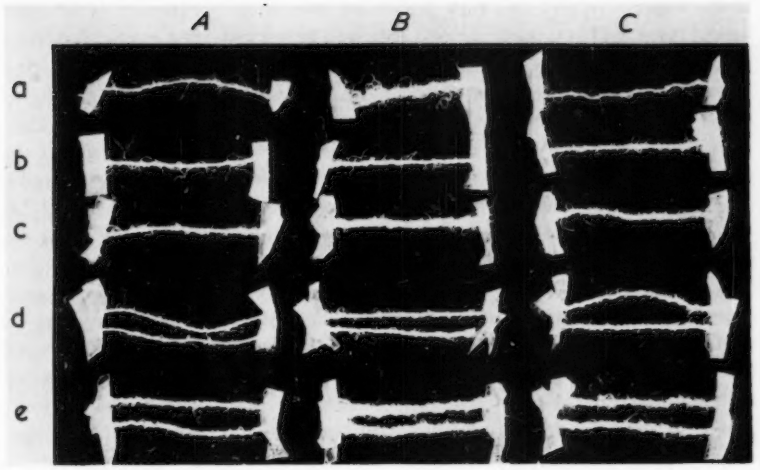

Fig. 3. The effect of releasing short lengths of various yarns in water. Magnification 0.75×. Yarns photographed in "air-dry state" after indicated treatments. Initial lengths not identical. Pieces fastened down loosely for photography. *Treatment.* A, original state; B, released freely in water; C, released with ends held to prevent untwisting. *Yarns.* a, singles worsted; b, doubled worsted; c, woolen; d, doubled worsted; e, woolen. a, b, c as spun; d and e taken out of fabrics.

vidual fibers in water. For the woolen, therefore, the conclusion reached in Part I for the worsted holds: the apparent loss of set is more correctly described as a masking of the permanent set by the superposition of a cohesive set.[2] The shape of fibers from the unpleated regions was only slightly changed when the fabric was washed to this extent, the "crimp" of the projected helices being a little deepened.

The Strains in the Fibers

It is clear that the mechanism of felting in this woolen fabric is essentially different from that observed in the worsted fabric examined previously. In both cases rootward migration of some regions of some fibers (microfelting) is an essential preliminary to felting, but in the woolen a very low level of microfelting triggers off a considerable shrinkage. Felting in the woolen appears to be intimately associated with the change in shape of the helices. It was suspected that this change might be due to recovery from strain. As is customary, relaxation shrinkage was separated from felting shrinkage by relaxing the fabrics, before washing, in water at 50° C. with a wetting agent, but this treatment does not release the individual fibers from all or even most of the strains from which an isolated fiber could recover under the same conditions, since the fibers in the fabric are held in strained configurations by their neighbors. Relaxation of the fabric allows individual fibers to recover from strain only so far as they can do so cooperatively. This is not very far; the relaxation shrinkage of either fabric in one treatment is only a few percent, and the red fibers show very little change of shape. If, however, relative movement of the fibers is produced by washing, the opportunity is provided for some recovery from strain. Recovery from the helical form necessitates an untwisting movement, the occurrence of which was readily demonstrated by the following simple experiments.

Release of short lengths of yarn.—Pieces of yarn 4 or 5 cm. long were immersed in cold water. The woolen yarn, whether as spun or teased out of the fabric, untwisted, becoming shorter and thicker. If held so that it could not untwist, it still contracted and thickened to a considerable extent. The singles worsted yarn, tested as spun, untwisted so vigorously and completely that the yarn structure was sometimes completely destroyed; if held so that it could not untwist, it showed a strong tendency to snarl. The two-ply worsted yarn produced by folding the singles yarn, whether tested as spun or as teased out of the fabric, began to untwist on wetting, but soon stopped, since untwisting of the folding twist necessitated insertion of singles twist.

The end results of these movements are shown in Figure 3.

Release of individual fibers.—Lengths of individual fibers (4 or 5 cm.) were removed from the same yarns with as little straining as possible. Their movements were watched when they were immersed in water and when they were floating on the surface

[2] Cohesive set is set which is produced by drying the deformed fiber at room temperature. It is removed when the fiber is relaxed in water at room temperature.

of the water. In all cases they untwisted from their helical form. This untwisting was followed or sometimes accompanied by bending and twisting into a new configuration similar to that adopted by fibers from the raw fleece when they are released individually in water. When the fibers were confined to the surface of the water, self-entanglement sometimes prevented them from untwisting completely (cf. [3, 20]), but any portions which were free to untwist always did so.

It is clear that in all the yarns the individual fibers have been cohesively set in a strained helical state during spinning, and that when wetted they will recover from this strain by untwisting if they are at the same time released from the constraints imposed by their neighbors. In the 2-ply yarn, however, such release is impeded by the twofold nature of the twist in the yarn.

Discussion

The Mechanism of Felting in the Woolen Fabric ("Release" Mechanism)

From the foregoing it may be deduced that the mechanism of felting in the woolen fabric studied is as follows.

Agitation of the fabric in water causes a rootward displacement of some fibers as a result of the difference of friction between the two directions along the fiber. This has always been observed in felting, although why water is necessary has not been fully explained. The details of the movement are discussed below. These movements slacken some parts of the moving fibers and change the positions at which they touch other fibers; the general effect is that there is some release of the mutual constraints and many of the fibers begin to untwist. Most of the length of each fiber untwists, but not as a whole; the short lengths between points of constraint untwist independently. The net result is a shortening and widening of all the helices, with consequent shrinkage and thickening of the fabric. The small degree of rootward migration is able to trigger off considerable shrinkage and entanglement basically because the subsequent movement is one of untwisting, not merely of contraction.

It is proposed that this mechanism should be called the "release" mechanism of felting.

Several workers [2, 7, 13, 17] have suggested that recovery from strain occurs during milling or scouring (although Schofield [13] excluded this from the category of felting). These authors, however, have not explicitly recognized that the movement involved is one of untwisting; for example, Speakman, Stott, and Chang [17] say: "The longer fibers produced during yarn production by the removal of crimp will strive to recover their original wavy form." Chaikin [2] has suggested that the recovery from longitudinal strain might be responsible for the shrinkage of warp-spun yarn on scouring, via the effect of this recovery on the geometry of the yarn loop. Although both these configurational changes must be of some importance, it is clear that the movements involved in untwisting from the helical form occur throughout a much greater volume than those involved in a simple contraction or even in flexing to a crimped form, and therefore provide far greater opportunity for entanglement of fibers.

Other authors (e.g., [3, 4, 8, 9, 20]) recognize that the tendency of wool fibers to twist or curl when their regain is varied (as of fur fibers to curl under certain conditions [1, 6]) is an important factor, though not the only one, in felting. They do not, however, refer to *un*twisting or recovery from the helical shape. Twisting and untwisting may be expected to produce somewhat similar effects, and it may well be that spontaneous twisting or curling plays the same part in the felting of loose wool that untwisting plays in the felting of fabrics.

The Nature of the Strains in the Helical Fibers

When a yarn is spun the component fibers are first straightened to a greater or smaller extent and then twisted into helices. The residual stresses left in the fibers manifest themselves predominantly as untwisting torques. Although the question is not directly relevant to the description of the "release" mechanism of felting, it is of some interest to consider what evidence is available as to the types of deformation responsible for these torques.

The main types of deformation to be expected as the result of spinning are longitudinal extension, flexure, and torsion about the fiber axis. Which of these is responsible for most of the untwisting torque depends on the characteristics of the fibers and the yarn, and on the spinning process. Platt, Klein, and Hamburger [12] have discussed the relative magnitudes of the contributions of torsion and bending, but have not considered the contribution due to extension, which Chaikin (private communication and [2]) considers to be the most important.

Conditions Responsible for the Dominance of Different Mechanisms in Different Fabrics

In the worsted fabric studied previously the "release" mechanism is much less important than in the present woolen, principally because the worsted is woven from a 2-ply yarn, a construction which very severely limits the extent to which the fibers can untwist. All worsteds made in Australia are woven with 2-ply yarn in the warp and may therefore be expected to show little release felting in this direction. The much closer packing of fibers in the worsted fabric compared with the woolen also impedes untwisting. "Release" felting can, however, be important in some worsted fabrics; the fiber shapes observed by van der Vegt [18], at various stages of washing, in a 3-ply worsted yarn spun for handknitting are very similar to those shown in Figure 2 here; they would presumably be the same in a fabric made from this yarn. The odd number of plies and the more open structure apparently permit "release" felting to occur in this yarn.

In the worsted fabric Shorter's mechanism of felting[3] was shown to become important when the rootward displacements of fibers were great enough. In the woolen this mechanism has less opportunity to come into operation; an essential feature of it is the development of relatively taut regions in some fibers, and such tautness cannot be maintained long in any fiber in the woolen fabric, owing to the rapid shinkage of the surrounding matrix of fibers which occurs as a result of the "release" mechanism.

It is reasonable to expect that yet other mechanisms of felting may be found to be of major importance under other conditions, e.g., in different types of fiber assembly or when different methods and conditions of felting are used.

The Role of Rootward Migration in the "Release" Mechanism

In principle, felting by the "release" mechanism need not depend on rootward migration of the fibers; any displacement of individual fibers sufficient to release them and their neighbors from their mutual constraints should cause it to occur. Shorter's mechanism, on the other hand, depends essentially on unidirectional migration, and most though not all of the theories of felting put forward at various times have taken the rootward migration of fibers to be an essential feature. In practice all types of felting depend on rootward migration; no case has ever been reported of tipward displacement of any substantial number of fibers in any type of felting, and in both the woolen and the worsted fabrics used in these studies, 98% of the fibers which moved relative to their neighbors did so towards their root ends. (The methods of investigation have been described in Part I.)

The with-scale frictional coefficient between wool fibers is very low under most conditions [10], and the against-scale coefficient is much higher. Whereas in Shorter's and most other suggested mechanisms of felting the difference itself is essential to produce sufficient fiber movement for felting, in the "release" mechanism it may be the low value of the with-scale coefficient which is essential; possibly if all three coefficients (with-scale, anti-scale, and mixed) were very low, movement both ways might occur and might initiate felting by the "release" mechanism. To test this possibility it would be necessary to apply a very effective lubricant to a loom-state woolen fabric shrinkproofed by a degradative method so as to eliminate the frictional difference completely. It is stressed that this suggestion is relevant only to the "release" mechanism.

Some authors, while accepting rootward migration as established, regard it as an end-result of very small elementary oscillatory movements; e.g., Moncrieff [11], discussing Shorter's and Arnold's views, presents the picture of extremely small elementary displacements in either direction, of which all those directed towards the tips are subsequently lost and all those directed towards the root are held. Van der Vegt and Schuringa [18] consider that in the middle range of intensity of the applied forces the fibers can move in only one direction, but that at higher forces they can move in both directions, and that the movement towards the root is always greater than the movement towards the tip. Shorter [14], on the other hand, considered that the areas of interfiber contact which are important in felting are of two types: those at which movement is possible only towards the root end and those at which no movement is possible. At other points of contact, movement may be possible in both directions, but this does not contribute to felting. There is no direct evidence as to whether small oscillatory movements do occur. If they do, they are probably individually too small to release the fibers from constraints or to initiate felting by any mechanism which has been suggested.

[3] Described on page 442 of Part II.

Possible Macroscopic Differences Among Felts Produced by Different Mechanisms

There has in the past been considerable disagreement among different workers as to whether felting increases the density of an assembly of fibers. In Speakman's [16] and Harrison's [7] milling experiments no increase in density of the fabric was observed (the figures, in fact, suggest an initial slight decrease, which they apparently found not to be significant). Schofield [13], on the other hand, found an increase in density when he felted loose wool, and it is generally accepted that the density of a fur hood increases during felting processes.

The root of the disagreement may lie in the existence of different mechanisms of felting. It is difficult to see how the "release" mechanism could increase the density of a fabric, but Shorter's mechanism appears to be capable of doing so. It is obviously desirable that the question of changes in density should be investigated more fully, although the measurements are not easy to make.

The Stability of Pleats

As reported above, pleats which are fast to relaxation in hot water are destroyed by much lighter washing in the woolen than in the worsted weave, and at a much lower level of microfelting. This is explicable in terms of the different mechanisms of felting which are dominant in the two fabrics. During the initial stages of washing, each individual fiber in the worsted has to move longitudinally for a distance of about half of the diameter of the orthogonal yarn (about $\frac{1}{4}$ mm.) before it contributes appreciably to blurring the apex of the pleat. In the woolen, on the other hand, although the yarn diameter is larger, a much smaller longitudinal displacement is sufficient to release the migrating fiber and some of its neighbors from their mutual constraints sufficiently for them to begin untwisting. It is the untwisting movements, rather than the longitudinal displacements, which blur the apex in this case.

The Definition of Felting

Some authors (e.g., Schofield [13]) consider that no process which depends on recovery from strain should be called felting. A case can be made for this view and also against it. On the whole, it seems both reasonable and convenient to class the "release" mechanism as felting. To justify this it is necessary to consider the definition of felting.

"Felting" is something which assemblies of animal fibers do under certain conditions. The possible forms of the assemblies are so various—staple, carded, combed, spun, or woven wool; blown or hardened fur—that it is very difficult to give a useful definition which will cover all cases. Most criteria which might be used to define felting are ruled out by the basic differences between the felting of ordered assemblies, such as yarns and fabrics, and of disordered assemblies, such as loose wool or fur, and carded webs. This applies to density, tensile strength, isotropy, and linear and superficial shrinkage. In a disordered assembly of fibers, felting causes an increase in density and tensile strength, but in an ordered assembly the density does not necessarily increase (it may possibly even decrease), and there are apparently no data for the tensile strength. In an ordered assembly of fibers, felting increases the isotropy of the assembly, but in a disordered assembly this is not always true; for example, felting may introduce considerable anisotropy into fur hoods if they are not frequently rotated. Linear shrinkage, applicable to yarns and fabrics, and superficial shrinkage, applicable to fabrics, are both inapplicable as a rule to disordered assemblies.

It appears therefore that, as most authors have maintained, the one characteristic feature of a felt is entanglement of the fibers. However, this is not sufficient to define the *process* of felting. Entanglements can be achieved with synthetic fibers, or with cellulose fibers, but the forces applied in these cases have to be carefully directed specifically to produce entanglement. The characteristic feature of felting is that it is in one sense spontaneous: although under all practical conditions external forces are necessary to cause felting, they need not be specifically chosen to produce entanglements, but will do so unavoidably, whatever their type, as long as they are strong enough. The following definition of felting is therefore suggested.

Felting is the process of progressive entanglement of the fibers in an assembly, occurring as a direct result of agitation by *undirected* external forces.

This definition does not provide a basis for a quantitative definition of the degree of felting of an assembly until the degree of entanglement is defined quantitatively. It is therefore permissible to use any feature appropriate to a given assembly, e.g. linear or superficial shrinkage of a fabric or yarn, as a measure of felting, so long as it is kept in mind

that these measures are different from each other and are not the only possible ones.

The above definition is based on more or less macroscopic features. Until a case of felting without rootward migration is observed, it would be permissible to set up an equivalent microscopic definition: felting is the process of progressive entanglement of the fibers in an assembly occurring as a result of persistent rootward migration of fibers or parts of fibers produced by agitation by undirected external forces. It may be noted that rootward migration alone is not sufficient to define felting; it can occur without felting if entanglement is not possible, as in the case of uncarrotted rabbit fur.

Even these broad definitions, macroscopic and microscopic, fail to cover a few cases of theoretical though not of practical interest. These may be regarded as limiting cases rather than as exceptions. For example, the agitation may be produced by forces internal to the fibers; this covers the cases of the entanglement of fibers placed together on the surface of water [3, 20] and of felting produced by prolonged cycling of the humidity of the atmosphere [9, 15]. In the former case felting is very limited in extent, and in the latter it is extremely slow.

The "release" mechanism of felting conforms to both the macroscopic and the microscopic definitions suggested above. It cannot occur without migration of some fibers, which partially releases others from their constraints.

Conclusions

In some fabrics, felting is due principally to a mechanism for which the name "release" mechanism is proposed. Rootward migration of some fibers releases the mutual constraints between fibers which then begin to recover from the state of strain imposed when they were twisted into helices during spinning. The net effect of limited untwisting by all the fibers in short lengths acting independently is a contraction and widening of all the helices, with consequent shrinkage and thickening of the cloth.

This mechanism was found to be very important in a loom-state woolen woven from single-ply yarn. It was much less important in the loom-state worsted which was studied previously, because this fabric was woven from two-ply yarn, a construction which severely limits the extent of possible untwisting of the fibers. The closer packing of the fibers in the worsted also hinders untwisting.

When the "release" mechanism is operative the fabric shrinks rapidly on washing, and the shrinkage is considerable even when the degree of microfelting (rootward migration) is very small. Pleats are destroyed at a very low level of microfelting because a very small longitudinal displacement of any one fiber can trigger off untwisting movements in several.

Because of the rapid shrinkage which occurs when the "release" mechanism is operative, Shorter's mechanism (described on page 442 of Part II) is not able to play as large a part in shrinkage of the woolen as in the worsted.

On the basis of a discussion of the characteristic features of felting, it is proposed that felting should be defined as the process of progressive entanglement of the fibers in an assembly, occurring as a direct result of agitation by *undirected* external forces.

Acknowledgments

The author wishes to thank Mr. W. L. Hindmarsh for his assistance with this work and Dr. K. L. Baird for valuable discussion.

Literature Cited

1. Berg, G., *Melliand Textilber.* **18**, 438 (1937).
2. Chaikin, M., *J. Textile Inst.* **49**, P578, P579 (1958).
3. Dobozy, O. K., TEXTILE RESEARCH JOURNAL **28**, 717 (1958).
4. Freney, M. R., Deane, K. R., and Anderson, J. R., *Nature* **157**, 664 (1946).
5. Harrap, B. S., *J. Soc. Dyers Colourists* **75**, 106 (1959).
6. Harris, M., *Am. Dyestuff Reptr.* **34**, 72 (1945).
7. Harrison, W., *J. Textile Inst.* **30**, T42 (1939).
8. Leveau, M., Varney-Cebe, N., and Parisot, A., *Proc. Int. Wool Text. Res. Conf. Aust.* **D**, 211 (1955).
9. Leveau, M., *Bull. inst. textile France* **67**, 19 (1957).
10. Lindberg, J., TEXTILE RESEARCH JOURNAL **18**, 470 (1948).
11. Moncrieff, R. W., "Wool Shrinkage and its Prevention," London, National Trade Press, 140 (1953).
12. Platt, M. M., Klein, W. G. and Hamburger, W. J., TEXTILE RESEARCH JOURNAL **28**, 1 (1958).
13. Schofield, J., *J. Textile Inst.* **29**, T239, T282 (1938).
14. Shorter, S. A., *J. Soc. Dyers Colourists* **39**, 274 (1923).
15. Speakman, J. B., *J. Soc. Dyers Colourists* **60**, 328 (1944).
16. Speakman, J. B., *J. Textile Inst.* **29**, T280 (1938) and references therein.

17. Speakman, J. B., Stott, E., and Chang, H., *J. Textile Inst.* **24**, T273 (1933).
18. van der Vegt, A. K., Thesis, Fibre Research Institute TNO (Pub. No. 7), The Netherlands; p. 88, Fig. 45 (1955).
19. van der Vegt, A. K., and Schuringa, C. J., TEXTILE RESEARCH JOURNAL **29**, 199 (1954).
20. Zilahi, M. and Dobozy, O. K., *Acta Technica Acad. Sci. Hung.* **9**, 65 (1954).

Manuscript received February 15, 1960.

The Bilateral Structure of Crimped and Steely Wools and the Origin of Fiber Crimp

D. F. Louw

South African Wool Textile Research Institute, Grahamstown, South Africa
and
Deutsches Wollforschungsinstitut, Aachen, Germany

Abstract

Observations have been made on the behavior of root and tip sections of normal and steely wools towards treatment with 0.1 *N* NaOH at 50° C. The results are considered in the light of available knowledge of the chemical composition of such fibers and the changes due to weathering damage. The data obtained lead to a concept that the formation of crimp in wool is dependent upon differences in the rate rather than in the final extent of keratinization in the two cortex segments. The lack of well-defined crimp in steely fibers, which still show very definite segmentation into ortho- and paracortex, is explained on the basis of the slower keratinization of fibers deficient in trace elements as compared to normal.

Introduction

Various aspects of the morphological structure of wool have been investigated by making use of differences in reaction rate of the component parts of the wool fiber. The bilateral structure of the cortex of a normal crimped fine Merino wool fiber was revealed by differential staining [15] and led Horio and Kondo [8] to define the so-called dye-accessible (DA) and non-dye-accessible (non-DA) sections. Experiments by Mercer [13] confirmed these observations, and the terms ortho- and paracortex were coined to replace the DA and non-DA nomenclature. The paracortex was regarded as the more stable, "more vulcanized" (or more keratinized) and the orthocortex as the more "rubbery" section.

Attention was also drawn to an apparent relation between bilateral structure and crimp in keratin fibers [3]. A greater degree of symmetry of ortho and para components coincides with lower crimp. At one extreme is to be found fine highly crimped Merino wools with definite segmentation into approximately equal sections of ortho and para components and, at the other, straight human hair, which may be regarded as "pure" paracortex, and slightly wavy kid mohair, regarded as "pure" orthocortex [12]. Coarser types of wool, e.g., Lincoln, are not so highly crimped as the finer quality Merino, and Fraser and MacRae [3] indicated a symmetric distribution of cortex segments in the former: a nucleus of ortho component surrounded by a sheath of paracortex. This was also found to be the case with a crimpless Merino wool. Adult mohair revealed a symmetric distribution of the two cortex types, but in this case the specific cells were more or less randomly intermixed. Ahmed and Lang [1] found that Pakistan carpet wools ranged from the finer (and more highly crimped) types, resembling Merino wools in their bilateral structure, to the coarser (less crimped) fibers with a central orthocortex.

It therefore seemed logical to expect differences in bilateral structure between normal and steely

Merino wools of comparable fiber diameter because the latter, as a result of copper deficiency in the natural pastures, can be quite hairlike and almost devoid of crimp. Fraser and Rogers [4] reported that their staining method showed differentiation in steely wool which was not as distinct as in normal wool. This could not be verified by Haly [7], and no bilateral structure was detected when water-saturated fibers were viewed under the microscope, but treatment in alcoholic KOH and dyeing with Coomassie Violet did show up the bilateral nature of such steely fibers. He came to the conclusion that the physical and chemical properties of the orthocortex of steely wool must be less different from those of the paracortex than is the case in normal wool.

Some chemical and physico-chemical differences between normal and steely wools have been observed, of which the abnormally high cysteine content [2], alkali solubility, and dye absorption are the most noticeable [11]. From this was concluded that copper deficiency in the sheep's diet results in incomplete keratinization of the fiber even at the stage when it has appeared above the skin level. The process of cross-linking through oxidation of free thiol groups to disulfide linkages may then continue under atmospheric conditions, and most fiber characteristics approach normal by the end of approximately six to eight months' growth, with the exception that the steely nature is retained.

No clarity has as yet been reached on the number of disulfide linkages in the specific cortex components. Mercer, Golden, and Jeffries [14] stated that the cystine content of the paracortex appeared to be almost twice that of the orthocortex. Fraser, Lindley, and Rogers [6] found the "H" segment to be cystine-rich and concluded that the greater degree of disulfide cross-linking was responsible for the resistance of this segment to swelling in alkali. Analytical results were, however, not conclusive because of possible admixture of cortex cells with cystine-rich cuticle components, and Leveau [10] favored a theory of a predominantly interchenic character of disulfide bonds in the paracortex and an intrachenic nature of such linkages in the ortho component.

Structural investigations by Menkart and Coe [12] led to the observation that the paracortex of Merino fibers retained birefringence and remained relatively unswollen when the fibers were boiled for 2 hr. in 0.4 N H_2SO_4 and then immersed in 2% NaOH solution. Such treatment, however, resulted in considerable swelling of the ortho segment and complete loss of its birefringence. Kid mohair fibers swelled greatly (500% in diameter) with almost total loss of birefringence, whereas human hair remained practically unswollen and completely birefringent under similar treatment.

A variation in technique enabled Satlow [16] to formulate a theory on the interdependence of the state of cystine linkages in a wool fiber and the birefringence of the cortex segments. Reduction of about half of the cystine linkages in wool by treatment at pH 5.0 in 0.3 N calcium thioglycollate solution resulted in a loss of birefringence of the orthocortex of the fibers upon embedding in 0.1 N NaOH. Re-formation of such broken linkages by oxidation with H_2O_2 returned the fibers to their original state of resistance to swelling and complete retention of birefringence upon embedding in hot alkali. It is thus possible to study the nature of the cortex segments microscopically and thereby to obtain an indication of normal cross-linking through disulfide bonds by observing fiber behavior upon treatment with hot dilute alkali. Satlow could not, however, decide conclusively between the theories of Mercer et al. and of Leveau, and he assumed that both the degree and the nature of the disulfide cross links

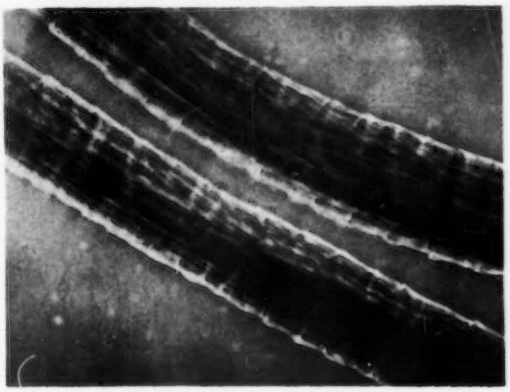

Fig. 1. All fiber sections shown were treated for 10 min. in 0.1 N NaOH at 50° C. and then photographed under crossed Nichols through a Gypsum Red I filter under a magnification of 400×. This and the following reproductions are black-and-white prints from black-and-white negatives made from the original Agfa CN17 color negatives. Root sections (AR) of a crimped South African Merino wool. The bottom section is closer to the middle of the staple.

were responsible for differences between the behavior of ortho- and paracortex.

A modification of the embedding technique of Satlow [17] was applied in a microscopical study of normal and steely wools in an effort to link up structural differences and birefringence with variations in chemical constitution and reactivity and with the presence or lack of crimp in the fiber.

Wool Samples

The root and tip third sections (AR and AT) of a normal good quality South African Merino wool from the Karoo area and corresponding sections (ER and ET) of fibers from a Merino sheep that had suffered from copper deficiency in its diet throughout the total growing period of the wool were compared. These fiber sections were carefully purified by iso-electric scouring and Soxhlet extraction with alcohol and ether, as described elsewhere [11].

The root sections could be regarded as protected against weathering, whereas the tips were considerably damaged.

Experimental Procedure

The following reaction conditions were found optimal for obtaining good differentiation between root and tip sections and between normal and steely wools.

About 10 ml. of 0.1 *N* NaOH is heated in a test tube placed in a thermostatically controlled waterbath at 50° C. A small sample of the purified wool section (10 mg.) is dropped into the alkali and rapidly wetted out by shaking; the test tube is stop-

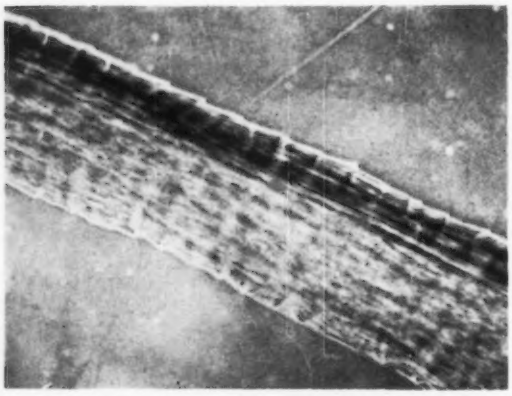

Fig. 2. Root section (ER) of a steely Merino wool.

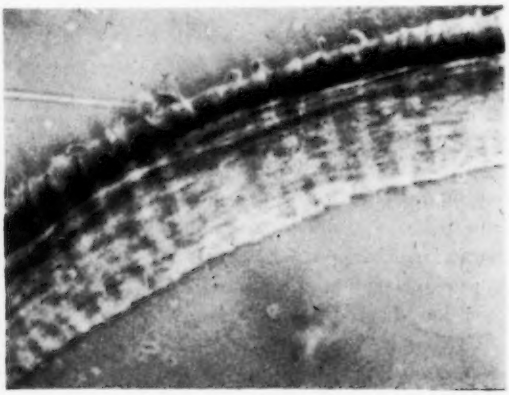

Fig. 4. Tip section (ET) of the same steely wool close to the middle of the staple.

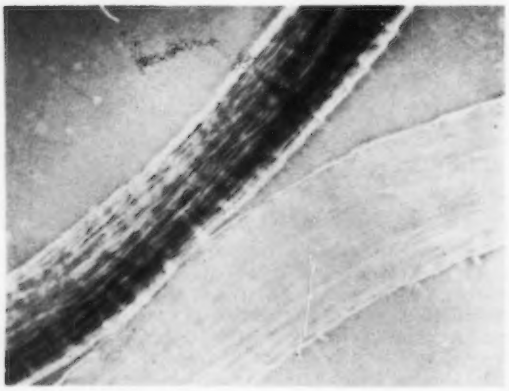

Fig. 3. Tip sections (AT) of the same crimped wool. The top section is closer to the middle of the staple, and the bottom section belongs to the extreme tip.

Fig. 5. Tip section (ET) of the steely wool showing a section near the extreme tip.

pered and left in the bath for 10 min. A portion of the wool fibers is then removed by means of two dissecting needles and placed on a microscope slide with a few drops of cold 0.1 *N* NaOH, covered with a cover slip, and viewed between crossed Nichols through a Gypsum Red I filter on the microscope.

Photomicrographs were originally taken on Agfa color negative film (CN17) under a magnification of 400×. Reproduction of these photographs in black-and-white as given here (see Figures 1–5) are much less satisfactory than the original red-and-green color prints, which show much more detail and indicate very clearly the borders between ortho- and paracortex as well as any variations in birefringence. For reasons of economy the black-and-white prints are reproduced here. It should be remembered that the paracortex, originally photographed in green, is here shown as the darker of the two sections.

Observations

Upon treatment in dilute alkali, the root sections of sound crimped fibers (AR) show very little swelling and are almost completely birefringent throughout both cortex segments (see Figure 1). Some fiber sections nearer to the middle of the staple (bottom fiber in Figure 1) reveal slight traces of a loss of birefringence in the one component, which presumably is the ortho, as is shown by its greater susceptibility to attack by alkali. Under identical treatment the steely root sections (ER) show considerable swelling and almost complete loss of birefringence of the orthocortex, whereas the para segment has withstood the action of alkali to a reasonable extent in both respects (Figure 2).

The thinner of the two fibers shown in Figure 3 is a tip section of normal wool closer to the middle of the staple, whereas the other is a section of the badly weathered extreme tip portion, both after treatment with dilute alkali. The former can be compared with the fiber shown in Figure 4, which is a comparable section of the steely wool, being closer to the middle of the staple than the portion shown in Figure 5. It is quite clear that in this case the steely wool is again more vulnerable than the crimped fiber towards dilute alkali. Greater swelling occurs and there is more loss of birefringence, especially in the orthocortex of the copper-deficient wool.

Comparison of Figures 2 and 4 reveals the increased resistance to attack by alkali in sections of steely wool closer to the middle of the staple. This is indicated by the more intense black of the paracortex as well as by the deeper shading of the ortho component.

These remarkable differences in resistance to attack by alkali disappear in the extreme tip sections of both crimped and steely wools, as can be seen in Figure 3 (the thicker fiber on the right-hand side) and Figure 5 respectively. Both fibers show extensive swelling and complete loss of birefringence. It is, however, still possible to discern the original outlines of the two cortex components, the para segment being slightly coarser in texture than the ortho.

Discussion

The observations recorded above constitute a confirmation of earlier findings [4, 7] that steely wool shows distinct bilateral asymmetry. The observed reactions of root and tip sections of crimped and steely wools also fit in with the analyses recorded previously [11] in connection with an investigation of the effects of weathering on the chemical composition of such fibers and on their physico-chemical behavior.

The wool sections dealt with in this paper were fully analyzed and the data reported in the previous paper, from which the following values for cystine, cysteine, and cysteic acid are quoted.

Analysis of Wool Sections

Section	Description	$\%(CyS)_2$	%CySH	$\%CySO_3H$
AR	Normal	12.1	0.21	0.05
AM	Normal	12.4	0.22	0.07
AT	Normal, weathered	11.1	0.34	0.17
ER	Steely	10.8	1.00	0.35
EM	Steely	11.1	0.46	0.36
ET	Steely, weathered	10.0	0.35	0.90

On that basis it was concluded that weathering of normal wool on the sheep's back results in a decrease in the cystine content and an increase in cysteic acid and also of cysteine. Evidence of this rupture of disulfide linkages was also found in the higher swelling of normal weathered fibers in aqueous solution, greater dye absorption, and increased alkali solubility.

Steely wools were found to be affected differently; the initial high cysteine content of the root sections is decreased and the cystine content remains prac-

tically constant or can even show an increase in the middle portions. The tip sections have lower values for cystine as a result of continued weathering. This was interpreted as evidence that the root sections of copper-deficient steely wools can be regarded as incompletely keratinized and that the process of keratinization, partly brought about by slight weathering, continues during aging of such wool on the sheep's back. The sum total of these processes results in lower swelling, dye absorption, and alkali solubility of the middle sections of steely wools as compared with the root portions. As a result of excessive weathering the tip sections, however, react in a manner similar to that of crimped weathered wools.

The weathering process can now be followed on the photomicrographs of the root and tip sections of the crimped wool (Figures 1 and 3). Initially weathering seems to affect the orthocortex, this segment apparently being more vulnerable. As the extent of weathering increases, so many disulfide bonds are progressively destroyed that the orthocortex soon loses birefringence and eventually even the more resistant paracortex is affected to such an extent that the two segments react similarly towards 0.1 *N* NaOH.

In the case of the steely wool (Figures 2 and 4) the initial increase in birefringence from root to middle section is evidence of an increase in resistance to alkali which parallels the formation of disulfide bonds out of a relative abundance of free thiol groups present in the root sections. This supports the theory of continued keratinization during at least the first six to eight months of fiber growth.

The fact that the extreme tips of steely (Figure 5) and crimped wools (the thick fiber in Figure 3) react in an identical manner indicates that weathering, with the associated rupture of disulfide bonds, tends to equalize the initial chemical and physicochemical differences between the fiber types.

Differences in chemical composition and fiber behavior can now be related to the degree of crimping and lead to conclusions on some of the factors responsible for the formation of fiber crimp and the connection with animal metabolism.

It is generally accepted that normal keratinization of the fiber inside the wool follicle sets in on the side adjacent to the thinnest follicle wall and that the cortex segment formed on that side is the one ultimately known as the paracortex. The main chemical reaction involved in this process seems to be the oxidative linking of free thiol groups through disulfide bonds, although dehydration and elongation of cells also may come into play [9].

The presence of crimp in wool has become associated with the existence of bilateral asymmetry and with the curvature and slant of the follicle in the skin. Similarity between the behavior of a bimetallic strip and the wool fiber with definite segmentation has been indicated. The case has now arisen where a segmented fiber with definite ortho and para components lacks the well-defined crimp due to trace element deficiency and the above explanation no longer seems applicable.

Fraser and Rogers [5] observed that differentiation of the H (para) and S (ortho) segments in dried plucked wool roots occurs even in the earliest stages of fibril formation. According to these authors the possibility exists that this differentiation may even originate in the germinal layers of the bulb where the ultimate differences in amino acid content of the two cortex components could arise. The fact that they did not observe segmentation in the case of freshly plucked roots can be explained in the light of a recent finding by Kassenbeck [9] that the morphological structure of keratinic fibers is determined in the basal layers of the follicle by the rate of proliferation of the cells and by their water content. Mere dehydration could therefore presumably give rise to a certain degree of differentiation. It has, however, to be borne in mind that an increased rate of cross-linking through oxidation during drying of the freshly plucked roots could also be the real basis of the observed differences, as will be explained below.

The photographs, combined with previous analytical data, indicate that the orthocortex of steely wools, especially in the case of the root sections, is definitely far less cross-linked than that of crimped fibers and is also more incompletely keratinized than the para component of the copper-deficient fibers. In all probability the paracortex in steely root wools also lacks the high degree of keratinization of the paracortex in normal wools. In this context keratinization is basically regarded as the process of linking up of free thiol groups through disulfide bonds by a metabolic oxidation–reduction process. This can be accompanied by dehydration and elongation, finally resulting in hardening of the cells, as proposed by other authors.

Arguments on the actual chemical differences between the ortho- and paracortex of normal wools

have not led to final conclusions, but at this stage it seems acceptable that a difference in sulfur and cystine content and/or probable differences between the types of disulfide linkages (inter- or intrachenic) do exist, as was concluded by Satlow [16]. Other factors apart from straightforward chemical differences must, however, be involved in the production of crimp in normal wools and in the lack of crimp in cases of trace element deficiency.

The assumption [4] that the germinal layers of the bulb are responsible for the production of the proteins ultimately found in the ortho- and paracortex respectively and differing in chemical composition seems acceptable. These primary secretions may be in the form of free amino acids or of peptides with relatively low molecular weights which later combine to form the usual long chains present in the normal wool protein. In the case of copper deficiency this peptide formation is affected in such a manner that shorter chains are produced, as postulated by Burley and de Kock [2].

These peptide chains of the two cortex segments are presumably not, or only slightly, cross-linked by disulfide bonds in the prekeratinization zone. The next stage in fiber development, involving the formation of cystine linkages in the keratinization zone, is believed to be basically responsible for the production of crimp in normal wools and for the lack of well-defined crimp when the animal has been restricted to grazing too low in available copper.

It is maintained that, in the case of the normal wool fiber, cross-linking through disulfide bonds proceeds from the thin side of the follicle wall at a relatively high rate associated with a form of catalysis as a result of the presence of sufficient copper in the animal body. The paracortex, probably containing more and/or different disulfide bonds than the ortho-, is keratinized at a higher rate and to a greater extent, and this is responsible for the bimetallic strip construction. This "tying down" of one segment of the fiber, probably together with dehydration and other processes and coupled with the slant of the follicle, results in a crimped fiber.

The absence of sufficient copper in the animal metabolism retards the rate of cross-linking taking place in the fiber cortex in the keratinization zone. This slowing down is so considerable that the process is incomplete even at the stage when the fiber emerges above the skin level. It seems reasonable to accept that only small differences in keratinization of the two cortex segments obtain within the follicle at a stage when the outside cuticle layers are already formed and hardened to an extent which suffices to keep the fiber permanently in its state of comparative uncrimpedness. The steely character is retained even when more marked segment differentiation arises subsequently as a result of continued keratinization through the action of the limited amount of copper catalyst, accompanied by the effects of oxidation upon prolonged exposure of the protein to air and sunlight. Thus copper deficiency results in the production of a steely wool in which distinct segmentation, as detected in the shorn wool, does not appear in the earlier stages of fiber formation [7].

Summary

Photomicrographs have been taken of normal and steely wools as viewed through crossed Nichols and a Gypsum Red I filter after treatment of the keratin fibers in 0.1 *N* NaOH at 50° C. for 10 min. Original photomicrographs, taken in color, show a wealth of detail and differentiation. The black-and-white reproductions are less satisfactory.

The existence of a bilateral asymmetry in both normal and steely wools has been verified.

Weathering damage of the two fiber types tends to eliminate differences in behavior towards alkali.

It is inferred that copper deficiency in a sheep's diet results in the production of a relatively uncrimped fiber, because of the fact that keratinization assumes significant proportions at a late stage in fiber formation when the fiber as such has already been stabilized in its steely form.

Crimp in fibers seems to be the result of catalyzed keratinization which, proceeding more rapidly in the para than in the ortho component and probably resulting in more and/or different cystine linkages in the former segment, results in crimp formation while the fiber structure is still relatively unstable and pliable.

Acknowledgment

Appreciation is expressed to Dr. G. Satlow of the Deutsches Wollforschungsinstitut, Aachen, Germany, where this work was carried out, for valuable suggestions on experimental technique.

Literature Cited

1. Ahmed, N. and Lang, W. R., Textile Research Journal **26**, 954 (1956).
2. Burley, R. W., *Nature* **174**, 1019 (1954).
3. Fraser, R. D. B. and MacRae, T. P., Textile Research Journal **26**, 618 (1956).

4. Fraser, R. D. B. and Rogers, G. E., *Biochim. Biophys. Acta* **12**, 484 (1953).
5. Fraser, R. D. B. and Rogers, G. E., *Biochim. Biophys. Acta* **13**, 297 (1954).
6. Fraser, R. D. B. et al., *Biochim. Biophys. Acta* **13**, 295 (1954).
7. Haly, A. R., TEXTILE RESEARCH JOURNAL **27**, 82 (1957).
8. Horio, M. and Kondo, T., TEXTILE RESEARCH JOURNAL **23**, 373 (1953).
9. Kassenbeck, P., *Bull. Inst. Text. France* **83**, 25 (1959).
10. Leveau, M., *Bull. Inst. Text. France* **74**, 75 (1958).
11. Louw, D. F., TEXTILE RESEARCH JOURNAL **30**, 462 (1960).
12. Menkart, J. and Coe, A. B., TEXTILE RESEARCH JOURNAL **28**, 218 (1958).
13. Mercer, E. H., TEXTILE RESEARCH JOURNAL **23**, 387, 388 (1953).
14. Mercer, E. H. et al., TEXTILE RESEARCH JOURNAL **24**, 615 (1954).
15. Ohara, K., *Melliand Textilber.* **19**, 407 (1938).
16. Satlow, G., *Textil-Rundschau* **14**, 446 (1959).
17. Satlow, G., *Z. gesam. Textilind.* **12**, 497 (1959).

Manuscript received December 9, 1959.

Studies on Wool

Part V: Partial Hydrolysis in Acid Reducing Medium[1]

Pierre Pigache and Gerard Biserte[2]

TENTH-NORMAL sulfuric acid at boiling temperature slowly hydrolyzes wool keratin, solubilizing a complex nitrogenous fraction comprised of free amino acids, among which aspartic acid predominates, and a mixture of oligo- and polypeptides characterized by their relative lack of cystine and richness in tyrosine. After 64 hr. of hydrolysis, the residual wool becomes very rich in cystine sulfur (6.2%) as well as in proline [1].

To complete this study, it seemed interesting to us to study the action of dilute sulfuric acid in the presence of a reducing agent such as thioglycollic acid, capable of cleaving the disulfide linkages of the wool.

Techniques Used

Material

The experiments were effected on a Merino wool (fineness 21–22 μ), washed industrially in neutral medium with a non-ionic detergent and subsequently degreased with ether in a Soxhlet apparatus.

Analytical Methods

Nitrogen was estimated by a micro-Kjeldahl method. Sulfur (thiol and disulfide) was estimated by the method of Shinohara [11]. The identification of the amino acids was realized either by two-dimensional chromatography (butanol : acetic acid : water (4 : 1 : 5) in the first direction and phenol in ammonia atmosphere in the second) or by coupling chromatography with paper electrophoresis according to the method of Biserte, Paysant, and Boulanger [3].

Experimental Conditions

Wool (5 g. dry weight) was hydrolyzed under reflux for varying times by a mixture of 0.1 *N* sulfuric acid (198 ml.) and thioglycollic acid[3] (2 ml.). The hydrolysis medium thus contained 0.2 gram-equivalents of acidic hydrogen per liter. After hydrolysis the wool was exhaustively rinsed in running tap water, neutralized overnight with a 1% solution of pyridine in water, again rinsed in running water and then in distilled water, dried at 100–105° C., and weighed. Some of the hydrolyses were effected in a mixture of 0.02 *N* acetic acid (198 ml.) and thioglycollic acid (2 ml.).

Experimental Results

Kinetics of the Solubilization of Nitrogen and Sulfur

The solubilization of the wool keratin is quite rapid in dilute sulfuric acid containing a reducing agent (Table I). In the early stages of hydrolysis,

[1] For the previous publications in this series, see [1, 2, 9].

[2] Laboratoire de Chimie Biologique de la Faculté mixte de Médecine et Pharmacie de Lille (Prof. P. Boulanger) and Laboratoire de Chimie Organique de la Faculté Libre des Sciences de Lille. We wish to thank M. Bernard Waeles for his technical assistance.

[3] Quality "for investigational use"; density 1.3253. Final concentration of the solution, 1 : 100 (vol. : vol.) or 1.3253 : 100 (wt. : vol.).

it is remarkable to note that the solubilization of the nitrogen is superior to that of the wool itself. This discordance is explained by the rapid hydrolysis of the amide linkages of the asparaginyl and glutaminyl residues of the insoluble protein. The rate of hydrolysis is greatly superior to that observed in 0.1 *N* sulfuric acid without reducing agent (Column 4 of Table I). It is interesting to point out that 0.1 *N* sulfuric acid solubilizes in 5 hr. 45% of the wool oxidized by peracetic acid[4] [8]. Thus, no matter how the disulfide linkages are cut, the kinetics of the solubilization of the wool by the sulfuric acid are very similar. In the medium 0.02 *N* in acetic acid and containing thioglycollic acid, the solubilization is much less rapid than in the reducing sulfuric acid medium (0.1 *N*); in 4 hr., the sulfuric acid hydrolysis solubilizes 47% of the initial nitrogen, the acetic acid hydrolysis only 23% (Table I). The final pH of the acetic acid hydrolysate (2.8) is higher than that of the sulfuric acid hydrolysate (1.8). This difference explains the variation in rates observed between the two types of hydrolysis.

The solubilization of sulfur (thiol + disulfide) follows a kinetic pattern virtually parallel to that of the nitrogen: after 12 hr. of hydrolysis, the percentages of nitrogen and of sulfur (thiol + disulfide) solubilized are identical (Tables I and II). Except during the first 2 hr. of hydrolysis, the residual wool becomes progressively poorer in sulfur (thiol + disulfide). After 12 hr. of hydrolysis, the level of sulfur, initially 3%, has gone down to 2.6% (Table II). These last results are contrary to those we have observed during hydrolysis by 0.1 *N* sulfuric acid alone since, after 12 hr., the level of sulfur, which had progressively increased, was 3.72% [1].

TABLE I. Kinetics of the Solubilization of Nitrogen in Reducing Acid Medium

Time of hydrolysis, hr.	Wool solubilized (% of the initial wool)*	Nitrogen solubilized (% of the initial nitrogen)†	
	Hydrolysis by 0.1 *N* sulfuric acid		
		in presence of thioglycollic acid	in absence of thioglycollic acid
1	13	20	1.4
2	27.5	33	3.2
4	47.5	47.5	5.9
8	56.5	58.2	10.7
12	70	74.5	17.3
	Hydrolysis by 0.02 *N* acetic acid in presence of thioglycollic acid		
1	8	10	—
4	19.5	23.5	—

* Determination by weighing the insoluble residue from the hydrolysis medium.

† Original wool: total nitrogen, 16.55%; sulfur (thiol + disulfide), 3%.

TABLE II. Kinetics of the Solubilization of Sulfur (Thiol + Disulfide)

(Hydrolysis by 0.1 *N* sulfuric acid in the presence of thioglycollic acid)

Time of hydrolysis, hr.	Sulfur content of the residual wool, g.	Amount of sulfur solubilized, % of initial sulfur
0	3	0
2	3.37	18
4	3.05	47
8	2.67	60
12	2.6	74

Composition of the Solubilized Nitrogenous Fraction

Existence of "thermosoluble polypeptides." The hydrolysates in reducing acid medium let settle out on cooling a group of "thermosoluble polypeptides," as we had already noted in the case of the hydrolyses with sulfuric acid alone. The fact that the polypeptides precipitate in reducing medium shows that their insolubility, at least in the cold, does not depend on the existence or absence of disulfide linkages. This insolubility certainly depends on the existence of hydrogen bonding, for addition of urea to the hydrolysate cooled to 20° C. brings about a total solubilization of these polypeptides. However, paper electrophoresis of these polypeptides in 8 *M* urea solution containing 1% thioglycollic acid and adjusted to pH 7.0 was not successful. These thermosoluble polypeptides are rich in tyrosine and cystine. However, the levels of tyrosine and cystine diminish as a function of the time of hydrolysis.

Nondialyzable fraction. After dialysis of the hydrolysate and removal of the thermosoluble polypeptides, the hydrolysate still contains nondialyzable peptides only poorly separated by paper electrophoresis at pH 3.9 and containing a high proportion of tyrosine and cystine.

Dialyzable fractions. After demineralization and fractionation of the dialyzable fraction on an ion-

[4] Under these conditions, the residues of cystine are transformed into residues of cysteic acid.

exchange column (Amberlite IR-120), the "amino-acid fraction" (ammoniacal elution of the resin) was studied by paper electrophoresis (Figures 1 and 2) and by two-dimensional chromatography.

After 4 hr. of hydrolysis in reducing acid medium, the only free amino acids found were aspartic acid and glutamic acid, the amount of aspartic being 7–8 times that of the glutamic. Similar results had been obtained during the course of the hydrolyses in sulfuric acid alone. After 8 hr. of hydrolysis, other amino acids appear (glycine, alanine), but the level of aspartic acid, which is always clearly predominant, continues to increase (Figure 2). The dialyzable fraction contains also a number of oligopeptides. After total hydrolysis of the ammoniacal eluate from the Amberlite IR-120, paper electrophoresis (Figure 1) and chromatography reveal the presence of all the constituent amino acids of the wool. The levels of glutamic acid, glycine, serine, threonine, alanine, histidine, and lysine are especially important. The level of aspartic acid is virtually identical before and after total hydrolysis of the ammoniacal eluate; the aspartic acid, then, is almost entirely in the free form in the dialyzable fraction. After oxidation by performic acid, the cystine present in the total hydrolysate of the dialyzable fraction is changed into cysteic acid, which may easily be identified by paper electrophoresis; its level is relatively high (Figure 3) and increases with time of hydrolysis.

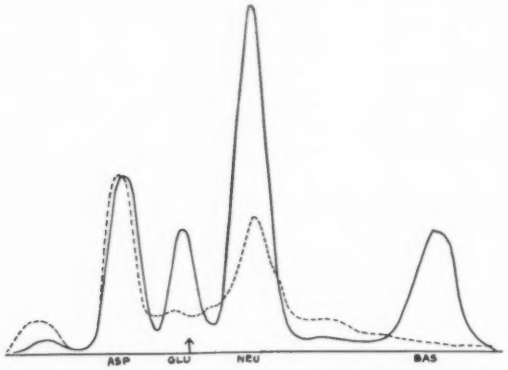

Fig. 1. "Amino acid" fraction of the hydrolysate. Photodensitometric recording of the ninhydrin coloration after paper electrophoresis of the amino acids of the dialyzable solubilized fractions (pyridine-acetic acid buffer, pH 3.9, 6 hr., 400 volts). Broken line: free amino acids and peptides (note the large proportion of free aspartic acid). Full line: total hydrolysate of the dialyzable solubilized peptides. Augmentation of the levels of glutamic acid (GLU), neutral amino acids (NEU), and of the basic amino acids (BAS) is particularly evident. The aspartic acid, which does not increase after total hydrolysis, must then be entirely in the free form in the hydrolysate of wool by 0.1 *N* sulfuric acid in the presence of thioglycollic acid.

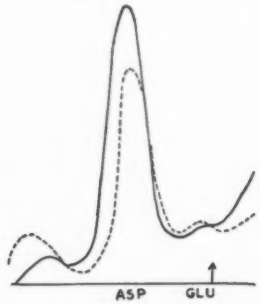

Fig. 2. Comparison of the levels of free aspartic acid at different times of hydrolysis. Photodensitometric recording of the ninhydrin coloration of the paper electropherograms at pH 3.9. Broken line: free aspartic acid in the hydrolysate after 4 hr. at 100° C. in 0.1 *N* sulfuric acid in the presence of thioglycollic acid. Full line: free aspartic acid after 8 hr. of hydrolysis.

Discussion of Results

The results we have just exposed present a certain number of points common with those obtained during the hydrolysis of wool keratin, wool cortical cells, and horn keratin by 0.1 *N* sulfuric acid alone. In effect, in reducing acid medium, the liberation of aspartic acid occurs in a preferential fashion [1, 4, 5, 7]; furthermore, the hydrolysate also contains high molecular weight peptides that present a common physico-chemical characteristic: their thermosolubility in dilute sulfuric acid.

Nevertheless, during hydrolysis in reducing acid medium, one can observe notable differences. First of all, the rate of hydrolysis and solubilization is greatly accelerated; in reducing acid medium 75%

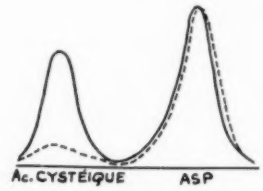

Fig. 3. Cystine content of the dialyzable peptides solubilized in reducing acid medium. Photodensitometric recording of the ninhydrin coloration of the total hydrolysates of the peptides separated by paper electrophoresis at pH 3.9. Broken line: total hydrolysates. Full line: total hydrolysates oxidized by performic acid. During the oxidation, the cystine is transformed into cysteic acid, which is easily detected on the electropherograms at pH 3.9. The high proportion of cysteic acid is clearly seen in the dialyzable peptides of this hydrolysate (8 hr. at 100° C., 0.1 *N* sulfuric acid in the presence of thioglycollic acid).

of the nitrogen is solubilized in 12 hr.[5] To obtain the same degree of hydrolysis in non-reducing acid medium, the hydrolysis must be prolonged for 50 hr. [1].

Other differences are seen concerning solubilization of sulfur (thiol + disulfide). In reducing acid medium, solubilization of the sulfur is not only rapid, but follows a curve practically parallel to that of the nitrogen; for instance, in 8 hr. of hydrolysis, 58% of the nitrogen and 60% of the sulfur are solubilized (Tables I and II). In non-reducing acid medium, solubilization of the sulfur is always less than that of the nitrogen; for instance, in 32 hr. of hydrolysis by the 0.1 *N* sulfuric acid, 51.8% of the nitrogen and 24.6% of the sulfur are solubilized.

Furthermore, the chromatographic analyses of the peptide fractions solubilized in reducing acid medium allowed us to show that their content of cystine was appreciable. Finally, contrary to that which we observed during the hydrolyses in acid medium alone, the cystine content of the residual wool of the reducing hydrolysis diminished progressively (Table II).

Therefore, in 0.1 *N* sulfuric acid, the "enucleation" of the aspartyl residues of the peptide chains occurs in a preferential fashion. In weak acid medium (acetic acid), the specific liberation of aspartic acid does not occur. In non-reducing medium the integrity of the disulfide linkages limits the solubilization of the peptide fragments formed and leads to the formation of a resistant "core" rich in cystine. In thioglycollic acid medium, the rupture of a considerable number of the disulfide bridges favors the solubilization of numerous peptides which can contain a greater or lesser proportion of cysteine.

However, in acid thioglycollic medium, the reduction of the disulfide bonds is not total [6]; at pH 5, the thioglycollic acid reduces only 45% of the disulfide bonds present, and this percentage is increased only in alkaline medium. One conceives, then, that the rate of solubilization of the nitrogen and the sulfur, while considerably accelerated in acid reducing medium, can slow down as a function of the time of hydrolysis. In our experiments, about 50% of the wool was solubilized in 4 hr. and 70% in 12 hr (Table I). This limitation is explained by the fact that after 4 hr. of hydrolysis the residual wool, impoverished in aspartic acid, is less selectively hydrolyzed by the dilute sulfuric acid, and also by the fact that the percentage of reduced disulfide bonds has greatly diminished.

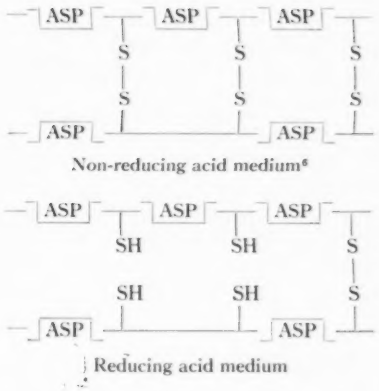

Literature Cited

1. Biserte, G. and Pigache, P., *Bull. Soc. Chim. Biol.* **33**, 1379 (1951); **34**, 51 (1952).
2. Biserte, G. and Pigache, P., *Bull. Soc. Chim. Biol.* **36**, 159 (1954).
3. Biserte, G., Paysant, P., and Boulanger, P., *Pathologie-Biologie* (Semaine des Hôpitaux de Paris) **7**, nº 13–14, 1529 (1959).
4. Bull, H. B., Hahn, J. W., and Baptist, V. H., *J. Am. Chem. Soc.* **71**, 550 (1949).
5. Leach, S. J., *Proc. Int. Wool Text. Res. Conf. Austr.* **C**, 181 (1955).
6. O'Donnell, I. J. and Woods, E. F., *Proc. Int. Wool Text. Res. Conf. Austr.* **B**, 49 (1955).
7. Partridge, S. M. and Davis, H. F., *Nature* **165**, 62 (1950).
8. Pigache, P., "Contribution à l'étude de la structure chimique de la kératine de Laine," These d'Ingénieur-Docteur, Faculté des Sciences, Lille, nº 21 (1956).
9. Pigache, P. and Biserte, G., *Bull. Soc. Chim. Biol.* **40**, 591 (1958).
10. Savige, W. E., TEXTILE RESEARCH JOURNAL **30**, 1 (1950).
11. Shinohara, K., *J. Biol. Chem.* **109**, 665 (1935); **112**, 671, 683 (1936).

Manuscript received March 28, 1960.

[5] Savige [10] has also studied the solubilization of wool in reducing acid medium. In thioglycollic acid medium at 60° C. during 24 hr., the dissolution of the wool is considerable (40% in 0.5 *M* medium, almost 100% in 10 *M* medium). On the other hand, in 0.01 *M* reducing sulfuric acid medium (mercaptoethanol 0.4 *M*, final pH 2.1), the solubilization of the wool, after 24 hr. at 60° C., is slight (of the order of 3%), while in 3 *M* reducing acetic acid medium (mercaptoethanol 0.4 *M*), 40% of the wool is solubilized. Thus, taking into account the results of Savige, it would seem that the results we have obtained in thioglycollic sulfuric acid medium should be interpreted not as a direct solubilization but rather as a veritable "directed" chemical hydrolysis of the wool.

[6] In this simplified scheme, we have shown only the interpeptide disulfide bridges.

Letters to the Editor

Short communications in the form of Letters to the Editor are intended to provide prompt publication of significant new research results and to permit an exchange of views on papers previously published in the JOURNAL. These communications are not submitted to formal review as are research papers, and the editors do not assume any share of the author's responsibility for the information given or the opinions expressed. When work previously published in the JOURNAL is the subject of critical comment, the authors of the original paper are given an opportunity to submit a reply, which will be published concurrently when possible.

A Ballooning Apparatus with Linear Yarn Movement

Manchester College of
Science and Technology
Manchester 1, England
April 19, 1960

To the Editor
TEXTILE RESEARCH JOURNAL

Dear Sir:

The limitations of existing types of apparatus used to simulate yarn balloons have been discussed previously [1]. A particular limitation of such apparatus is that once an equilibrium balloon profile has been achieved, no movement of yarn in the direction of the balloon axis can occur, thus excluding the influence of Coriolis, acceleration, and certain air drag forces directly attributed to linear yarn movement. These forces are an important feature of balloons formed during unwinding and during twisting processes having high linear yarn speeds.

A new type of ballooning apparatus has been described recently [2] which simulates actual ballooning conditions more closely than was hitherto possible. This equipment employs a closed loop of yarn having continuous linear movement, while a portion of the loop is simultaneously rotated about its axis. Referring to Figure 1, an endless length of yarn SCHG is given linear movement by means of a driven twin-grooved pulley at S, around which the yarn is lapped. At the same time, the length of yarn between H and G is rotated by means of the driven ballooning head at H, shown in more detail in Figure 2. The upper disc of the ballooning head contains a guide-eye E which can be moved diametrically in a slot in order to adjust the initial radius of the balloon. The yarn is threaded up the hollow bearing shaft to the guide eye E, which consists of a miniature ball bearing, the object of which is to prevent twist disturbance in the yarn. Thus, the ballooning head could be described as a zero efficiency false twister.

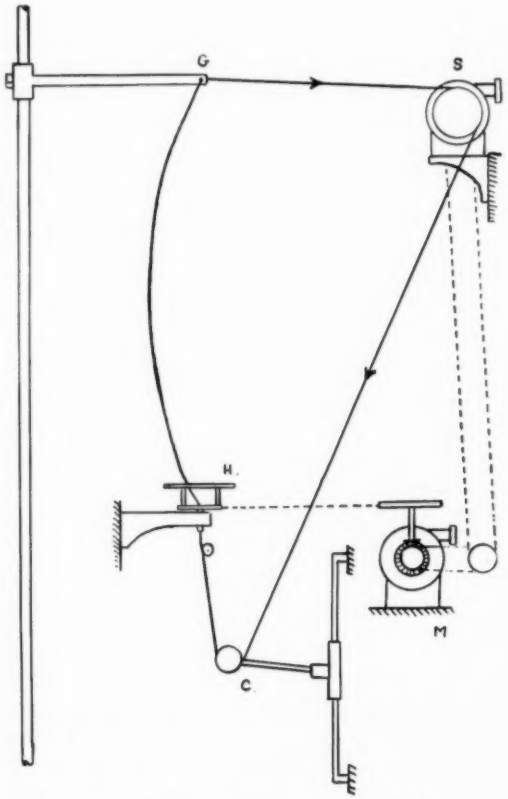

Fig. 1. The ballooning apparatus. M, driving motor; H, ballooning head; S, yarn winding unit; G, guide-eye; C, tension compensator.

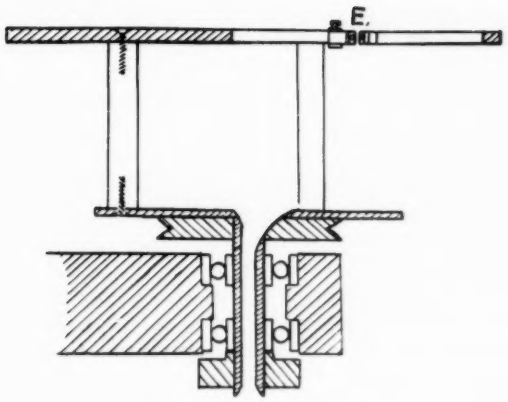

Fig. 2. The ballooning head.

The drive to the ballooning head is taken from a ¼ horsepower motor at M, through a stepless variable speed gear box, to give a maximum balloon speed of over 10,000 rpm. At the same time, another drive is taken through a second variable-speed gear box to the yarn pulley at S to give a maximum linear yarn speed of 2,000 yd./min. with a 3-in. diameter pulley.

The height of the guide at G can be adjusted to vary the height of the yarn balloon above the ballooning head, this height being variable between zero and 36 in. in the particular apparatus described. Any slack yarn is taken up by the jockey pulley at C, which is also used to pretension the yarn before it passes to the ballooning head. Although pulley C is used to add tension to the yarn, it cannot be used to measure the ballooning tension (i.e., the axial component of the yarn ballooning tension). At present, the yarn tension is measured using a standard hand tension meter immediately after guide G, suitable allowance being made for the effect of friction at this guide. However, it is intended to incorporate a strain gauge or other transducer in the arm carrying guide G in order to obtain a direct reading of the ballooning tension.

Preliminary experiments indicate that special attention must be paid to obtaining a smooth joint in the yarn which forms the closed loop. If a bulky knot occurs, there will be a certain amount of disturbance in the balloon form, hindering the maintenance of equilibrium profiles and tensions. For ease of operation, various ply and cable yarns have been employed which could be spliced to give a smooth joint. No evidence of yarn twist disturbance was detected, and it is thought that, for most yarns, twist redistribution will be negligible.

Comparisons with the results of tests on a ballooning apparatus having no linear thread movement are most interesting. It is now possible to commence with rotation of the ballooning head alone, maintaining the driving pulley at S stationary. Movement of pulley S is next introduced, at first slowly and later as fast as is required up to the maximum speed available. During such an experiment, changes in balloon shape and tension directly attributable to the linear yarn movement are immediately evident.

Finally, it should be mentioned that even this improved apparatus is unable to simulate unwinding conditions exactly. During overend withdrawal from a package, while it is possible to know exactly the distance between the point where the yarn first moves on the package and the point of the balloon apex at the first guide, the amount of yarn slippage on the package surface before entering the balloon is a variable quantity dependent upon several factors. Thus, while in the ballooning apparatus we have a predetermined balloon height, during unwinding there is one further degree of freedom which cannot be directly simulated at present. During ring and cap spinning, however, the simulation of the actual conditions is very close.

Literature Cited

1. Brunnschweiler, D. and Mohammadain, I. S., TEXTILE RESEARCH JOURNAL **29**, 119 (1959).
2. Cotterill, P. J., M.Sc. Tech. Thesis, University of Manchester (1959).

D. BRUNNSCHWEILER [1]
P. J. COTTERILL [2]
N. HODGKINSON

[1] Present address: Leesona Holt Limited, Darwen, England.

[2] Present address: British Nylon Spinners Limited, Pontypool, Monmouthshire, England.

Cotton Fiber Weight Distribution

The Arvind Mills Limited
P. O. Box 56
Ahmedabad 2, India
March 16, 1960

To the Editor
TEXTILE RESEARCH JOURNAL

Dear Sir:

In a recent article in this Journal [1] the authors have discussed fiber fineness distribution according to fiber length group. The authors have shown that the short fibers are finer than the long ones varying by fiber length group.

It is our day-to-day experience that shorter fibers of a cotton sample are coarser than the longer fibers. Fiber weighing technique is used as a routine test to determine fiber fineness in our laboratory. Tufts of fibers of different group length are taken from the Baer-sorter pattern, spread on a microscope slide, counted under low power microscope, collected, and weighed on a microbalance. The fiber weight per inch of each length group is determined and the average is reported.

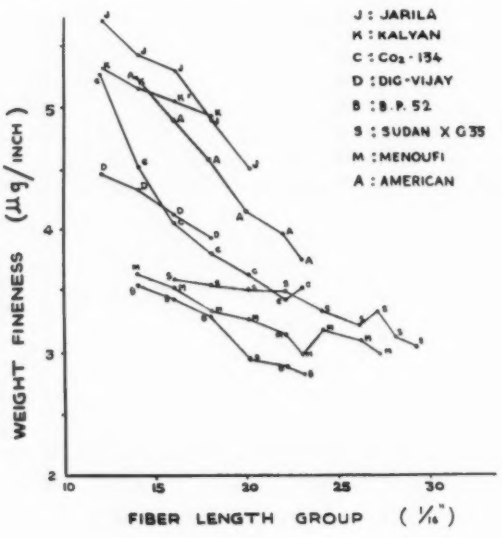

Fig. 1.

Iyenger and Turner [2] have reported that fibers of longer length of given *G. hirsutum* cottons have a lower fiber weight per inch and that *G. herbaceum*, *G. neglectum*, and *G. indicum* cottons do not generally show a large change in fiber weight with fiber length. Lord [3] has also reported that shorter fibers are coarser than longer ones. The shorter fibers give higher fiber weight fineness even though they are more immature.

Figure 1 gives the fiber weight distribution according to length groups of different varieties of cottons. It is very clear that shorter fibers show higher weight fineness than longer fibers, which is contrary to the data given in the above-mentioned article. In Figure 1 only the broad varieties of cottons are given. The Jarila, Kalyan, CO-2/134, and Dig-Vijaya are some of Indian varities, B.P.52 is a representative of African cotton variety, Sudan XG3S represents one of the Sudan cottons, Menoufi (X-Menor) represents one of the Egyptian cottons, and American (Californian G.M. $1\frac{5}{32}$") is an American cotton. Many more varieties of cottons are tested in this laboratory and all show the same trend.

Literature Cited

1. Fiori, Louis A., Louis, Gain L., and Sands, Jack E., TEXTILE RESEARCH JOURNAL **29**, 706–716 (1959).
2. Iyenger, R. L. N. and Turner, A. J., Indian Central Cotton Committee, Technological Laboratory, Technical Bulletin Series, B. No. 7 (1930).
3. Lord, E., *J. Textile Inst.* **47**, T16–47 (1956).

JAMNADAS SHAH

Linear Densities of Fibers in Selected Length Groups of 42 Domestic and Foreign Cottons

Southern Utilization Research
and Development Division
1100 Robert E. Lee Boulevard
New Orleans, Louisiana
May 18, 1960

To the Editor
Textile Research Journal

Dear Sir:

The authors have read with interest the Letter to the Editor by Mr. J. Shah and offer the following comments.

Admittedly, the statement by Fiori et al. [2] to which Mr. Shah objects was somewhat broad and open to conflicting interpretations. According to Mr. Shah's figure, he apparently did not consider or measure length groups shorter than $^{12}/_{16}$ to $^{14}/_{16}$ in. long, whereas Fiori et al. in their Figure 1 showed the fineness–length distribution for all groups $^{5}/_{16}$ in. and longer. It will be noted that the shorter fine fibers occur below the $^{12}/_{16}$-in. point. Attention was called in the paper to the curvilinear relationship which is often found. The linear density or weight fineness was measured in accordance with the recommended ASTM test method [1].

Table I is presented as further evidence of the relationship to be found between linear density and length distribution within a cotton. It shows the linear densities, as measured at the Southern Regional Research Laboratory, of 42 different cottons including both American and foreign growths. The first 35 cottons listed are in approximate order of increasing staple length, ranging from $^{29}/_{32}$ to $1^{7}/_{16}$ in. It is evident that, in the preponderant number of cases, the shorter length groups have lower linear densities than the intermediate groups. However, the longest groups also have lower densities than the intermediate groups.

Therefore, we do not agree with Mr. Shah that linear density decreases with increasing length over the entire length distribution. It is possible that Mr. Shah's misconception is due to the fact that he did not measure length groups shorter than $^{12}/_{16}$ to $^{14}/_{16}$ in. Also, our findings do not corroborate the general findings of Iyenger and Turner [3] that fibers of the longer lengths of *G. hirsutum* cottons have lower linear densities than those of the shorter lengths.

As pointed out above, the linear densities shown in Table I were not obtained by the cut fiber technique used by Iyenger and Turner, the employment of which, they indicate, may give substantially different results. Also, the cottons they measured were

TABLE I. Linear Density of Selected Length Groups of 42 Domestic and Foreign Cottons

Type or variety	Selected Length Groups—$^{1}/_{16}$ inch				
	5 μg/in.	9 μg/in.	13 μg/in.	17 μg/in.	21 μg/in.
Upland	3.85	5.25	5.25	3.90	—
Upland	3.60	4.58	5.55	4.60	—
Upland	4.85	5.60	5.65	4.80	—
Upland	4.70	5.45	5.60	4.75	—
Upland	3.05	3.45	4.25	3.90	—
Upland	4.25	4.55	4.40	4.40	—
Upland	3.45	4.60	4.75	4.55	—
Upland	3.55	4.00	4.40	4.30	—
Upland	5.30	6.50	6.05	4.90	—
Upland	4.35	4.80	4.80	4.20	—
Upland	2.65	3.40	3.75	3.80	—
Interspecies	3.00	4.00	4.15	3.90	3.20
Upland	3.25	4.65	4.80	4.55	3.85
Empire	2.65	3.50	3.70	4.40	3.70
Upland	3.70	3.90	4.10	4.45	3.70
Upland	3.30	3.50	4.05	4.70	4.00
Upland	2.45	3.15	3.10	3.90	3.40
Upland	3.25	3.95	4.55	4.40	3.80
Rowden	7.25	6.10	6.75	5.60	4.55
Hopi Acala 50	3.45	3.70	3.70	3.70	3.25
Deltapine	3.60	4.20	4.50	4.70	3.90
Upland	4.40	5.20	5.45	5.25	4.60
Upland	3.15	3.45	4.35	4.80	3.80
Upland	3.30	4.15	4.35	4.50	4.20
Coker 100 Wilt	4.10	4.40	4.50	4.35	4.00
Upland	4.00	3.65	4.30	4.20	3.60
Upland	2.95	3.15	3.75	3.95	3.55
Deltapine	4.50	4.75	4.50	4.90	4.20
Tanguis	4.30	5.05	4.90	4.95	4.80
Hopi Acala 54	6.70	4.65	5.00	4.70	4.30
Karnak	2.15	2.70	2.80	2.90	2.85
Wilds	4.05	4.20	3.85	3.95	4.00
Pima S-1	2.80	3.00	3.40	3.30	3.05
Upland	3.25	3.70	4.05	4.30	3.80
Strain #330	3.30	3.25	3.65	3.55	3.70
Russian Pervyi	4.75	4.75	4.80	4.90	3.85
Russian Otbornyi	4.60	4.35	4.90	4.75	4.05
Belgian Congo	2.95	3.05	4.15	3.65	3.40
Pakistan 289F	3.35	4.10	3.65	3.65	3.60
Pakistan Ayad	3.95	4.20	4.60	4.05	—
Uganda #701	2.90	2.85	3.20	3.50	3.20
Ethiopian	2.65	3.85	4.20	3.95	3.95

from the 1923–26 crops, whereas all of the cottons listed in our table were grown since 1940.

Literature Cited

1. Am. Soc. Testing Materials, Committee D-13, ASTM Standards on Textile Materials (with related information), Philadelphia, ASTM Designation D1442-54.
2. Fiori, L. A., Louis, G. L., and Sands, J. E., TEXTILE RESEARCH JOURNAL **29**, 706–716 (1959).
3. Iyenger, R. L. N. and Turner, A. J., *J. Textile Inst.* **21**, T417–440 (1930).

JACK E. SANDS
GAIN L. LOUIS
JOHN D. TALLANT

A Note on the Effects of Humidity and Actinic Exposure on Fabric Strength[1]

Georgia Institute of Technology
Engineering Experiment Station
Atlanta, Georgia
April 18, 1960

To the Editor
TEXTILE RESEARCH JOURNAL

Dear Sir:

In connection with a WADC research program, initiated primarily to estimate the effectiveness of specific commercial fungicidal applications, a considerable amount of data was collected to evaluate the effects of actinic exposure, humidity, temperature, and rainfall on the tenderization of a cotton sateen fabric.

Fabric panels were weathered outdoors for periods up to and including 12 months at test sites in Alaska, New Mexico, and Florida. The panels were exposed on racks facing south, fixed at a 45° angle to the horizontal. Breaking strength measurements were made on both 4 × 6 in. and 1 × 6 in. specimens cut from these panels. The amount of actinic exposure and rainfall and the extremes of temperature and humidity were recorded daily at each of the exposure sites.

It is a well established fact that the exposure of cotton fabrics to ultraviolet radiation produces a marked strength loss. Although the exact chemical mechanism of this reaction is unknown, chemical kinetic theory suggests that temperature and relative humidity would affect the rate of this fabric tenderizing reaction. The latter is of importance because it controls the equilibrium moisture content of the fabric. Our understanding of this reaction has not been developed to the point where a theoretical mathematical model can be prescribed to relate these variables. For this reason, a simple linear model given in Equation 1 was employed. Aside from this arbitrary selection of the model, all other conditions of the experiment were such that estimates of the constants β_0, β_1, β_2, β_3, and β_4 could best be made by the standard method of least squares; i.e., the observational errors in the X's are negligible and the random errors in the Y's, denoted by ϵ_n below, are independent of the X's and have a constant dispersion.

$$Y_n = \beta_0 + \beta_1 X_a + \beta_2 X_r + \beta_3 X_t + \beta_4 X_h + \epsilon_n \quad (1)$$

where Y_n = percent breaking strength retention

$$= 100 \times \frac{\text{breaking strength after the first } n \text{ days of outdoor weathering}}{\text{breaking strength before weathering}}$$

X_a = cumulative actinic exposure in kilo langleys (10^3 g.cal./cm.^{2})

$$= \sum_{i=1}^{n} a_i$$

where a_i = total kilo langleys of actinic exposure at the exposure site in question on the ith day.

X_r = cumulative total inches of rainfall

$$= \sum_{i=1}^{n} r_i$$

[1] This note was taken from WADC Technical Report 57-711, ASTIA Document No. 151-127.

where r_i = total inches of rainfall at the exposure site in question on the ith day.

X_t = weighted average temperature (° F.)

$$= \frac{\sum_{i=1}^{n} t_i a_i}{\sum_{i=1}^{n} a_i} = \frac{\sum_{i=1}^{n} t_i a_i}{X_a}$$

where t_i = high temperature at the exposure site in question on the ith day.

X_h = weighted average humidity (%)

$$= \frac{\sum_{i=1}^{n} h_i a_i}{\sum_{i=1}^{n} a_i} = \frac{\sum_{i=1}^{n} h_i a_i}{X_a}$$

where h_i = average relative humidity at the exposure site in question on the ith day. ϵ_n = random error, assumed to be independent of the X's and having a constant variance for all values of n. β_0, β_1, β_2, β_3, and β_4 are constants.

The above definitions of the independent variables evolved from a desire to express Y as a percent strength retention based on the original fabric strength; with this definition, the relationship between these variables seemed less artificial than with other definitions considered. Since Y was based on the original fabric strength, all of the X's must be defined on a cumulative basis; the above choice of definitions for the X's seemed best from a chemical reaction viewpoint.

TABLE I. Results of Least Squares Regression of Fabric Strength Retention on Outdoor Weathering Data

	4 × 6 In. specimens	1 × 6 In. specimens
	Regression equations	
Four variables	$Y_N = 137.1 - .24X_a - .10X_r - .044X_t - .41X_h$	$Y_N = 125.9 - .21X_a - .20X_r - .059X_t - .34X_h$
Two variables	$Y_N = 141.4 - .27X_a - .51X_h$	$Y_N = 134.0 - .25X_a - .52X_h$

Partial correlation coefficients

	X_a	X_r	X_t	X_h	X_a	X_r	X_t	X_h
Four variables	−.59	−.05	−.07	−.25	−.50	−.09	−.09	−.14
Two variables	−.82	—	—	−.58	−.79	—	—	−.55

TABLE II. Computed and Observed Values of Breaking Strength Retention Corresponding to the 12 Basic Outdoor Weathering Conditions

Site	Months of outdoor weathering	X_a	X_h	4 × 6 in. specimens Y_c*	Y_0	Y_c* − Y_0	1 × 6 in. specimens Y_c†	Y_0	Y_c† − Y_0
Florida	2	22.6	80.2	94.4	93.1	+1.3	86.6	88.2	−1.6
	4	49.7	80.5	86.9	85.1	+1.8	79.7	81.2	−1.5
	8	109.1	77.8	72.3	72.0	+0.3	66.3	69.6	−3.3
	12	163.3	77.7	57.7	56.8	+0.9	52.8	51.4	+1.4
New Mexico	2	37.9	45.1	108.2	104.6	+3.6	101.1	95.6	+5.5
	4	74.0	44.8	98.6	97.7	+0.9	92.2	93.2	−1.0
	8	147.3	33.7	84.4	83.4	+1.0	79.7	80.8	−1.1
	12	224.3	38.1	61.4	61.7	−0.3	58.1	57.2	+0.9
Alaska	2	12.4	67.9	103.4	103.5	−0.1	95.6	95.7	−0.1
	4	14.4	67.9	102.9	103.1	−0.2	95.1	97.4	−2.3
	8	73.6	58.7	91.6	96.0	−4.4	85.1	91.4	−6.3
	12	125.9	61.0	76.3	74.9	+1.4	70.8	72.1	−1.3
				Absolute average		1.4%			2.2%
				Standard deviation‡		1.9%			2.8%

* $Y_c = 141.4 - 0.27X_a - 0.51X_h$; for 4 × 6 in. specimens.

† $Y_c = 134.0 - 0.25X_a - 0.52X_h$; for 1 × 6 in. specimens.

‡ Standard deviation = $\sqrt{\sum_{i=1}^{12} \frac{(Y_{ci} - Y_{0i})^2}{12 - 1}}$.

Twelve basic exposure conditions were present in the data utilized in making the correlation calculations; these conditions consisted of four different periods of outdoor weathering at each of the three test sites. Thirty-six lot (10 specimens each) mean breaking strength retentions were available for each basic exposure condition. The quantitative results of this analysis are given in Table I. A simplified analysis involving only humidity and actinic exposure was also made because of the relative unimportance of rainfall and temperature as shown by their small parital correlation coefficients.

By use of the equations for 4 × 6 in. and 1 × 6 in. specimens involving two variables, the percent breaking strength retentions were computed for each of the 12 basic exposure conditions described above. These computed values, denoted by Y_c, are given in Table II along with the observed average percent breaking strength retentions for the 36 test lots comprising each of the 12 basic exposure conditions; these observed values are denoted by Y_0. The agreement between the predicted or calculated values and the observed or measured values was quite good. The standard deviation of the differences, $(Y_c - Y_0)$, was only 1.9% for the 4 × 6 in. and 2.8% for the 1 × 6 in. specimens. An analysis of the random errors in determining the lot mean breaking strengths indicates that an appreciable portion of the differences $(Y_c - Y_0)$ are due to random sampling and measurement errors; i.e., most of the contribution to ϵ_n in Equation 1 was from errors in determining the lot mean breaking strength and only a small contribution from inadequacies of the model.

It is therefore concluded that a linear combination of the cumulative langleys of actinic exposure and the weighted average relative humidity, as given in Table I, explain almost all of the variation in the percent strength retention after outdoor exposure

JOSEPH J. MODER

The X-Ray Diffraction Pattern of Iodinated Wools

Wool Research Laboratories
Division of Textile Physics
Commonwealth Scientific and
Industrial Research Organization
338 Blaxland Road
Ryde, N.S.W., Australia
March 4, 1960

To the Editor
TEXTILE RESEARCH JOURNAL

Dear Sir:

Harrison and Speakman [6] found that when wool was treated in a propanolic solution of iodine, less iodine was bound than when an ethanolic solution was used. They concluded that the "fine structure" of wool was inaccessible to molecules larger than those of n-propanol. Previously, Fraser and MacRae [4] had reported that ethanolic iodination resulted in the appearance of a *new* x-ray reflection with a spacing of 34 Å and in the intensification of the reflection at 25 Å.

We have treated Lincoln wool samples in solutions of iodine in both ethanol and propanol. The technique of Harrison and Speakman [6] was carefully followed, an important feature of the method being that the wool was dry during iodination. Treatment in the propanol solution was for 70 days, and in the ethanol solution for 40 days, both at 20° C. Cross sections of fibers from the samples immediately after removal from the iodine solutions showed that in both cases the fibers were heavily stained throughout. In Table I are shown mean values of tyrosine contents of the treated wools. Tyrosine was determined by the method of Bernhart [1]. Apparently the washing of wool in an alkaline solution of sodium thiosulfate (the method used for removing excess iodine) caused a small loss of tyrosine. The table shows a comparison of the present results with data taken from the paper of Harrison and Speakman [6]. These authors determined combined iodine in the wool; the losses were deduced on the assumption that all combined iodine was in the form of di-iodotyrosine. Under these circumstances agreement between the results is satisfactory.

Photographs showing the x-ray diffraction patterns of the iodinated Lincoln wools were obtained.

TABLE I. Tyrosine Contents of Treated Wool Samples

Treatment	Tyrosine content, (% of weight of dry untreated wool)	Tyrosine loss, %	Tyrosine loss (Harrison and Speakman), %
Cleaned only	3.42 ± 0.07	—	—
Cleaned and given all treatments except iodination	3.13 ± 0.06	8.5	—
Cleaned and iodinated in ethanol	0.48 ± 0.07	86	98
Cleaned and iodinated in propanol	2.10 ± 0.04	39	41

The sample iodinated in ethanol solution showed a prominent meridional reflection with a spacing of 34 Å, but there was no appreciable intensification of the 25 Å reflection. A 34 Å reflection was absent in the case of the sample iodinated in propanol, the pattern differing only in minor details from that due to untreated wool.

Simpson and Woods [7] suggested that the 25 Å reflection which they found in reduced wool treated with silver nitrate resulted from the occurrence of cystine residues at 25 Å intervals along the fiber axis. If this is correct, the absence of the 25 Å reflection indicates that the present method of ethanolic iodination leaves intact the regularly repeating cystine residues. The major difference in technique between this iodination and that of Fraser and MacRae [4] was that in the latter case no attempt was made to exclude water during iodination.

It is reasonable to assume that the 34 Å reflection is due to regularly repeating di-iodotyrosine residues in the direction of the fiber axis. These residues must be associated with organized regions, presumably microfibrils. The obvious working assumption to make is that both ethanol and propanol solutions iodinate tyrosine residues in the matrix, but only the ethanol solution produces iodination of tyrosine in the microfibrils. It does not follow that the propanol solution iodinates *all* the tyrosine in the matrix.

There are reasons from D–H exchange [5], x-ray diffraction, and mechanical studies [3] to suppose that microfibrils are by no means as completely hydrated as matrix when wool fibers are placed in water. Furthermore, Bradbury's work [2] shows that the volume sorbed by wool fibers in water, methanol, ethanol, or n-propanol is nearly the same, so that it is probably unrealistic to consider that the additional "penetration" of ethanol solution of iodine over that of the proparol solution is more than a few angstroms. If these propositions are correct we are led to the view that the regularly repeating tyrosine residues are near the outside of the microfibrils. Simpson and Woods [7] arrived at a similar conclusion in the case of regularly repeating cystine residues.

We are most grateful to Mr. T. P. MacRae, who took the x-ray diffraction photographs, and to Mr. L. M. Dowling for the tyrosine analysis.

Literature Cited

1. Bernhart, F. W., *J. Biol. Chem.* **123**, x (1938).
2. Bradbury, J. H., TEXTILE RESEARCH JOURNAL **27**, 829 (1957).
3. Feughelman, M., TEXTILE RESEARCH JOURNAL **29**, 223 (1959).
4. Fraser, R. D. B. and MacRae, T. P., *Nature* **179**, 732 (1957).
5. Fraser, R. D. B. and MacRae, T. P., *J. Chem. Phys.* **28**, 1120 (1958).
6. Harrison, D. and Speakman, J. B., TEXTILE RESEARCH JOURNAL **28**, 1005 (1958).
7. Simpson, W. S. and Woods, H. J., *Nature* **185**, 157 (1960).

A. R. HALY
M. FEUGHELMAN

The Differential Thermal Analysis of Textile and Other High Polymeric Materials

Textile Research Institute
Princeton, New Jersey
May 17, 1960

To the Editor
TEXTILE RESEARCH JOURNAL

Dear Sir:

Recently the thermal behavior of various textile fibers and other high polymers has been studied by differential thermal analysis (DTA). In DTA thermally detectable transitions or reactions that occur as a substance is heated at a constant rate through the temperature range of interest are measured. This is done by determining the temperature difference (ΔT) that obtains between a thermally inert reference substance (calcined aluminum oxide was used in this work) and the substance being examined. ΔT is usually continuously recorded as a function of sample or furnace temperature to yield a curve or thermogram of ΔT in degrees Centigrade plotted against T in degrees Centigrade that is uniquely characteristic for each different sample substance. The DTA curve is characterized by the appearance of peaks due to deflections from the thermally steady state. The technique has been fully described in the literature [14, 17] and was first reported in 1922 [14]. However, the application of DTA to high polymers is of recent date and has been limited largely to a few general surveys [5, 12] and more detailed investigations of the simple transitions occurring at temperatures below 300° C. [4, 9, 10], with the exception of work by Morita [13] and a very recent paper by Anderson and Freeman [1]. Very little is reported on textile fibers [5, 19], and no detailed study of the high-temperature degradation of textile materials by DTA has been reported in the literature at this writing.

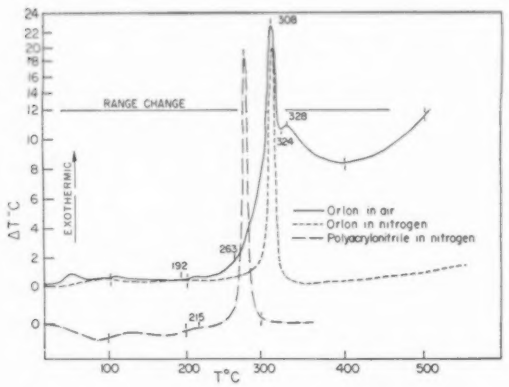

Fig. 1. DTA curves of Orlon and polyacrylonitrile.

Fiber and fabric samples of 75–150 mg. were heated at a rate of 10° C./min. from room temperature to 550° C. The techniques and apparatus employed were based on the work of Gordon and Campbell and others [7, 17] and will be described at a later date. The results obtained have been shown to be quite reproducible.

In Figure 1 the thermograms obtained in air and in nitrogen for Orlon[1] and in nitrogen for pure polyacrylonitrile (PAN) of molecular weight 200,000, in an amorphous form, are shown. In the case of Orlon both curves are dominated by a sharp exothermic reaction with a peak at 308° C. The air curve shows a second, less important, exothermic peak at 328° C., followed by a dip. These latter reactions have been eliminated under a nitrogen atmosphere. There is also a notable lack of any endothermic reaction, which suggests that Orlon does not undergo depolymerization as do cellulose and nylon. In nitrogen, PAN yields a DTA curve essentially identical in configuration with that of Orlon except that the sharp exotherm now occurs at 272° C. instead of 308° C. Since the primary differences between these two materials are those of crystallinity and chain orientation, it is suggested that the difference of 36° C. is related to these structural features. This prominent exothermic reaction, which is nonoxidative in character, is believed to represent the cross-linking of the PAN chains by the elimination of HCN and/or the formation of naphthyridine-like rings along the chains, as first suggested by Houtz [8] in his discussion of "black Orlon" since reactions such as cross-linking or cyclization should in general be of an exothermic character. Pyrolysis studies on PAN have indicated that HCN is liberated above 200° C., and evidence for the formation of fused rings along the PAN chains has been obtained [3]. Madorsky suggests that

[1] Du Pont trademark.

PAN becomes stabilized on heating by cross-linking, with additional stability conferred by the formation of conjugated double bonds in the chains [11].

In Figure 2, curves for drawn Dacron [1] fiber in air and nitrogen are shown together with the curve obtained for undrawn Dacron fiber under nitrogen. In the case of the drawn fiber, the endothermic reaction with a peak at 260° C. in air and 262° C. in nitrogen represents polymer melting; the melting points so obtained compare favorably with literature values [15]. In air, exothermic activity occurs following melting, followed by a sharp rise in the curve at about 440° C. to a prominent peak at 470° C. Under nitrogen, the suppression of oxidative reactions reveals an exothermic reaction at 390° C., followed by an important endothermic reaction with a peak at 447° C. This latter reaction probably represents the depolymerization of polyethylene terephthalate polymer. The DTA curve for undrawn Dacron is quite different from that of drawn Dacron up to 230° C. and quite similar thereafter. Scott [16] has examined powdered amorphous polyethylene terephthalate by DTA up to a temperature of 300° C. and has found a second order transition at 70° C., followed by an exotherm at 140° C. said to be due to polymer crystallization. The determination of glass transition temperatures for nonfibrous polymers by DTA has indicated that the change in specific heat occurring at the glass transition results in a shift in the base line of the DTA curve [10]. Thus the DTA curve for undrawn Dacron fiber in Figure 2 indicates a second order transition at 77° C., followed by a crystallization process at 136° C. The curve then follows the same pattern as that found for the drawn fiber. The disparity in the depth of comparable peaks and in the area under comparable peaks in the drawn and undrawn fiber is due to the fact that sample size was larger for the undrawn fiber.

In Figure 3, thermograms for nylon 66 fabric are shown. Around 100° C., a weak endotherm appears in both curves due to the loss of sorbed water. In air an exothermic reaction initiating around 185° C. is interrrupted by a small endotherm which is polymer melting (m.p. *ca.* 255° C.). In nitrogen the exothermic reactions are completely eliminated, suggesting that those reactions were oxidative in nature. The two endotherms in nitrogen represent sharp melting of the polymer, followed by a depolymerization reaction beginning around 350° C. and completed at or near the peak temperature of 406° C. It should be noted here that different mechanisms

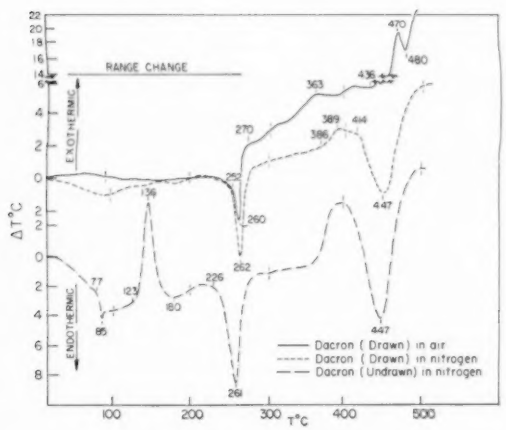

Fig. 2. DTA curves of Dacron.

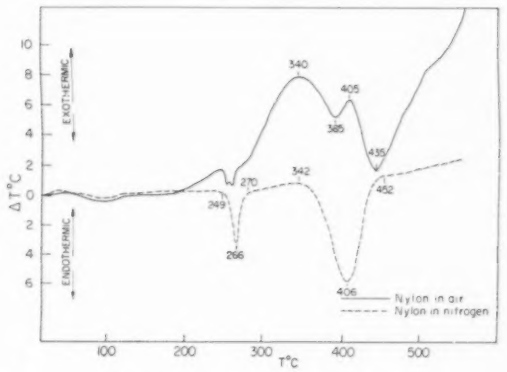

Fig. 3. DTA curves of nylon 66.

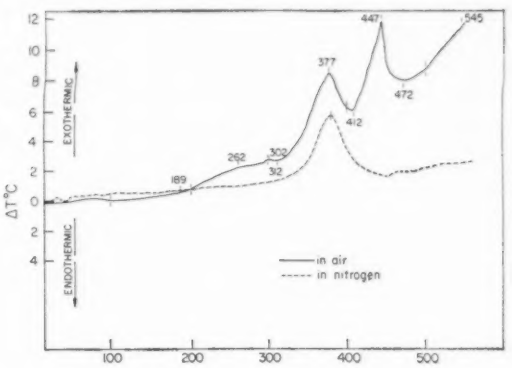

Fig. 4. DTA curves of Neoprene W.

may be operative during the thermal degradation of a polymer in air and in nitrogen.

The DTA curves for Neoprene W are given in Figure 4. The interesting feature in these curves is the exothermic reaction with a peak at 377° C. that persists under a nitrogen atmosphere. Since HCl may be eliminated by heating Neoprene rubber, it seems reasonable to assume that the polymer is being cross-linked at this temperature, as indicated by the nonoxidative exothermic reaction. Roff [15] reports that Neoprene hardens by cross-linking at elevated temperatures. Other textile fibers examined include cotton, nylon 6, cellulose acetate fiber, Arnel,[2] and polypropylene. In addition, other polymers such as butyl rubber, chlorosulfonated polyethylene, and polyethylene have been studied.

From the results obtained it would appear that specific reactions that occur during the thermal degradation of polymers such as rearrangements, cross-linking, and depolymerization may be detected and identified. Other results have also indicated that relatively small changes in polymer composition or the presence of substituents on the polymer backbone can readily be detected by DTA. The indications are that DTA may be a powerful technique for mechanism studies, as well as a means for the characterization of textile materials and evaluation of the thermal stability of textile fibers and fabrics. The study of the degradation reactions at high temperatures in textile fibers represents a new application of DTA. When used in conjunction with pyrolysis studies and thermogravimetric analysis (TGA), it is expected that many of the reactions and reaction mechanisms involved in the thermal decomposition of high polymers will be clarified. The area under a DTA peak is reported to be proportional to the heat of reaction, ΔH, so that quantitative data may also be obtained [2, 6]. Ke [9] has recently determined the crystallinity of isotactic polypropylene from the heats of fusion obtained from DTA data. Thus it is further suggested that crystallization processes, degree of crystallinity, and orientation phenomena in textile fibers may also be studied by DTA.

We are grateful for valuable discussions with W. J. Kauzmann. We are also indebted to the U. S. Naval Supply Research and Development Facility for supporting this work.

Further details of this work will be submitted for publication in this journal in the near future.

[2] Celanese trademark.

Literature Cited

1. Anderson, D. A. and Freeman, E. S., *J. Appl. Polymer Sci.* **1**, 192 (1959).
2. Borchardt, J. J. and Daniels, F., *J. Am. Chem. Soc.* **79**, 41 (1957).
3. Burlant, W. J. and Parsons, J. L., *J. Polymer Sci.* **22**, 249 (1956).
4. Chackraburtty, D. M., *J. Chem. Phys.* **26**, 427 (1957).
5. Costa, D. and Costa, G., *Chimica e industria (Milan)* **33**, 71 (1951).
6. Erikkson, E., *Ann. Agri. Coll. of Sweden* **19**, 127 (1952).
7. Gordon, S. and Campbell, C., *Anal. Chem.* **27**, 1102 (1955).
8. Houtz, R. C., TEXTILE RESEARCH JOURNAL **20**, 786 (1950).
9. Ke, B., *J. Polymer Sci.* **42**, 15 (1960).
10. Keavney, J. J. and Eberlin, E. C., *J. Appl. Polymer Sci.* **3**, 47 (1960).
11. Madorsky, S. L., *J. Research Nat. Bur. Standards* **63A**, 261 (1959).
12. Morita, H. and Rice, H. M., *Anal. Chem.* **27**, 336 (1955).
13. Morita, H., *Anal. Chem.* **28**, 64 (1956).
14. Murphy, C. B., *Anal. Chem.* **30**, 867 (1958).
15. Roff, W. J., "Fibers, Plastics, and Rubbers," New York, Academic Press (1956).
16. Scott, N. D., *Polymer* **1**, 114 (1960).
17. Smothers, W. J. and Chiang, Y., "Differential Thermal Analysis: Theory and Practice," New York, Chemical Publishing Company Inc. (1958).
18. Varma, M. C. P., *J. Appl. Chem.* **8**, 117 (1958).
19. White, T. R., *Nature* **175**, 895 (1955).

ROBERT F. SCHWENKER, JR.
LOUIS R. BECK, JR.

Ultraviolet Light and Conduction in Keratin

Wool Research Laboratories
Division of Textile Physics
Commonwealth Scientific and
Industrial Research Organization
338 Blaxland Road
Ryde, N.S.W., Australia
March 8, 1960

To the Editor
Textile Research Journal

Dear Sir:

In connection with a study of the effect of ultraviolet light on keratin it was found that radiation in the wave length range 2400–4000 Å had no observable effect on the electrical conductivity.

A single horsehair was cleaned by washing in cold petroleum ether, alcohol, and distilled water. Several changes of distilled water were used to ensure removal of ionic impurities.

The hair was mounted between clamps ≈ 1 mm. apart in an apparatus which has already been described [1], and a high-pressure mercury-in-quartz lamp (125 watts) was placed ≈ 30 cm. from the hair. A stream of air at $20 \pm 0.1°$ C. was blown over the hair at a velocity sufficient to ensure isothermal conditions for the fiber. The required relative humidity was achieved by including a sulfuric acid–water solution in the circulating system. Resistance measurements were made with a recording electrometer [1]; the standard resistors with which the hair was compared were 10^{13} Ω and 10^{11} Ω.

In the early stages of the experimental work irradiation appeared to change the conductivity, but the same effect was observed when the ultraviolet beam was interrupted.

Heat conducted from the lamp housing to the cell containing the hair produced this change. When this was remedied by thermally insulating the lamp housing a new conductivity change was observed. This effect remained when the fiber was removed, and was assumed to be caused by photo-emission from the brass electrodes since the effect was increased when dry nitrogen was substituted for the dry air. Nitrogen does not absorb UV radiation in the wave length range used and consequently an increased amount fell onto the electrodes.

To overcome the photo-emission an aperture-type collimator was then set up so that a thin beam of UV fell onto the hair alone. Under these conditions no change of conductivity was observed when the UV lamp was switched on whether the hair was dry or in an atmosphere of 90% RH.

The smallest change in resistance which could have been detected when the fiber was dry was a change from the dry resistance of 10^{17} Ω to a resistance of 0.5×10^{17} Ω. This is equivalent to a current change of 10^{-15} amperes.

The absence of any observable effect of UV on the conductivity indicates that conductivity carriers are not being generated, as they are in electronic semiconductors, even though the energy barrier to conduction (30 kcal./mole) is such that UV should have sufficient energy to release them. The result consequently implies that Baxter's proposal [2] of electronic semiconduction in keratin is not verified. A possible solution to the problem is that the conduction process in keratin is protonic even in the dry state, as has been proposed by Riehl [4] for gelatin.

Niven [3] has claimed that infrared radiation produces an increase in the conductivity of gelatin. Since UV had no observable effect on the conductivity of keratin it is suggested that the increase in conductivity in Niven's experiments was due to a temperature rise following the absorption of infrared radiation.

Literature Cited

1. Algie, J. E. Textile Research Journal **29**, 1 (1959).
2. Baxter, S., *Trans. Faraday Soc.* **39**, 207 (1943).
3. Niven, C. D., *Can. J. Phys.* **31**, 1095 (1953).
4. Riehl, *Kolloid Z.* **151**, 66 (1957).

J. E. Algie
A. R. Haly

Continuous Simultaneous Measurements of Rigidity and Regain in a Filament During a Sorption Process

C.S.I.R.O. Wool Research Laboratories
Division of Textile Physics
Ryde, N.S.W., Australia
April 11, 1960

To the Editor
TEXTILE RESEARCH JOURNAL

Dear Sir:

The changes in the mechanical properties of textile fibers and filaments during the processes of sorption and desorption of water are of considerable interest in helping to elucidate the relations between fiber structure and mechanical behavior and also from a practical viewpoint in providing a better understanding of the behavior of yarns and fabrics during manufacture and use.

The simple technique described here allows continuous simultaneous determination of the dynamic torsional rigidity of a fiber (or yarn) and of the uptake of water vapor (or other sorbate vapor) by the same fiber. Vapor uptake is measured by the vibroscope method [1, 6], in which the mass of the fiber is measured in terms of its natural frequency of transverse vibration, while rigidity is simultaneously measured by determining the period of oscillation of the torsion pendulum formed by the fiber and its tensioning weight.

The arrangement of the fiber as a vibroscope is shown in the diagram, a small tensioning weight being attached at its lower end. Excitation of the fiber to transverse resonance and detection of the motion may be by any convenient means; we have found electrostatic excitation [6] and optical detection to be very satisfactory. The amplitude of oscillation of the fiber is extremely small; about one fiber diameter is found satisfactory. The exciting frequency may be derived from a manually-adjusted audio-frequency oscillator, or the vibroscope may be of the self-oscillatory type [3] in which the excitation is from an amplifier coupled to the detector. The latter arrangement, being continuously self-adjusting, is preferable when sorption proceeds rapidly in the fiber.

Regain r of the fiber at any instant is given by

$$r = \frac{f_0^2}{f^2} \qquad (1)$$

where f_0 is the resonant frequency of the fiber when dry and f is the instantaneous resonant frequency. Expression 1 assumes that errors [3, 5, 7, 9] due to fiber stiffness, nonuniformity, etc. are negligibly small. It also assumes that the length of the fiber is unchanged during sorption; this is frequently true to a good approximation. In cases of appreciable length change the appropriate formula is

$$r = \frac{1}{1 + \frac{\Delta l}{l_0}} \left(\frac{f_0}{f} \right)^2 - 1 \qquad (2)$$

where Δl is the change from the "dry length" l_0.

Dynamic torsional rigidity of the fiber is determined by setting it manually in oscillation as a torsion pendulum and measuring the period with the aid of a stop watch. The amplitude of transverse oscillation is so small as to have negligible effect on the torsional oscillation. A fine wire attached to and projecting from the tensioning weight provides a convenient point which may be touched to set the weight rotating. Care is needed to set the weight in rotation only, and not swinging laterally as in a gravity pendulum. The torsional oscillations become damped out by internal friction in the fiber; in a typical sorption process it will be found necessary to excite the oscillations a number of times to obtain a complete picture of the variation in rigidity. Fre-

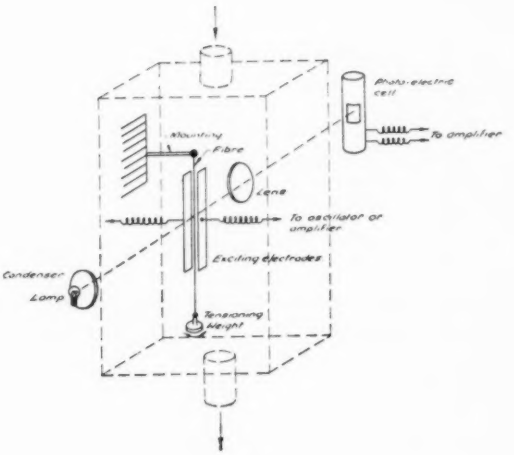

Fig. 1.

quently the absolute rigidity is not required but only the change relative to the rigidity in the dry state (in this note rigidity is taken to mean the restoring torque per unit angular displacement of the tensioning weight). Relative rigidity may be expressed simply as

$$\frac{N}{N_0} = \left(\frac{T_0}{T}\right)^2 \tag{3}$$

where N_0 is the rigidity of the dry fiber and T_0 the corresponding period of oscillation, while N and T are the rigidity and corresponding period at any instant during sorption. If it is required to determine the change in modulus of rigidity then from the expression

$$N = \frac{\pi}{2}\frac{nR^4}{l} \tag{4}$$

where n = modulus of rigidity, R = fiber radius, and l = fiber length, we find that

$$\frac{n}{n_0} = \left(\frac{T_0}{T}\right)^2 \frac{l}{l_0}\left(\frac{R_0}{R}\right)^4 \tag{5}$$

where the subscripts $_0$ refer to the fiber in the dry state. Determination of the variation in n thus requires knowledge of changes in l and R during sorption.

In practice, deviations from simple torsion-pendulum behavior may sometimes be observed, due to imperfect behavior of the fiber as a spring material; e.g., the observed period of oscillation may depend on the size of the initial deflection or the damping due to internal friction in the fiber may be large enough to prevent free oscillation. In such cases judgment must be exercised in interpreting the results.

The technique has proved useful in studying transient variations in the rigidity of wool fibers during sorption of water vapor [4].

Literature Cited

1. Gonsalves, V. E., TEXTILE RESEARCH JOURNAL **17**, 369 (1947).
2. Kinsler, L. E. and Frey, A. R., "Fundamentals of Acoustics," New York, Wiley (1950).
3. Mackay, B. H. and Downes, J. G., TEXTILE RESEARCH JOURNAL **28**, 467 (1958).
4. Mackay, B. H. and Downes, J. G., *J. Appl. Polymer Sci.* **2**, No. 4, 32 (1959).
5. Montgomery, D. J., *J. Appl. Phys.* **24**, 1092 (1953).
6. Montgomery, D. J. and Milloway, W. T., TEXTILE RESEARCH JOURNAL **22**, 729 (1952).
7. Stauff, D. W. and Montgomery, D. J., *J. Appl. Phys.* **26**, 540 (1955).
8. Stokes, J. J., "Non-Linear Vibrations," New York, Interscience (1950).
9. Voong, E. T. L. and Montgomery, D. J., TEXTILE RESEARCH JOURNAL **23**, 821 (1953).

B. H. MACKAY
J. G. DOWNES

Book Reviews

Physical Methods of Investigating Textiles. Edited by R. Meredith and J. W. S. Hearle. New York, Textile Book Publishers, Inc., a Division of Interscience Publishers, Inc., 1959. ix + 411 pages. Price $13.00.

Reviewed by Joseph H. Dusenbury, Textile Research Institute, Princeton, New Jersey

A little over a year ago this reviewer was asked by a physical chemist, with an advanced degree and new to the fiber field, to recommend a book describing experimental methods used to characterize the molecular structure and physical properties of textile materials. At the time, the physical chemist was told that such a book was nonexistent and was given instead a list of review articles and texts. The situation is different today; with the publication of "Physical Methods of Investigating Textiles," the requested book is now available. And it is a first-rate book, in which its two editor-authors and the other authors presented in it may take considerable pride.

According to its Preface, the work originated from a 1956–1957 course of lectures given at the Manchester College of Science and Technology, and some of the contributions are from specialists working in fields other than those concerned with textiles. The scope of the book is indicated from a listing of the titles and authors of its fourteen different chapters. These are (1) X-ray Techniques, by D. R. Holmes, (2) Infra-red Spectroscopy, by C. G. Cannon, (3) Electron Microscopy, by J. A. Chapman, (4) Optical Microscopy, by R. Barer, (5) Fibre Dimensions, by S. L. Anderson, (6) Density, Moisture and Swelling, by J. W. S. Hearle, (7) Yarn and Fabric Structure, by W. E. Morton, (8) Mechanical Properties of Fibres and Yarns, by R. Meredith, (9) Some Mechanical Properties of Fabrics, by J. C. Guthrie, (10) Transmission of Heat, Moisture and Air, by G. King, (11) Frictional Behaviour of Textiles, by J. W. S. Hearle and D. Tabor, (12) Optical Properties, by R. C. Faust, (13) Electrical Properties, by J. W. S. Hearle, and (14) Applications of Nuclear Physics, by J. W. S. Hearle. Where practicable throughout these chapters, intelligent use has been made of review articles and texts, with the result that there is room for and discussion of newer techniques. For most of the contributions, the literature through about 1956 appears to be well-covered; as could be expected for a book whose Preface is dated July 1958, the coverage appears less complete for 1957–1958.

It is a tribute to the present rate of research in the fiber field that it causes a book such as this to have some out-of-date aspects by the time it is printed. Thus, for example, no mention is made of papers presented at the 1958 Textile Institute Conference on "Mechanical Properties of Textile Materials," held in Gothenburg. It is unfortunate also that mention could not be made of Klein's 1959 paper describing the two-dimensional load–extension tester for fabrics developed at Fabric Research Laboratories and that direct mention is not made of the two-dimensional tester described in 1953 by Reichardt, Woo, and Montgomery. This reviewer also believes that the discussion of such tests ought to have been in the chapter on fabric mechanical properties rather than in that on "Mechanical Properties of Fibres and Yarns." Another example of "time marches on" is to be found in the necessary omission in the chapter on "Electrical Properties" of the important 1958 paper by Levy et al., in which the relation of charge to frictional work is described in connection with the static electrification of textiles. In this same chapter, an incorrect description is given of the use of a Faraday cage in the "rather elaborate apparatus" of Hersh and Montgomery.

As usually happens with a book of this type, a reader looks for coverage of certain specific topics and is sometimes disappointed to find these topics—important in his view—either inadequately treated or omitted. This reviewer is no exception in this regard. In the chapter on "Fibre Dimensions," for example, it would have been preferable, in discussing the equation for the vibroscopic determination of fiber linear density, to have pointed out that the "extra" part of the "bracketed term" is associated with fiber stiffness. Moreover, it is the reviewer's experience that, in contrast to the statement in the text, the correction for fiber stiffness often needs to be made

for fibers whose test-specimen length is greater than the 2 cm. mentioned in the text. Since crimp is mentioned in the chapter on "Fibre Dimensions," where its nuisance value in fiber-length measurements is considered, and in the chapter on "Yarn and Fabric Structure," where it is considered in connection with the crimp imposed on yarns by fabric geometry, it seems a pity that in the chapter on "Mechanical Properties of Fibres and Yarns" no mention is made of evaluating fiber crimp by analysis of the low-extension region of the fiber load–extension curve. In the chapter on "Some Mechanical Properties of Fabrics," it is interesting that a fair amount of attention is paid to the handle of fabrics, with a good brief discussion given of the relation between subjective and objective tests. Later in this same chapter, it is implied that abrasion testing is viewed with considerably less suspicion in the USA than in Great Britain, because the ASTM has described five different tentative tests for fabric abrasion resistance in its "1955 Book of ASTM Standards," but in Great Britain "no method has yet been the subject of a British Standard Test." From what this reviewer knows of the situation, the present view of abrasion tests in the USA is less sanguine than indicated in this book and is also thus indicated in the "Introduction" portion of the ASTM descriptions of tentative abrasion tests.

The book appears to be relatively free of trivial errors, although some are present and involve inaccurate literature references. The figures—there are 208—and tables have been carefully selected and add considerably to the value of the text. The author and subject indexes have been carefully prepared and also serve to enhance the book's worth. The book's attractive format is up to the usual high Interscience standards.

Advances in Carbohydrate Chemistry, Vol. 13. M. L. Wolfrom, ed. New York, Academic Press, 1958. xi + 387 pages. Price $11.00.

Reviewed by Eugene Pacsu, Princeton University, Princeton, New Jersey

This new volume of the by now indispensable *Advances* contains ten articles by twelve authors giving valuable and much needed information on less familiar topics, such as the formazan reaction, four-carbon saccharinic acids, glycosyl ureides, the chemical nature of the sialic acids, polysaccharide hydrocolloids (polysacolloids), methyl ethers of the amino sugars, and starch nitrate. It also presents up-to-date theoretical discussion on the extension of Richard E. Reeves' pioneering work on sugar-ring conformational analysis and on important sugar-alkali reactivity of general interest. An obituary of the renowned biochemist, Carl Neuberg, appears as a tribute written by Professor F. F. Nord, one of his former students.

The contents of this volume are as follows: Formation and Cleavage of the Oxygen Ring in Sugars, by F. Shafizadeh (222 refs.); The Lobry De Bruyn–Alberda Van Ekenstein Transformation, by John C. Speck, Jr. (133 refs.); The Formazan Reaction in Carbohydrate Research, by L. Mester (166 refs.); The Four-Carbon Saccharinic Acids, by James D. Crum (36 refs.); The Methyl Ethers of 2-Amino-2-Deoxy Sugars, by Roger W. Jeanloz (61 refs.); Glycosyl Ureides, by Irving Goodman (55 refs.); The Nonulosaminic Acids [Neuraminic Acids and Related Compounds (Sialic Acids)], by F. Zilliken and M. W. Whitehouse (127 refs.); Polysaccharide Hydrocolloids of Commerce, by Leonard Stoloff (26 refs.); Alkaline Degradation of Polysaccharides, by Roy L. Whistler and J. N. BeMiller (201 refs.); and Starch Nitrate, by George V. Caesar (70 refs.).

In addition to an Author Index (15 pp.) and a Subject Index (14 pp.), the volume also contains a Cumulative Author Index (5 pp.) and a Cumulative Subject Index (6 pp.) for Vols. 1–12.

Acrylic Resins. Milton B. Horn, New York, Reinhold Publishing Corporation, 1960. vii + 184 pages. Price $4.50.

Polyester Resins. John R. Lawrence. New York, Reinhold Publishing Corporation, 1960. ix + 251 pages. Price $5.75.

Reviewed by Richard K. Toner, Textile Research Institute, Princeton, New Jersey

These volumes are the fourteenth and fifteenth in a series being published by Reinhold. Like others in the series, they are only semi-technical in content and can be read by anyone with a little chemical background. For this reason they will appeal more to the industrial man than to research personnel. They may also prove interesting reading for those wishing to get an over-all picture of the application of acrylic polymers and polyester resins.

Information for Contributors

Requirements for copy submitted to TEXTILE RESEARCH JOURNAL conform, in general, with those for other scientific publications. This outline is intended to point out several differences in content and style.

Subject Matter

The JOURNAL covers the broad field of textile research with papers on pure science, engineering, and technology; it includes studies relating to chemistry, physics, and physical chemistry.

Types of Papers.—There are five principal classes of contributions suitable for the JOURNAL. *Fundamental research articles* should present new information and data and should represent distinct contributions to science. *Technical papers* may describe development work, engineering advances, and innovations in manufacture and processing. *Laboratory techniques* should include brief descriptions of practical methods developed which may be helpful to workers in other laboratories. In describing new instruments or modifications of existing apparatus, experimental data illustrating the utility of the instrument should be included. *Letters to the Editor* are intended for prompt publication of new discoveries and observations, or for informative comment on papers previously published in the JOURNAL; rarely should they exceed 1,000 words. *Review articles* of an authoritative and critical nature are occasionally published when judged to be of sufficient interest and importance.

Acceptance.—Papers are submitted to qualified persons for review, critical comment, and suggestions. Names of reviewers are not disclosed except with their consent.

Preparation of Manuscripts

Arrangement.—Any logical arrangement of the subject matter is acceptable. The order used by many authors is *Abstract, Introduction, Experimental Procedure, Results, Discussion, Conclusion, Acknowledgment,* and *Literature Cited,* with variations suitable to the particular subject. Subheadings are an aid in following the exposition.

Style.—The JOURNAL's style guides are "Webster's Unabridge Dictionary" and the "Government Printing Office Style Manual," with few exceptions. For situations not covered in these references, consult a recent issue.

Authors' Names and Affiliations.—This information should be given exactly as it is to appear in print. If the author is no longer with the company where the work was done, his new affiliation should be given in a footnote.

Typing.—Manuscripts should be typed, double-spaced; two copies should be submitted. They should be in *final form* and *checked for accuracy* to eliminate changes after the article is set in type.

Abstract.—A brief abstract (about 150 words) should accompany each paper. The abstract serves as an editorial lead and should give a simply worded preview of the paper.

Equations and Formulas.—All equations should be checked carefully by the author to avoid costly alterations which require hand-setting of type. Exponents should be legible and properly positioned. There should be a clear distinction between small and capital letters, between 1 (one) and l (el), and between the letter O and zero. Fairly simple structural formulas can be set in type; complicated ones should be lettered in India ink on a separate sheet of paper, from which a plate will be made. Greek letters should be written clearly; it is helpful to spell out the name of the symbol in the margin (lightly, in pencil) if an unfamiliar one is used. Equations are numbered in parentheses to the right; they are referred to in the text as Equation *2*, Equation 11a, etc. (no parentheses).

Description of Experiments.—The apparatus and procedures used should be described in sufficient detail to enable other investigators to repeat the experiments. Data should be included to substantiate conclusions drawn. To show a trend, graphical presentation may be best; to point out small differences, tabulation may be preferred; do not use both forms for the same data unless essential to the exposition.

Illustrations.—Drawings should be made in India ink on white paper or blue tracing cloth. Coordinate paper must be ruled in blue if the lines are not to show in the finished illustration. Clear photographic prints of drawings are also acceptable. The ultimate size of the illustration should be kept in mind when the originals are made; the table below gives a lettering guide for reduction to the usual 3-in. column width. Lettering in all capital letters usually is more legible than caps and lower case.

Size of Original	Height of Letters
4×5	2–3 mm.
8×10	4–5 mm.
10×16	8+ mm.

Letters and figures made by stencils are preferable; they should *never* be typewritten. Captions should not appear on the drawings; they are set in type below the figures and should be submitted together on a separate sheet. Blueprints, Verifax or Thermofax copies, or other reproductions may accompany the carbon copy.

Photographs.—Photographs should be glossy prints, clear, sharp, and as contrasty as possible without loss of detail. Identification of the figures should be made very lightly on the back with a soft pencil, as heavy writing or typing will appear on the printed figure; paper clips should be avoided or used on a part of the photo that will not be reproduced. To avoid cracks and creases, photos should be mailed flat, protected by heavy cardboard.

Tables.—Every table should have a caption above it and be identified with Roman numerals. For arrangement, see tables in current issues of the JOURNAL.

Literature Cited.—Data should be given in the following order: authors' names followed by initials (comma), name of publication (in quotes for a book, underlined for a journal, no punctuation following), volume number (comma), place and publisher for a book, (commas), inclusive page numbers (no punctuation following), and year of publication (in parentheses). If pagination is not consecutive throughout the volume, issue number and complete date of publication should also be given. Abbreviations of journal titles follow those used by *Chemical Abstracts.* Items are arranged alphabetically by author and numbered. Patent references include patent number, date, and assignee.

Galley Proofs–Reprints

Galley proofs are sent to the author for checking before publication. He is responsible for the accuracy of all text and tabular matter as well as numbering of figures, references, etc. It is urgently requested that the author confine his changes to corrections of errors and that he does not insert additions or make alterations, unless such material radically affects the conclusions drawn in the original work. If such alterations are extensive the paper may, at the editor's discretion, be again subject to review, and additional typesetting costs may be chargeable to the author.

A reprint order form is sent with galley proofs; it should be returned with them. Orders received after publication cannot always be filled, as type is destroyed after each issue and no extra reprints are made.